Universitat Autònoma de Barcelona

# Network Coding for Multi-beam Satellite Systems

**R. Alegre Godoy**

# Network Coding for Multi-beam Satellite Systems

author: R. Alegre-Godoy
advisor: Dr. M. A. Vázquez Castro

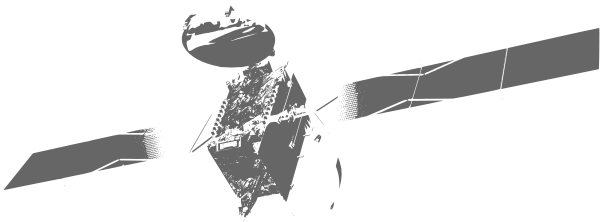

UAB
Universitat Autònoma de Barcelona

# NETWORK CODING FOR MULTI-BEAM SATELLITE SYSTEMS

PH.D. THESIS

AUTHOR: R. ALEGRE GODOY

ADVISOR: DR. M. A. VÁZQUEZ CASTRO


Ph.D. Programme in Telecommunications and Systems Engineering
Department of Telecommunications and Systems Engineering
Escola d'Enginyeria, Universitat Autònoma de Barcelona
Bellaterra, September 2016

*- voor mijn kleine vogeltje -*

# ABSTRACT

The last decade has witnessed a constant and increasing demand for the efficient distribution of personalized contents on the Internet over networks known to be highly throughput consuming. Design of upcoming satellite networks must address such demands with powerful new technological solutions in order to compete with the rapidly evolving terrestrial networks. The main objective of this thesis is to identify such solutions in order to enhance the offered throughput in multi-beam satellite systems, the main technology enabling High Throughput Satellite (HTS) systems. This objective is proposed to be achieved via alternative transmission schemes to the conventional frequency re-use and improved logical mechanisms based on Network Coding (NC), a new networking paradigm also being under consideration in the 5G and Wi-Fi terrestrial counterparts. The main contributions of this thesis are the following. First, a unified multi-beam satellite analytical system model has been developed. The model serves for the design and analysis of a large number of satellite systems enabling efficient comparison of the new technological solutions in terms of throughput. Second, a full design of a transmission scheme based on NC for the forward downlink of multi-beam satellite systems operating over an adaptive physical layer, a common feature on the lower layers of satellite systems. The proposed scheme shows multicast throughput gains of up to 88% employing the same amount of resources as traditional multicast schemes at the cost of a more complex but still realistic receiver. Third, a second full design of a transmission scheme based on NC, this time combined with Spatial Diversity (SD) and novel cognitive design elements. This scheme is particularly useful when severe packets losses impair the forward uplink of multi-beam satellite systems so that geographically distributed Gateways (GWs) can be jointly exploited. The design is shown to achieve more than one order of magnitude system outage probability advantage for a sufficient number of GWs. Furthermore, a methodology determining the optimal number of GWs and code-rate is derived.

# RESUMEN

La última década ha presenciado una constante y creciente demanda para la distribución eficiente de contenidos personalizados a través de Internet sobre redes conocidas por su alto consumo de *throughput*. El diseño de las nuevas redes satelitales debe tener en cuenta estas demandas mediante soluciones tecnológicas innovadoras para seguir compitiendo con las redes terrestres actuales, que estan evolucionando rápidamente. El objetivo principal de esta tesis es identificar estas soluciones para mejorar el *throughput* ofrecido en sistemas de satélite *multi-beam*, la principal tecnología habilitando sistemas de satélite de alto *throughput*. Se ha propuesto conseguir este objetivo mediante métodos de transmisión alternativos al típico reuso de frecuencia y mejorando los mecanismos lógicos basándose en *network coding* (*NC*), un nuevo paradigma de *networking* también bajo estudio por los homólogos terrestres 5G y Wi-Fi. Las contribuciones principales de esta tesis son las siguientes. Primero, el desarrollo de un modelo (analítico) unificado de sistemas de satélite *multi-beam*. El modelo sirve para el diseño y análisis de una variedad de sistemas *multi-beam* habilitando una comparación eficiente de las nuevas soluciones tecnológicas en términos de *throughput*. Segundo, el desarrollo de un esquema de transmisión completo basado en *NC* para el *forward downlink* de sistemas *multi-beam* con capa física adaptativa, un elemento común en las capas bajas de los sistemas satelitales. El esquema propuesto obtiene ganancias en *multicast throughput* de hasta el 88% usando los mismos recursos que esquemas de *multicast* tradicionales, sin embargo un receptor más complejo, aunque realista, es necesario. Tercero, un segundo diseño completo de un esquema de transmisión basado en *NC*, esta vez combinado con *spatial diversity (SD)*. Este esquema es particularmente útil cuando el *forward uplink* de sistemas de satélite multi-beam se ve afectado por altas pérdidas de paquetes, aprovechando los múltiples y geográficamente distribuidos *gateways (GWs)*. El diseño consigue mejoras en *system outage probability* de hasta un orden de magnitud para un número suficientemente grande de *GWs*. Además se propone una metodología para derivar el número óptimo de *GWs* y *code rate*.

# ACKNOWLEDGMENTS

This has certainly been a long long journey. The first person I would like to thank is my advisor Dr. María Ángeles Vázquez Castro. Working with her and learning from her has been a great experience that has taught me many important engineering and research lessons: passion, hard-work, motivation, being accurate and thorough *etc*. Some of these lessons I find to be applying myself now at work, others in my daily life. I would also like to thank her for her patience these last years where I did not have that much time to dedicate to the Ph.D. due to my job. Thank you for everything.

As a part of this Ph.D. I had the opportunity to work in the European Space Agency for 10 months under the ESA PRESTIGE programme. During my stage not only I found new directions and concepts for my thesis but I also discovered a whole new world, all the space activities carried out by the European Space Agency. I would like to thank Nader Alagha for his guidance during such time and the European Space Agency and the PRESTIGE programme for granting me such an unforgettable opportunity.

A journey is not a journey without companions to share it, in the good and in the not so good times. I would like to thank Alejandro, Marc, Moi, Mercè, Juanma, Mónica, del Peral and the many others I am sure I am forgetting for being part of my Ph.D. journey. But more especially I would like to thank my three office mates Smrati, Alejandra and Paresh since we have shared daily our successes and disappointments throughout several years. Circumstances have forced me to complete the last part of this journey abroad and alongside my job. I would like to thank my parents for keeping "funding" this project and for encouraging me to finish it even when it looked like it would hardly be finished. Gracias Jose María and Ilda. I would also like to thank my friends here in the Netherlands that have encouraged me to finish the Ph.D. and especially to my girlfriend Mieke who has encouraged me every day to work on it and she understood I had to spend many early mornings and late evenings in front of the computer. Thank you!

# CONTENTS

## LIST OF FIGURES



## LIST OF TABLES

# ACRONYMS

| | |
|---|---|
| **ACM** | Adaptive Coding and Modulation |
| **AWGN** | Additive White Gaussian Noise |
| **BH** | Beam Hopping |
| **BPA** | Binary Power Allocation |
| **CDS** | Content Download Services |
| **CONV** | Conventional |
| **C-PFM** | Combined-Proportionally Fair Multicast |
| **CR** | Cognitive Radio |
| **CSI** | Channel State Information |
| **Diffserv** | Differentiated services at IP level |
| **DSS** | Dual Satellite System |
| **DTN** | Delay Tolerant Network |
| **DVB-S2** | Digital Video Broadcasting over Satellite, 2nd Generation |
| **DVB-S2X** | DVB-S2 Extension |
| **FLEX** | Flexible |
| **GA** | Genetic Algorithm |
| **GW** | Gateway |
| **HPA** | High Power Amplifier |
| **HTS** | High Throughput Satellite |
| **IETF** | Internet Engineering Task Force |
| **LMB** | Live Multimedia Broadcasting |
| **LMS** | Land Mobile Satellite |
| **MODCOD** | Modulation and Codification |
| **NC** | Network Coding |
| **NOFR** | Non-Orthogonal Frequency Re-use |
| **NUM** | Numerical Utility Maximization |

| | |
|---|---|
| **OBO** | Output Back-Off |
| **PF** | Proportionally Fair |
| **PFM** | Proportionally Fair Multicast |
| **QoS** | Quality of Service |
| **RLNC** | Random Linear Network Coding |
| **SAR RLS** | Search and Rescue Return Link Service |
| **SD** | Spatial Diversity |
| **SINR** | Signal to Noise plus Interference Ratio |
| **SF** | Satisfaction Factor |
| **SLA** | Service Level Agreement |
| **SRLNC** | Systematic Random Linear Network Coding |
| **SS** | Spectrum Sensing |
| **SSS** | Single Satellite System |
| **UT** | User Terminal |
| **WCM** | Worst Case Multicast |
| **WSN** | Wireless Sensor Network |

# Part I

# DISSERTATION SUMMARY

# 1

# INTRODUCTION

## 1.1 MOTIVATION

The last decade has witnessed a constant and increasing demand for the efficient distribution of personalized contents in Internet based networks [ADI+12]. The delivery of this type of contents is well known for being highly throughput-consuming. Some examples of common applications are HD broadcasting, interactive TV, audio and video streaming, online gaming and file distribution and downloading.

In order to satisfy such throughput demand cellular networks moved from the 2G standard up to the current 4G, while already designing the upcoming 5G. The satellite industry, with the aim of competing with traditional cellular networks and offering Internet and broadband services, took also a big leap and moved from single-beam based satellite systems to multi-beam based satellite systems. Single-beam satellite systems are typically characterized by its wide coverage, given by a single antenna with a high aperture angle and thus providing limited antenna gain and throughput. On the other hand, multi-beam satellite systems board a number of high gain spot-beam antennas in the satellite platform, each of them covering a small region of the globe, typically of the order of hundreds of kilometers, and thus providing high throughput. Its coverage pattern, as seen from the satellite, resembles the one of cellular networks. Multi-beam technology has enabled High Throughput Satellite (HTS) systems, *i.e.* systems providing typically twenty times the throughput of a classic satellite system. HTS systems have recently started to be deployed by the satellite industry [FTA+16, FATS13] and the deployment of collocated HTS is foreseen in the future [CCO13, SCO14]. The multi-beam concept has unveiled a wide number of research areas ranging from the satellite hardware implementation to the system level design.

Beyond the aforementioned satellite-specific aspects it is also possible to satisfy the throughput needs by improving the logical mechanisms delivering the contents. In this sense the appearance of Network Coding (NC) in the seminal work by Ahlswede *et. al.* [ACLY00] has changed the paradigm of networking. Although originally meant for wired networks, it has been extended to terrestrial wireless networks and more recently to satellite networks. Among its advantages and implementation possibilities, studied in a vast number of articles, two of them are of special relevance to the multi-beam satellite case. First, its capability for improving the throughput of networks, especially under mul-

ticast scenarios where it is demonstrated to be a Shannon Capacity achieving technique [HMK+06]. Second, its easy implementation at the packet level of the system, *i.e.* without requiring any change at the physical level of the gateways or satellite which are costly and sometimes unapproachable for already deployed satellite systems.

This thesis focuses on the multi-beam satellite system modeling and on the introduction of transmission techniques that maximize the throughput offered to the users, the latter being mainly covered by the use of NC techniques. The literature covers well both topics, multi-beam satellite systems and NC, by separate. However, its joint application, addressing the particularities of multi-beam systems, has gained attraction only in the past few years [VSB10, VLA12a, VB09, VLA12b, VC13, AKO15, MMA13, MGdC14].

## 1.2 OBJECTIVES

The high level objectives of the thesis are the following:

*Objective 1: Develop a unified multi-beam satellite system model*

The multi-beam system model developed shall introduce a number of novelties with respect to other existing models in the literature. First, it should be representative of the three main types of multi-beam systems: Conventional, Beam-Hopping and Flexible. Second, it should introduce the effect on the user of the spot-beam antenna gain as a function of the antenna aperture angle. Thus, allowing easy analysis of the received signal strength regardless of the user location with respect to a beam. The developed multi-beam satellite system model shall also be the underlying tool used to carry out performance analysis and extraction of results.

*Objective 2: Design of NC transmission techniques for multi-beam satellite systems with adaptive physical layer*

Multi-beam satellite systems typically make use of an adaptive physical layer, the most common the Adaptive Coding and Modulation (ACM) feature of the Digital Video Broadcasting over Satellite, 2nd Generation (DVB-S2) and DVB-S2 Extension (DVB-S2X) standards. With the aim of improving the overall system throughput, proposed NC techniques shall be built upon this feature and respect as much as possible the multi-beam satellite systems reference architecture.

*Objective 3: Design of combined NC and Spatial Diversity (SD) transmission techniques for overcoming severe packet losses*

Occasionally, adverse atmospheric conditions can cause multi-beam satellite systems to operate out of the ACM range and produce severe packet losses.

This effect can occur for instance in the forward uplink, where the frequency band employed is high (Ku, Ka, Q and V bands) in order to exploit the higher amount of available bandwidth, and therefore more susceptible to deep fadings. Proposed NC techniques shall exploit the multiple geographically distributed GWs in order to improve the throughput when the system operates out of the ACM range and behaves as an ON/OFF channel.

## 1.3 STRUCTURE AND RATIONALE

This thesis is structured in three Parts. Part i contains a dissertation summary based on the journal papers, conference papers and book chapter contributions included in Part ii, iii and iv respectively. More specifically, in Part i:

- Chapter 1 has introduced the doctoral thesis. The main motivation, framework and objectives pursued have been presented. It also introduces the overall structure of the thesis and provides a brief analysis on the relevance of the publications annexed.
- Chapter 2 provides the reader with the necessary background and context. The chapter defines multi-beam satellite systems and describes its most typical architecture. The NC formulation at packet level and main figures of merit are also described. The work summarized in this chapter is partially based on the book chapter contribution in [VCAAG11] (not included in Part iv due to the generality of its content).
- Chapter 3 contributes to the achievement of Objective (1). It presents a unified system model for the three most common types of multi-beam satellite systems and also explores the physical satellite implementations of each of the types. Such model allows to perform an initial performance comparison between the different types of systems. The work summarized in this chapter is the result of the paper contributions C, D and E.
- Chapter 4 contributes to the achievement of Objective (2). It proposes a full multicasting scheme, that is, system architecture, scheduling policy and packet scheduling architecture, employing NC and built upon the ACM feature of the DVB-S2 and DVB-S2X. The work summarized in this chapter is the result of the paper contributions A, E and F.
- Chapter 5 contributes to the achievement of Objective (3) by proposing a combination of NC and SD for scenarios with multiple sources and one or two collocated satellites. The proposed system matches a number of satellite scenarios, among them the forward uplink of multi-beam systems. The work summarized in this chapter is the result of the paper contributions B and the book chapter contribution G.
- Finally, Chapter 6 discusses the main results of the doctoral thesis. Future lines of research are also proposed.

This is a thesis written by compendium of works. As such the annexed papers and book contributions represent the core of the thesis which include the thorough descriptions, discussions, mathematical developments and results. Part ii is the main annex and contains the published journals (A and B). Part iii and Part iv are complementary annexes containing the conference papers (C, D, E and F) and the book chapter contributions (G) respectively. The dissertation summary is meant to give an overall logical envelope by discussing the relevant related work in the literature and the main findings pointing the reader to the relevant papers where the complete descriptions can be found.

## 1.4 RELEVANCE OF PUBLICATIONS

The following analysis on the relevance of publications is based on the open-source SCImago Journal Rank [SCI] and Google Scholar [SCH]. The analysis in Table 1 shows that the publications annexed to this thesis have been published in journals in the first or second quartile *(Q1* or *Q2)* for the engineering category, and have been referenced by works in the literature.

Table 1: Analysis of relevance of publications. Quartile and IF values are referenced to the year of publication.

| **Title** | **Annex** | **Jour. / Conf.** | **Q#** | **IF** | **Ref.** | **Year** |
|---|---|---|---|---|---|---|
| Network Coding Multicast over Multi-beam Satellite Systems | A | Mathematical Problems in Engineering | Q2 | 0.68 | - | 2015 |
| Spatial Diversity with Network Coding for ON/OFF Satellite Channels | B | IEEE Communications Letters | Q1 | 2.44 | 4 | 2013 |
| Unified Multibeam Satellite System Model for Payload Performance Analysis | C | Personal Satellite Services Conference | - | - | 2 | 2011 |
| Heuristic Algorithms for Flexible Resource Allocation in Beam Hopping Multi-Beam Satellite Systems | D | AIAA International Communications Satellite Systems Conference | - | - | 1 | 2011 |
| Offered Capacity Optimization Mechanisms for Multi-beam Satellite Systems | E | IEEE International Communications Conference | - | - | 9 | 2012 |
| Multicasting Optimization Methods for Multi-Beam Satellite Systems Using Network Coding | F | AIAA International Communications Satellite Systems Conference | - | - | 4 | 2011 |

# 2

# PRELIMINARIES

## 2.1 MULTI-BEAM SATELLITE SYSTEMS DEFINITION

A multi-beam satellite features a number of high gain spot-beam antennas. The latter have a narrow beam, with a 3 dB beam-width of one to few degrees, thus providing coverage to a limited area of the earth, typically of the order of few hundreds of kilometers. The aggregate of beam coverage areas defines the multi-beam satellite antenna coverage. The typical (simplified) architecture of the system can be see in Figure 1 and consists of the following elements:

- A number of GWs, which can act cooperatively or cognitively, uplinking the data to the satellite through a high bandwidth feeder link in a separate frequency per Gateway (GW). Each GW is in charge of serving/managing a reduced number of beams within the overall system.
- A satellite featuring a multi spot-beam antenna and an on-board interconnection system routing the feeder links from the GWs towards the appropriate beams.
- A set of UTs, spread throughout the coverage, non-uniformly distributed and requesting a certain service.

The main advantage provided by multi-beam satellite systems is the increased power observed by the User Terminal (UT) due to high gain spot-beam antennas. On the other hand, the UT also observes an increased interference due to the antenna side lobes of beams in adjacent regions. To mitigate this effect a number of transmission schemes have been conceived, the main one based on conventional frequency re-use; however, other solutions are possible:

- Conventional (CONV) frequency re-use: Bandwidth is divided in a number of chunks and each beam is assigned an equal and fixed chunk. Since the number of beams is much higher than the number of bandwidth chunks, cellular colouring schemes are employed to assign the chunks to the ground cells minimizing the co-channel interference [AGVCJ11].
- Beam Hopping (BH): It defines a cyclic window of $W$ time-slots. Within each time-slot a subset of all the beams is activated or "*illuminated*" employing the entire bandwidth in a way that the offered throughput in each beam matches as much as possible the demanded throughput [AGVCJ11, AGAVC11].

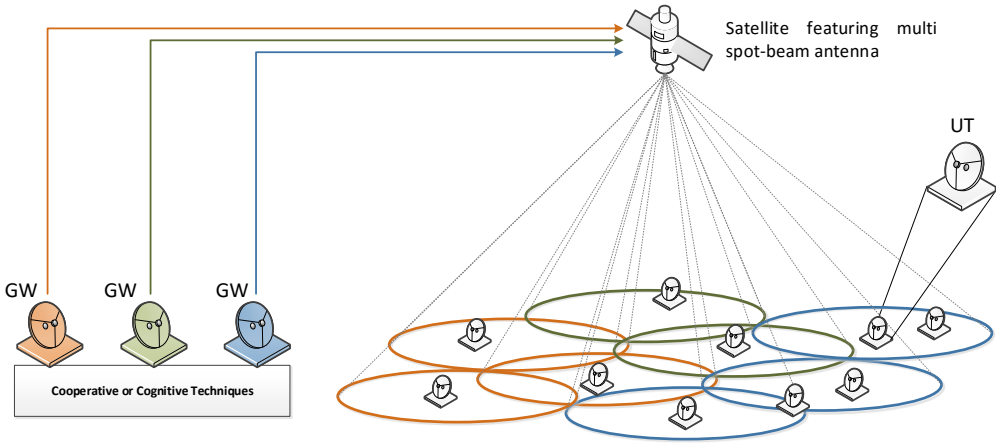


Figure 1: Multi-beam satellite system architecture.

- Non-Orthogonal Frequency Re-use (NOFR) or Flexible (FLEX): the total available bandwidth is divided in a number of frequency carriers. Each ground cell can be allocated a variable number of carriers depending on the traffic request. Carriers can be re-used throughout the coverage, but no restrictions are imposed on the frequency reuse, it should be given by the chosen resource optimization (*i.e.* interference minimization for a given traffic demand pattern) and will therefore be non-orthogonal [AGVCJ11, LVC11].

Figure 2 shows how the bandwidth assignment on the beam lattice would look like in each of the transmission schemes. The complexity of the final system lies on the antenna technology to generate a high number of narrow beams, the on-board interconnection matrices to forward the uplink carriers to the appropriate downlink beams (described in detail in Paper C) and the necessity for multiple GWs uplinking the high bandwidth carriers to the satellite at different frequencies.

## 2.2 PACKET-LEVEL RANDOM LINEAR NETWORK CODING

NC is, in this thesis, the main logical mechanism employed for improving the throughput. NC is based on the observation that nodes in a network can not only forward the incoming independent data flows, but also perform operations among them. Additional benefits besides the throughput improvement are enhanced reliability, energy saving and increased security [FS07]. These benefits can be easily demonstrated through the famous introductory example: *the butterfly network* [FyLBW06].

Among the number of existing network codes, Random Linear Network Coding (RLNC) is adopted due to its simplicity and capacity-achieving performance, although any other network code could be, in principle, applied to the presented schemes. Under RLNC, random linear coded packets are generated from $N_p$ native packets as follows. Let $L$ denote the length in bits of a native

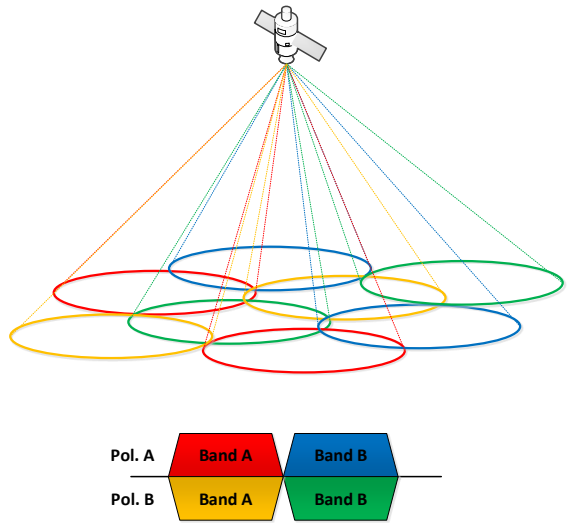


(a) CONV

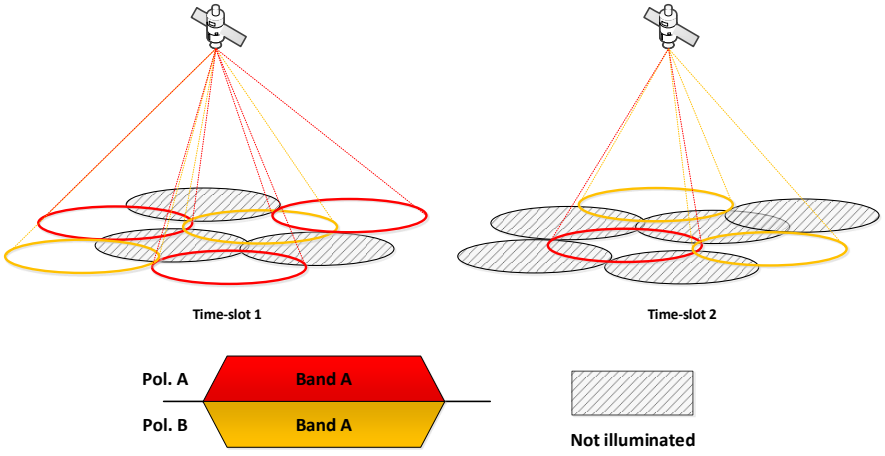


(b) BH

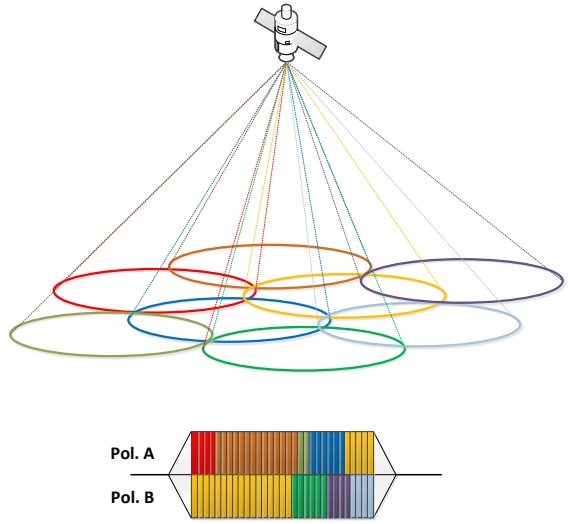


(c) NOFR or FLEX

Figure 2: Bandwidth assignment for CONV, BH and NOFR multi-beam satellite systems.

IP packet. Then, the payload of each packet $p_t$ is split into blocks of $\epsilon$ bits. Let $d_{tk}$ denote the $k$-th block of $t$-th packet, with $1 \leq k \leq L/\epsilon$. Next, we choose $N_p$ random coefficients $c_t$ from $\mathbb{F}_q$, with $q = 2^\epsilon$ . The $k$-th coded block of a coded packet is given by

$$C_k = \sum_{t=1}^{N_p} c_t d_{tk},\ 1 \leq k \leq L/\epsilon \tag{1}$$

The encoding coefficients $c_1, ..., c_{N_p}$ are added in the header of the packet unless pseudo-random codes are used and then only the code seed needs to be sent. In the receiver side, at least $N_p$ coded packets must be received to retrieve the original packets. The parameter $\epsilon$ is the size of the finite field and should be big enough to ensure that the probability of generating two linearly dependent (l.d.) coded packets is negligible.

## 2.3 PERFORMANCE METRICS

The main performance metric used to evaluate the proposed schemes is the offered throughput, normally measured in bits per second. Under the ACM specification of DVB-S2 and DVB-S2X assumed throughout the thesis, throughput is mainly a function of two factors:

- The system symbol rate $R_s$.
- The spectral efficiency $\eta$ (or equivalently MODCOD defined as a pair modulation and codification) derived from the Signal to Noise plus Interference Ratio (SINR) observed by the UT.

Since the schemes in this thesis aim to improve the throughput at a number of levels (user, multicast group, beam and system level) under a number of transmission schemes (CONV and BH), the specific throughput formulations are given in the associated chapters. The system outage probability is another performance metric used in this thesis. It is defined as the probability that the receiver is unable to collect all the information packets sent by the source. It is strictly related with the throughput since the lower the outage probability is, the higher the throughput will be.

# 3

# MULTI-BEAM SATELLITE SYSTEMS MODELING

## 3.1 INTRODUCTION

This chapter covers *Objective 1* of the thesis by introducing a unified model for multi-beam satellite systems and providing a system throughput performance comparison between the different types of multi-beam system. The model, described in Paper C, is representative of the main types of multi-beam satellite systems, CONV, BH and FLEX, capturing both its transmission schemes characteristics and technological satellite payload differences. Moreover, it also explicitly introduces the notion of angle between the UT location and a beam center as seen from the satellite. These two characteristics allow to:

1. Compute the SINR of a UT at each point of the coverage and per each type of multi-beam system (as Paper C shows). Subsequently, one can derive an overall multi-beam system throughput performance per each of the presented types. This is captured in Papers D and E for the CONV and BH systems and summarized in Section 3.3.

2. Reference the SINR of a UT to any of the beams. This allows to derive a SINR of a UT with respect to an adjacent beam easing the formulation of the algorithms presented in Chapter 4 where the UT can decode signals meant for an orthogonal beam.

At the point in time Paper C was written, a number of works had already introduced a multi-beam satellite system model, but lacked of the unified approach and/or did not specifically introduce the notion of angle between the beam center and the UT as seen from the satellite [LVC11, LVC10]. The work in [VCA12], developed later in time, presented a more refined model focusing on the decoding of signals from adjacent beams.

## 3.2 UNIFIED MODEL FOR MULTI-BEAM SATELLITE SYSTEMS

Let $\mathbf{x}_i = [x_{i1}, x_{i12}, ..., x_{iM}]$ be the symbols transmitted to a UT $i$ inside of beam $i$ and $\mathbf{n}_i$ a column vector of zero mean and complex circular noise with variance $N$. Let also $P_{sat}$ be the satellite transmitted power and $g_{ij} = \sqrt{g(\theta_{ij})}$ the square root of the antenna gain between the satellite transmitter antenna for beam $j$ and beam $i$, being $\theta_{ij}$ the angle that forms the receiver in beam $i$ towards the spot-beam center $j$ as seen from the satellite. Finally, $\beta_i = OBO_{hpa} L_{sat} L_{down} G_{gt}$

includes the gain and losses terms that do not depend on the angle $\theta_{ij}$ with $OBO_{hpa}$ the Output Back-Off (OBO) of the High Power Amplifier (HPA), $L_{sat}$ the satellite repeater output losses, $L_{down}$ the free space losses and additional rain, polarization, atmospheric and scintillation losses in the forward downlink, and $G_{gt}$ the ground terminal antenna gain. The derivations in Paper C lead to the following expressions for the received signal $\mathbf{y}_i(\theta)$ and $SINR_i(\theta)$ for a number of co-channel interferers $k$:

$$\mathbf{y}_i(\theta) = \sqrt{P_{sat}\beta_i g(\theta_{ii})}\mathbf{x}_i + \sum_{j=1, j\neq i}^{j=k} \sqrt{P_{sat}\beta_i g(\theta_{ij})}\mathbf{x}_j + \mathbf{n}_i \tag{2}$$

$$SINR_i(\theta) = \frac{P_{sat}\beta_i g(\theta_{ii})}{\sum_{j=1, j\neq i}^{j=k} \left(P_{sat}\beta_i g(\theta_{ij})\right) + N_i} \tag{3}$$

From the expressions above it can be noted that:

- The term $\beta_i = OBO_{hpa}L_{sat}L_{down}G_{gt}$ depends on the type of multi-beam system since their payloads have fundamentally different physical designs as Paper C shows. Therefore, specific SINR expressions can be extracted for each of the payloads, $SINR_i^{CONV}(\theta)$, $SINR_i^{FLEX}(\theta)$ and $SINR_i^{BH}(\theta)$, by replacing $\beta_i$ with $\beta_i^{CONV}$, $\beta_i^{FLEX}$ and $\beta_i^{BH}$ respectively.
- The derived expressions depend not only on the $\theta_{ii}$ (*i.e.* the angle between user $i$ and its beam center $i$) but also on the $\theta_{ij}$ with $i \neq j$ (*i.e.* the angle between user $i$ and each of the interferers $j$).

## 3.3 CONVENTIONAL VS BEAM HOPPING SYSTEM PERFORMANCE

Being a model applicable to each type of multi-beam system, one could attempt to establish a first comparison, in terms of overall system throughput, between the CONV, BH and FLEX options. Since the BH and the FLEX types are demonstrated to be dual [LVC11], an analysis of the BH also gives a hint of the performance trend of the FLEX type.

The chosen figure of merit is the Satisfaction Factor (SF) or percentage of useful throughput offered to the UTs given by the quotient of the overall useful throughput offered by the system and the total throughput requested by the UTs. This can be mathematically expressed as:

$$SF = \frac{\sum_{i=1}^{N_b} \left(\min(R_i, \hat{R}_i)\right)}{\sum_{i=1}^{N_b} \hat{R}_i} \tag{4}$$

where $N_b$ is the number of beams, $R_i$ is the offered throughput in beam $i$ and $\hat{R}_i$ is the required/demanded throughput by the UTs in beam $i$. For a CONV system deriving $R_i$ is relatively straightforward since all the beams are continuously

Table 2: Simulation results under a traffic distribution prediction for 2020. Results for predictions for other years available in Paper D.

| **Metric** | **CONV** | ***Convex*** | ***Genetic*** | ***minCCI*** | ***maxSINR*** |
|---|---|---|---|---|---|
| *SF* | 0.53 | 0.63 | 0.59 | 0.66 | 0.68 |

illuminated (see Figure 2a). Assuming a system based on DVB-S2 or DVB-S2X, $R_i$ is given by:

$$R_i = R_s f_{DVB-S2(X)}(SINR_i) \tag{5}$$

where $R_s$ is the system symbol rate, $SINR_i$ is the SINR at an intermediate point of the coverage of beam $i$ derived as shown in Eq. (3) and $f_{DVB-S2(X)}$ is a mapping function relating the DVB-S2 or DVB-S2X SINR to a certain spectral efficiency. On the other hand, in a BH system not all the beams are continuously illuminated but only a subset of them (see Figure 2b). Therefore $R_i$ can be expressed as:

$$R_i = \frac{R_s}{W} \sum_{j=1}^{W} T_{i,j} f_{DVB-S2(X)}(SINR_i^j) \tag{6}$$

where $W$ is the time-slot window length, $T_{i,j} \in \{0, 1\}$ is a flag indicating if beam $i$ is illuminated in time-slot $j$ ($T_{i,j} = 1$) or not ($T_{i,j} = 0$), and $SINR_i^j$ is the SINR at an intermediate point of the coverage of beam $i$ at time-slot $j$ derived as in Eq. (3) by selecting those co-channel interferers actually illuminated. The offered throughput will depend on how beams are illuminated as this factor determines the co-channel interference. How to perform such "illumination pattern" to optimize the SF in Eq. (4) is a non-convex optimization problem heuristically approached in Paper D and E. At the time these were written, the existing work on BH allocation algorithms either:

- Approached a simplified problem under the Binary Power Allocation (BPA) assumption, *i.e.* beam ON or OFF, through convex optimization [LVC11, ACDB+10].
- Or, adopted a computationally complex solution based on the Genetic Algorithm (GA) [ACG+10].

To the best of authors knowledge the heuristic algorithms presented in Paper D and E (*minCCI* and *maxSINR*) remain not only as the best performing solutions but also as computationally fast and flexible solutions taking into account a realistic representation of the BH payload. Beams can be allocated different transmitted powers by tunning the OBO (non BPA process) and the sharing of the amplification chains is modeled. The throughput improvement with respect to the CONV system ranges from the 20% to 28% depending on the traffic distribution. With respect to the best performing BH algorithm in the literature the improvement ranges from the 2% to 9%. Table 2 shows an example of the achieved throughput performances for year 2020. Figure 3 and Figure 4 show graphically the inflexibility of the CONV system with respect to the BH

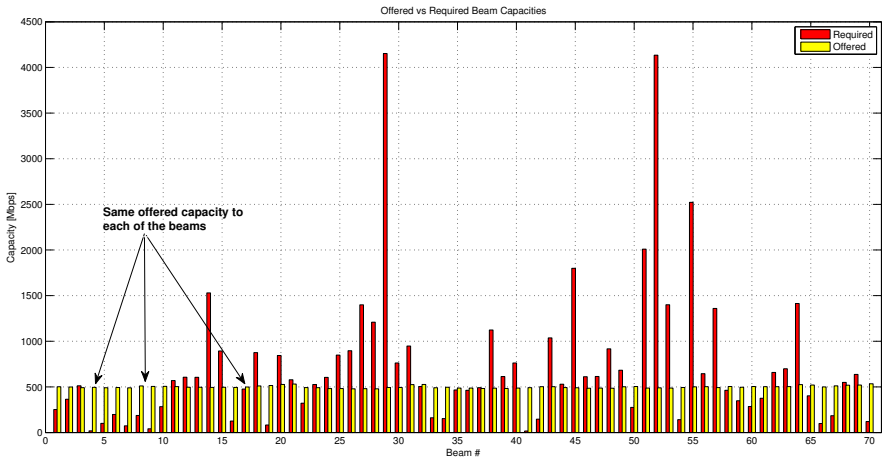


Figure 3: $R_i$ vs $\hat{R}_i$ for a CONV system under a traffic distribution prediction for 2020. Results for other years predictions available in Paper D.

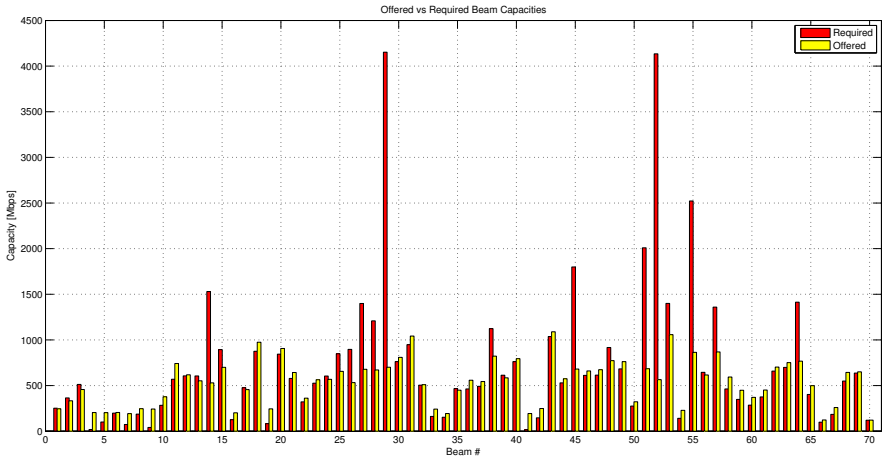


Figure 4: $R_i$ vs $\hat{R}_i$ for a BH system under a traffic distribution prediction for 2020. Results for other years predictions available in Paper D.

system. It can also be observed that the required throughput for some beams can not be satisfied which suggests that the future growth in throughput demand will overcome the physical limits of the present systems. Although new HTSs could be launched it would also be desirable to introduce improvements at the logical levels rather than the physical levels. Thus, the following chapters of this thesis analyze throughput improving techniques for multi-beam satellite systems based on NC and as a starting point for CONV systems.

# 4

# NETWORK CODING FOR ADAPTIVE PHYSICAL LAYER

## 4.1 INTRODUCTION

The unified multi-beam system model and system throughput performance comparison introduced in Chapter 3 were key elements to reveal that even advanced HTS systems may struggle to cope with the future throughput demands. As introduced in Chapter 1, besides of the specific satellite transmission aspects already discussed, it is also possible to increase the throughput by implementing the appropriate logical mechanisms at higher layers. The problem tackled in this chapter is the development of powerful NC mechanisms, and in particular based on RLNC, for improving the overall system throughput in HTS systems with an adaptive physical layer, covering thus the *Objective 2* of this thesis. In particular, the work in Papers A, E and F:

- Focus on the forward downlink of a CONV system.
- Exploit the fact that transmissions in orthogonal beams within an adaptive physical layer scheme show enough SINR to be decoded.
- Assumes multi-link reception, i.e. a UT able to syntonize different frequencies and polarizations, could access and decode the signal meant for adjacent beams.
- Target multicast applications for being an effective method to deliver throughput demanding applications such as audio/video streaming, online gaming, file distribution, and file downloading.

Paper F pointed out for first time that the exploitation of transmissions from orthogonal beams together with NC could bring important benefits in terms of throughput and reliability in multi-beam satellite systems. The concept has been later exploited by a number of works, focusing especially in the reliability enhancement for unicast transmissions [VLA12a, VLA12b]. The subsequent work in Papers A and E focus more on the throughput improvement for multicast applications which is little studied in the literature. The preliminary concept is introduced in Paper E whilst the full scheme, including scheduling policy based on the joint use of multi-link reception, NC and Proportionally Fair Multicast (PFM) and cross-layer packet scheduling architecture based on the Internet Engineering Task Force (IETF) Differentiated services at IP level (Diffserv) model, is introduced in Paper A.

At the point Paper A was written, the most similar work in terms of content (throughput improvement in the forward downlink of multi-beam satellite systems for multicast applications) and completeness was [PVC11]. It is also based on the adaptive physical layer concept and the authors propose a Numerical Utility Maximization (NUM) to trade delay and rate also accounting for Quality of Service (QoS) and multiuser diversity. With respect to this work, the concepts developed introduce the novelty of multi-link reception UTs together with NC which enables decoding orthogonal transmissions. Besides of the above mentioned work, multicast by itself has been little studied in the satellite domain from the resources allocation and scheduling point of view and most approaches opt for choosing MODCODs decodable by all or most of the UTs [SAEG09, PVC09a, PVC09b]. On the other hand, Paper A adopts a novel approach by adapting the unicast Proportionally Fair (PF) resource allocation [CG07, VVCSG06] to the satellite multicast scenario.

## 4.2 PRELIMINARY CONCEPT FOR EXPLOITING TRANSMISSIONS IN ORTHOGONAL BEAMS

The preliminary concept, described in Paper F, is based on the fact that a UT located in a beam of interest can decode transmissions from orthogonal beams, i.e. employ multi-link reception. Such effect is studied in detail in [VCA12] and caused by the gain of the antennas in the satellite that is so high that even UTs outside area of the beam observe enough SINR as to decode the signal. See for instance Figure 5 where the SINR values have been mapped to a MODCOD assuming the adaptive physical layer of DVB-S2 (ACM). The top plot shows per each location, the adjacent beam providing better SINR (the location and the adjacent beam with the strongest SINR are plotted in the same color and dashed lines separate the different areas). The mid and bottom plots show the achievable MODCODs from the own and determined adjacent beam transmissions, respectively. It can be observed that at any location of the beam it is possible to decode an orthogonal transmission and to do so UTs need to be equipped with multiple reception chains. Paper A discusses how such kind of terminals are already a reality.

Now, let us assume a GW multicasting certain video content, in this case Content Download Services (CDS) and Live Multimedia Broadcasting (LMB), to a set of UTs with multi-link reception capabilities spread in several beams as shown in Figure 6. Figure 7 shows two examples of the equivalent network representation. Since UTs can potentially receive packets from two paths employing the same MODCOD, the min-cut/max-flow theorem states that up to 2 different packets can be received simultaneously [FS07]. Due to the layout of the multi-beam network, the only way to ensure that all scheduled UTs will receive both packets is to send packets network coded. For instance, Figure 7a shows an example where one of the UTs would only receive one of the packets $p_1$ and $p_2$ independently of the packets sent by each queue. Instead, if every queue generated a single coded packet, as introduced in Section 2.2, all UTs would receive $p_1$ and $p_2$. Moreover, NC simplifies the scheduling because the

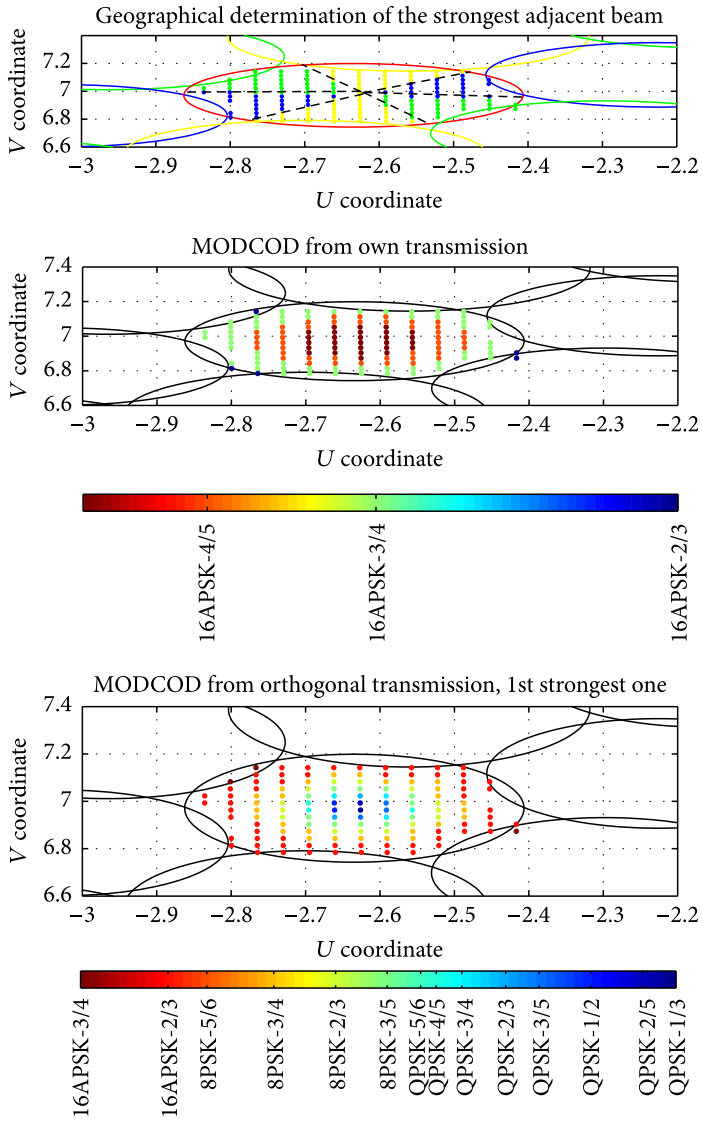


Figure 5: Achievable MODCODs for locations within a beam of interest.

system just transmits combined packets instead of looking at the topology of the network and deciding which packets should be selected in each queue for transmission. For instance, Figure 7b shows that all UTs can obtain $p_1$ and $p_2$ but previous knowledge of the topology is necessary to decide which packet forwards each queue. This simple examples show the power of multicasting in a network coded fashion. Advantages for multi-beam satellite systems are not limited to throughput improvement and simplified routing but also extend to the reliability domain as introduced in Paper F.

## 4.3 NETWORK CODING FOR THROUGHPUT IMPROVEMENT

A full understanding of the achievable gains in an actual multi-beam system requires a realistic and thorough assessment. In real multi-beam satellite systems GWs are assigned a subset of the beam lattice (normally higher than 3 beams),

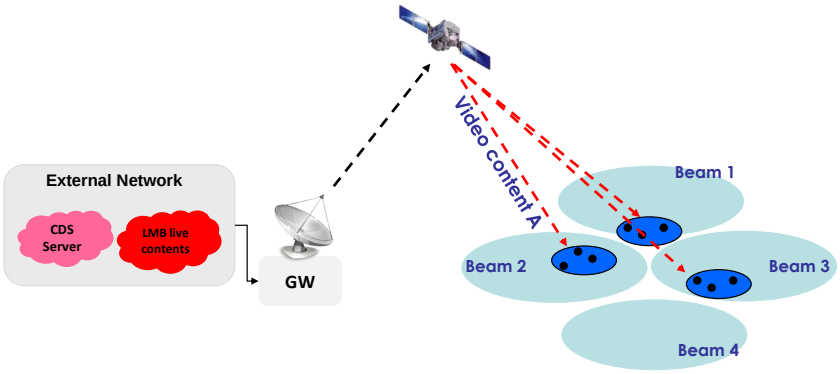


Figure 6: Multicast scenario of interest.

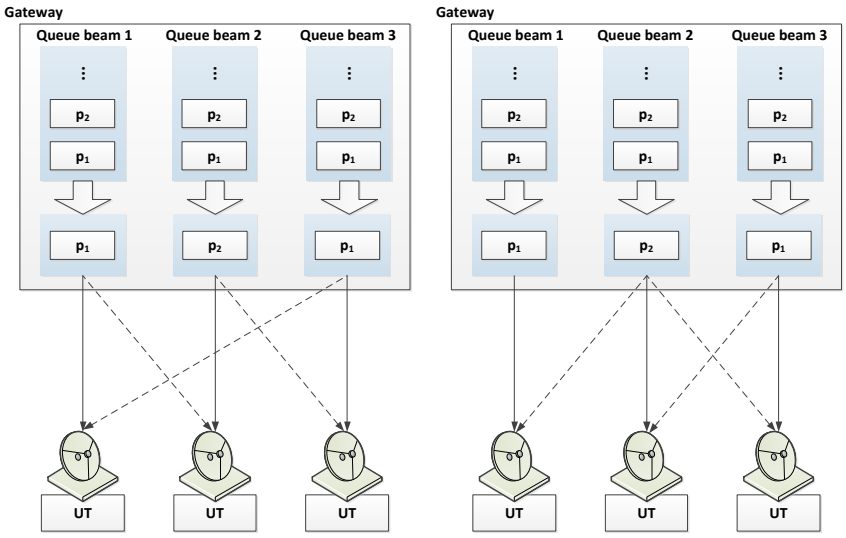


(a) (b)

Figure 7: Two examples of classical multicasting from a GW transmitting uncoded packets to three UTs in three beams. Continuous and dashed arrows represent transmissions from the own and best orthogonal beam, respectively.

UTs are non-uniformly distributed throughout the coverage and its distribution could change through time. The cases depicted in Figure 7a and Figure 7b assume equal throughput from the own and orthogonal transmission which is not necessarily true. Paper E points out that depending on the MODCOD assigned to each UT, which depends on its geographical location, weather conditions, scheduling scheme *etc.*, it may be more efficient to send the packets uncoded. Hence, a switching scheme between sending packets conventionally or network coded would be desirable. Paper A covers the above-mentioned aspects in order to propose a full multicasting scheme including:

- Combined-Proportionally Fair Multicast (C-PFM) scheduling policy based on PFM and a minimum Service Level Agreement (SLA), selecting the optimal MODCOD for the multicast service under adaptive physical layers based on DVB-S2 and DVB-S2X.
- Method to decide when to use the multi-link reception with NC feature.
- End-to-end system functional diagram including all the necessary new functions in the GW and UT side to implement the proposed multicast scheme based on NC and UT multi-link reception.
- Associated cross-layer packet scheduling architecture with respect to the IETF Diffserv model.
- Analysis and simulations performed over theoretical and realistic non-uniform UTs distributions.

Paper A demonstrates that the proposed scheme provides significant multicast throughput gains employing the same resources as traditional multicast schemes, especially when most of the UTs are located close to the edge of the beams. The specific algorithms are also described in Paper A, being the entire scheme is built upon the PFM concept. If a majority of UTs, subscribed to the same multicast service, can decode a certain MODCOD, that should be the transmitted mode by the satellite most of the time rather than transmitting according to the channel conditions of the worst UT [KK06]. This strategy that normally favours UTs in the center of the beam it is modified to take into account the orthogonal transmissions, *i.e.* UTs could simultaneously receive two packets (from the own and best orthogonal beam) at the MODCOD observed from the best orthogonal transmission. In order not to continuously burden UTs under degrade channel conditions an SLA mechanism consisting in periodically transmitting at a MODCOD decodable by all UTs is applied.

The proposed C-PFM scheme provides higher gains, compared to Worst Case Multicast (WCM), when UTs are located in the beam overlapping area or close to the edge of the beam concentrated in small (64%– 88%) or large areas (16%–27%). When UTs are located in the center of the beam, the gain is marginal (3%–5%). Ideally, if all the UTs were located in the beam overlapping area (*e.g.* in a regional satellite broadcast for a city), a 100% throughput gain could be achieved, except for the overhead bytes introduced when including the encoding coefficients in the network coded IP packets. Figure 8 shows a particular

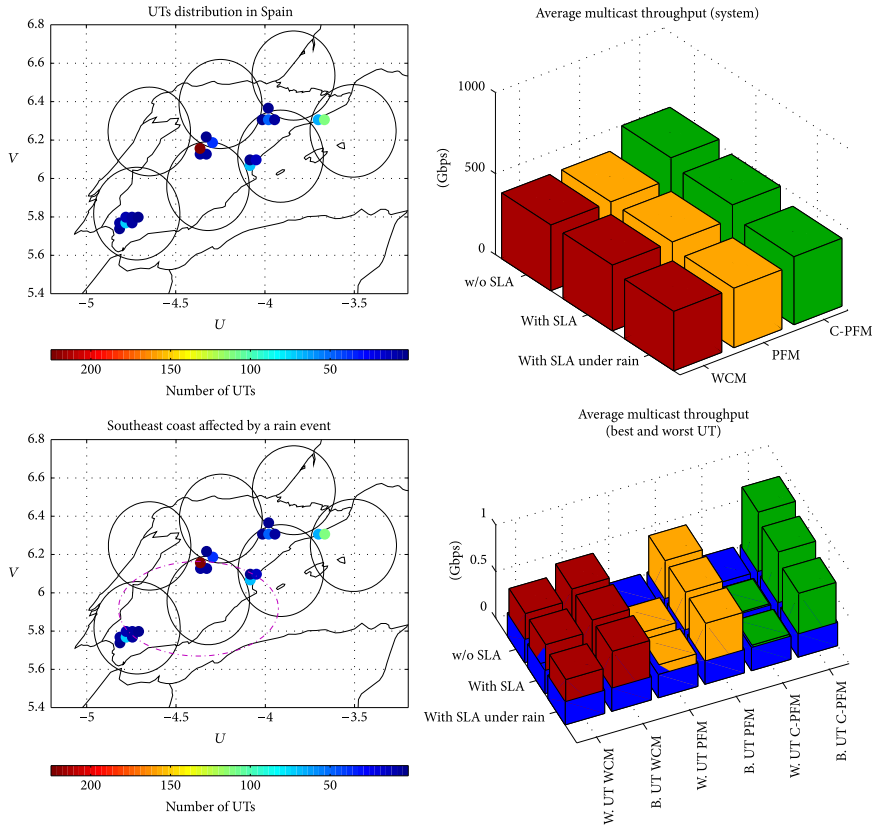


Figure 8: Average multicast throughput for a realistic UTs distribution in Spain.

case where a GW provides multicast services to Spain. The number of UTs subscribed to the multicast service is proportional to the number of inhabitants of the 5 largest Spanish metropolitan areas. The case without SLA gives the best average system multicast throughput improvement (32%) compared to WCM, however UTs are not guaranteed the minimum average throughput allocation (marked by the blue bar in the bottom plot). The cases with SLA under clear-sky and rainy conditions still show a significant throughput improvement, 21% and 15% respectively, while guaranteeing a minimum throughput allocation for all UTs.

# 5

# NETWORK CODING FOR SPATIAL DIVERSITY

## 5.1 INTRODUCTION

The work presented in Chapter 3 and Chapter 4 has mainly focused on the forward downlink of multi-beam satellite systems. However, the forward uplink plays a fundamental role. In order to provide with the necessary amount of bandwidth, feeder links have moved to Ku, Ka, Q and V bands, which are more susceptible to (deep) fading due to atmospheric impairments. The service availability is achieved by deploying an increased number of GWs, approximately 10 [FTA+16], over large geographical areas (SD) to decorrelate these impairments. This chapter covers *Objective 3* of the thesis by assessing the design of combined NC and SD techniques to improve the system availability (or its complementary, the system outage probability as defined in Section 2.3) in a general scenario that can be matched to the forward uplink of a multi-beam satellite system. More specifically, the work in Paper B and book chapter contribution G:

- Targets two scenarios. 1) A multiple sources, single satellite, single receiver scenario or Single Satellite System (SSS). 2) A multiple sources, dual satellite, single receiver scenario or Dual Satellite System (DSS).
- Assumes an ON/OFF channel producing severe packet losses. For a multi-beam satellite system this could be equivalent to operate out of the ACM range, for instance during heavy rain events.
- Assumes sources have exchanged a common set of packets and no Channel State Information (CSI) is available to them.

Paper B assesses the conventional scenario, with one satellite, and book chapter contribution G focus in the case where two collocated satellites provide final users with the desired throughput. In the latter, sources employ Cognitive Radio (CR) techniques in order to share the available spectrum efficiently. At the point in time Paper B was written, SD had already been applied to these type of scenarios where multiple sources cooperate and communicate with a single destination through one or two satellite relays in presence of deep fadings. See for instance [BM08, KETJ12]. With respect to these works, the contributions in this thesis introduce the novelty of NC. A number of posterior works have jointly applied NC and SD in the forward uplink of multi-beam satellite systems. Whilst both contributions B and G assume no CSI is available

and hence all sources continuously send packets network coded in order to increase the likelihood of the reception, [MMA13, MGdC14] apply a channel prediction algorithm in order to recover packet losses caused by inaccuracies on the prediction of the handover phase duration when shifting traffic from one source to another. Techniques and analysis are only provided for the SSS case while the contributions in this thesis also analyze the more advanced DSS case taking advantage of CR techniques. The proposed combined NC and SD techniques have also been applied to totally different scenarios, for instance in [AGS14] for the Search and Rescue Return Link Service (SAR RLS) of the Galileo system, demonstrating the generality of the scenario assessed.

## 5.2 SPATIAL DIVERSITY WITH NETWORK CODING FOR SINGLE SATELLITE SYSTEMS

Figure 9a shows the scenario under study where multiple sources are connected to a receiver through a single satellite. Each source-satellite link is modeled as an ON/OFF channel using a two state Markov chain. $N$ different packets, $P = \{p_1, p_2, \ldots, p_N\}$, are to be transmitted by $|S|$ sources, $S = \{s_1, s_2, \ldots, s_{|S|}\}$ with $N \leq |S|$. In a classical SD scheme sources $s_1$ to $s_N$ would transmit each a different packet $p_1$ to $p_N$ and sources $s_{N+1}, s_{N+2}, \ldots, s_{|S|}$ would correspondingly transmit packets $p_1, p_2, \ldots, p_{|S| \bmod N}$ (see Figure 9b). In the proposed SD+NC scheme each source employs RLNC to generate a coded from $N$ native packets as explained in Section 2.2 (see Figure 9c where coded packets are indicated as C(·)). The reason for the better behavior of the SD+NC scheme is two-fold:

- Avoids that duplicated versions of the same packet are received.
- Provides fair protection of the packets.

Each coded packet stores information from $N$ original packets, then if one source-satellite link is in bad state it equally affects to all the $N$ packets and not to a single packet as in the SD case. Hence, that for a large enough number of sources all the $N$ packets are likely to be received whilst for the SD scheme it completely depends on which specific links are in good or bad state. The main disadvantages of the proposed SD+NC scheme are:

- At least $N$ packets must be received to get useful information.
- Packets suffer from an extra delay due to the coding overhead.

Both disadvantages can be mitigated employing Systematic Random Linear Network Coding (SRLNC) where the first $N$ sources send uncoded packets and the last $|S| - N$ would be coded packets. Moreover, Paper B also proposes a design methodology for the optimal use of the scheme:

- Deriving the optimal value of $N$, $N_{opt}$, for a given number of sources $|S|$ to achieve a target system outage probability, *i.e.* the optimal code rate constrained to a maximum system outage probability.

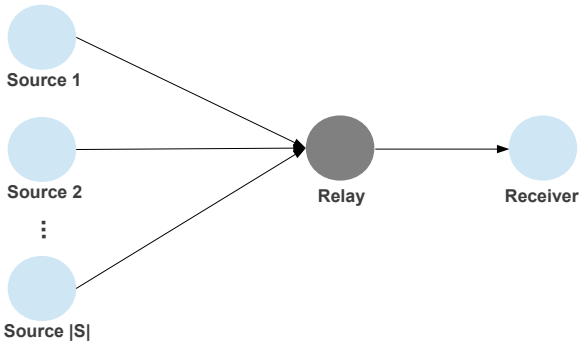


(a) Scenario under study.

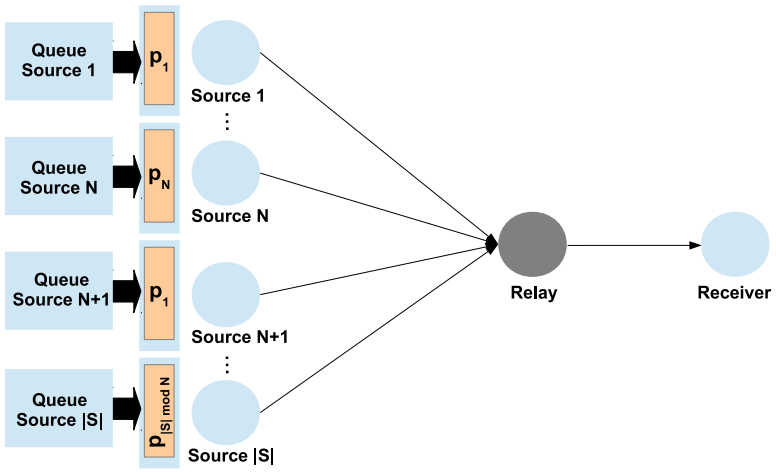


(b) SD scheme.

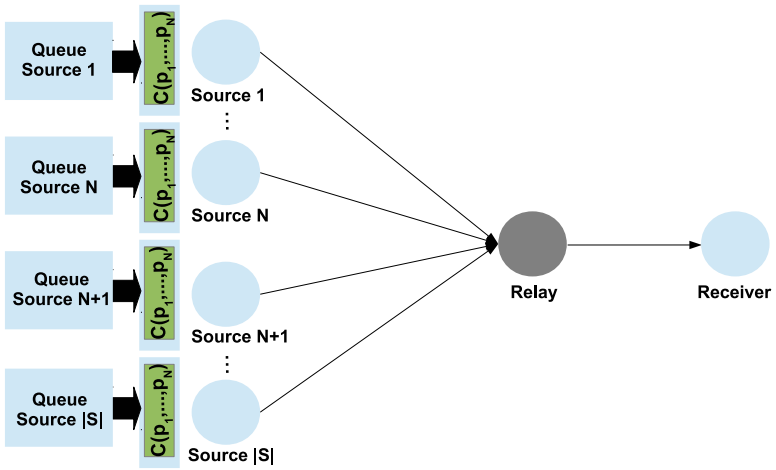


(c) SD+NC scheme.

Figure 9: Scenario under study and proposed schemes for SSS.

Table 3: Simulated multi-beam scenario.

| Parameters | Value |
|---|---|
| Packet size (bytes) | 1500 |
| Rate (kbps) | 10 |
| Propagation delay (s) | 0.250 |
| Number of sources | 1-10 |
| $E_G$ (s) | 1200 |
| $E_B$ (s) | 600 |
| $N$ | 2 |
| $m$ (Only in SD+NC) | 8 |
| Simulation time (s) | 10000 |
| Rounds | 10 |

- Deriving the minimum number of sources $|S|_{min}$ to achieve a certain system outage probability given the number of packets to be coded and transmitted in a certain time-slot.

Paper B shows results for Wireless Sensor Network (WSN) and Delay Tolerant Network (DTN) scenarios. For a multi-beam case we could consider the scenario shown in Table 3 where a number of GWs attempt to communicate with a UT. The packet size is set up to 1500 bytes (typical IP value) and the transmission rate is very low since the system operates at the edge of the ACM due to heavy rain conditions with mean durations of the good and bad states of 20 and 10 minutes respectively. Figure 10 and Figure 11 show the results in terms system outage probability (theoretical and simulated) and the optimal values of $N_{opt}$ and $|S|_{min}$. Figure 10 clearly shows that the SD+NC scheme achieves systematically lower system outage probabilities. For a large number of GWs, 9 or above, the difference is one order of magnitude. Figure 11 can be used to determine the optimal code rate (top plot) and the minimum number of GWs (bottom plot) to achieve a certain target system outage probability value. For instance, for a typical unavailability target of $10^{-2}$, the minimum number of GWs ranges from 6 to 13, with code-rates ranging from $1/6$ to $4/13$.

### 5.3 COGNITIVE RADIO SPATIAL DIVERSITY WITH NETWORK CODING FOR DUAL SATELLITE SYSTEMS

Figure 12a shows a scenario where multiple sources are connected to a receiver through two satellites. DSS are becoming every time more common. Not only the increase of traffic demand in certain regions has led to the launch of various platforms to cover a similar area, but also the co-existence of old single-beam systems with the new HTS and the replacement phase of old satellites with new ones form DSS. The co-existence of two satellites covering similar regions possesses a number of challenges such as limited spectrum, high interference and limited availability for which CR techniques are a promising so-

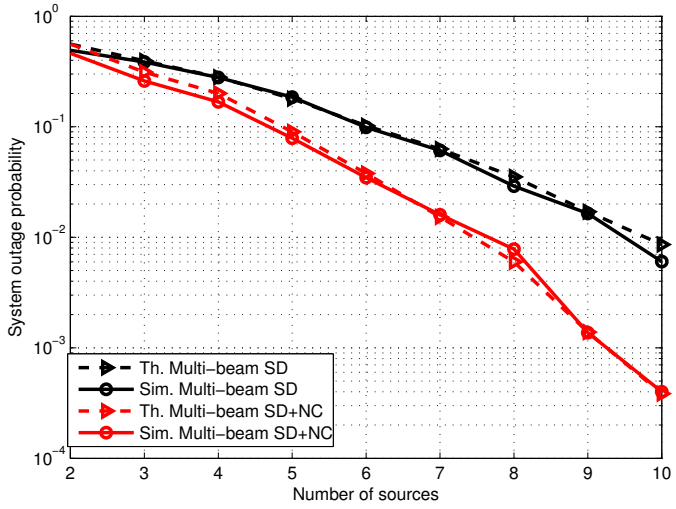


Figure 10: Simulation results and theoretical curves for the system outage probability in a multi-beam scenario.

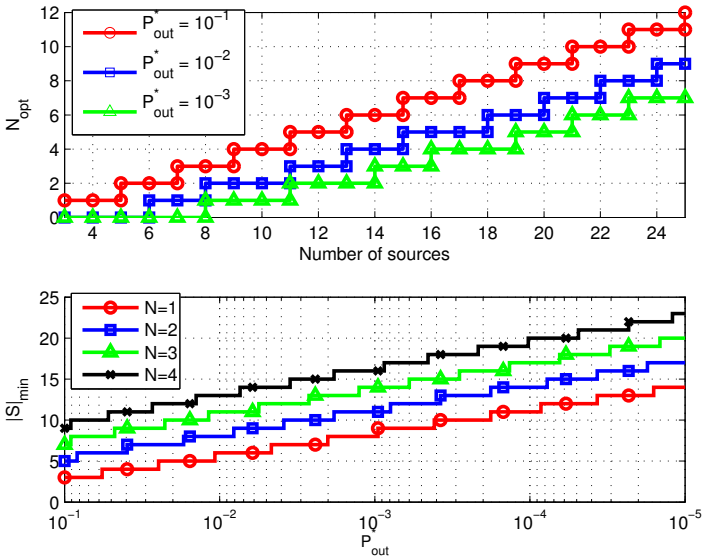


Figure 11: Upper sub-figure: Optimal value of $N$ for multi-beam scenario. Bottom sub-figure: Minimum value of $|S|$ to accomplish $P^*_{out}$ given $N$.

lution [CODG15]. Each source-to-satellite link is still modeled as an ON/OFF channel and hence the connection between each source and the satellites can be modeled as a pair "ON-ON", "ON-OFF", "OFF-ON" or "OFF-OFF". Depending on the frequency of the states, the source-to-satellites channels could be correlated, uncorrelated or totally correlated.

The transmission schemes for the CR SD and CR SD+NC schemes in Figure 12b and Figure 12c are equivalent to the ones presented in Section 5.2, however, the access to the medium is performed via Spectrum Sensing (SS), a CR technique. The fact that UTs exchange, accumulate and code packets before sending them makes the transition between busy and idle periods more predictable for which the SS becomes more effective [WSZL11, ZDL+13]. As before, the scheme with NC performs better because it limits the possibility to receive duplicated packets but the performance depends on the correlation of the source-satellite channels. Figure 13 shows a theoretical performance of the CR SD+NC compared to the CR SD for the system in Table 1. If the source-to-satellites channels were totally uncorrelated both schemes would perform equally since there would always be an available satellite and all packets would reach the receiver. On the other hand, when the source-to-satellites channels are totally correlated the performances shown in Section 5.2 apply because both satellites are available or not available (right plot of Figure 13 and the plot in Figure 10 are the same). For any degree of correlation in between, CR SD+NC offers always better performance compared to standalone CR SD and compared to a SSS since the fact of having two satellites is exploited (left plot of Figure 13 shows better performance than the plot in Figure 10).

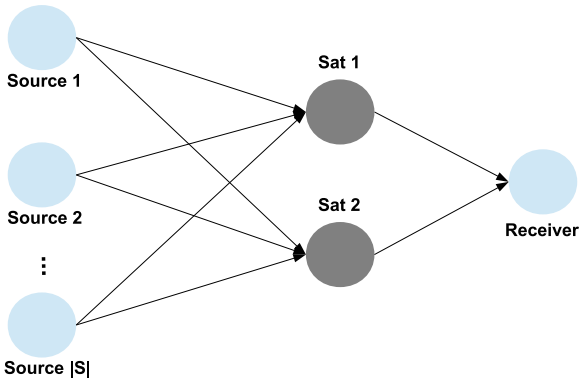


(a) Scenario under study.

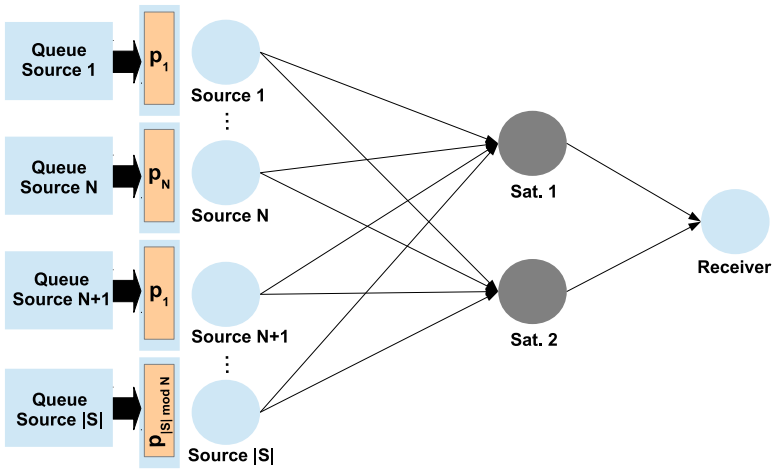


(b) CR SD scheme.

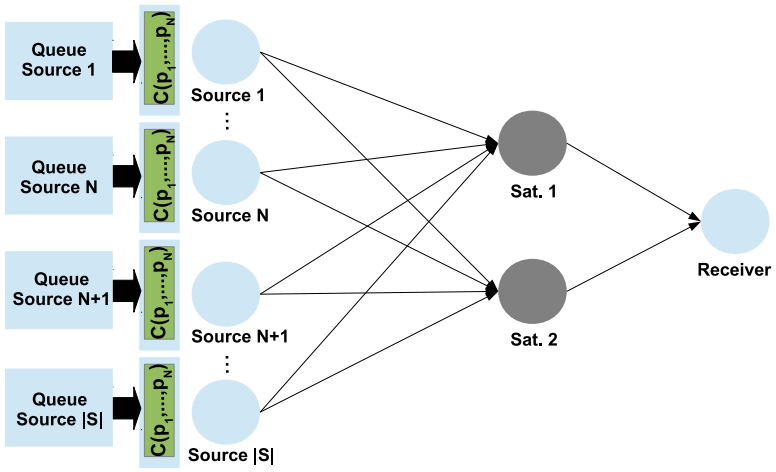


(c) CR SD+NC scheme.

Figure 12: Scenario under study and proposed schemes for DSS.

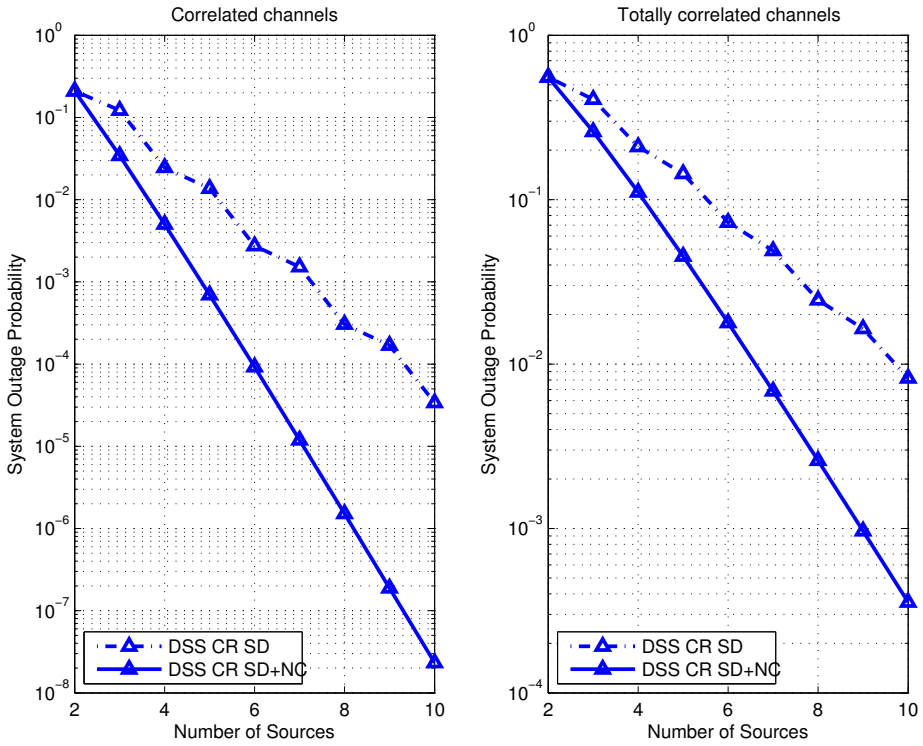


Figure 13: Simulation results for the system outage probability in a DSS multi-beam scenario.

# 6

# MAIN RESULTS OF THE DISSERTATION

## 6.1 CONCLUSIONS

The first chapter of this thesis has introduced a number of high-level objectives to systematically identify needs, develop and analyze NC techniques to improve the offered throughput in multi-beam satellite systems. The summary presented throughout Chapters 3 to 5 covers the objectives in Chapter 1 and allows to safely state that the objectives of the thesis have been achieved. The work presented is supported by a number of publications, annexed to the thesis: 2 journal papers, 4 conference papers and 1 book chapter contribution, whose relevance is analyzed in Chapter 1. More specifically, the contributions of this thesis against each of the objectives can be summarized as follows:

*Objective 1: Develop a unified multi-beam satellite system model*

Chapter 3 has introduced a unified model for multi-beam satellite systems. The work in this chapter is covered by Papers C, D and E contributing to the state-of-the-art in the modeling and system-level design of multi-beam satellite systems.

*Contributions on modeling*

The unified system model introduces two novelties with respect to the state-of-the-art. First, it is representative of the main types of multi-beam systems (CONV, BH and FLEX) capturing its transmission and satellite payload technological differences. Second, it introduces the notion of angle between the UT and any beam center allowing to derive SINR values not only for the beam where the UT is located but for any beam in the coverage.

*Contributions on system-level design*

With respect to the system-level design, the system model has been the underlying tool used for all the performance analysis. Through its implementation in a simulator it has provided fair and precise SINR values for the different types of multi-beam systems feeding the BH and NC algorithms of this thesis.

*Objective 2: Design of NC transmission techniques for multi-beam satellite systems with adaptive physical layer*

Chapter 4 has introduced a novel NC based scheme exploiting the adaptive physical layer of multi-beam satellite systems in order to improve the throughput delivered to UTs. The preliminary concept is covered by Papers E and F whilst the full scheme is covered in Paper A. The work in this chapter contributes to the state-of-the-art of multi-beam satellite systems at a number of levels: On satellite multicasting, at NC level and at system-level design.

*Contributions on satellite multicasting*

With regard to satellite muticasting, the technique proposed in this thesis adopts a novel point of view rather than the conventional approach based on multicasting according to the worst or average UT: PFM. Although similar frameworks had been proposed for satellite unicasting they are proposed here for first time for satellite multicasting enabling fair allocation of the multicast resources.

*Contributions on NC*

Based on the multi-link reception UTs and on the PFM concept, this thesis integrates these features with NC by proposing a novel technique for the joint use of multi-link reception, NC and PFM.

*Contributions on system-level design*

The aforementioned concepts are consolidated into a novel full multicasting scheme which provides high multicast gains employing the same amount of resources as traditional multicast schemes. The full end-to-end functional diagram, scheduling policy selecting the optimal MODCOD and enabling, when appropriate, the multi-link reception with NC feature and the packet scheduling architecture with respect to the IETF Diffserv model are provided. Finally, the analysis breaks the well-established and unrealistic assumption of uniformly distributed UTs to show performance results for a number of non-uniform UTs distributions.

*Objective 3: Design of combined NC and SD transmission techniques for overcoming severe packet losses*

Chapter 5 has introduced a combined NC and SD scheme for overcoming severe packet losses in the forward uplink of multi-beam satellite systems. The work in this chapter is covered by Paper B and Book Chapter G contributing mainly on the system-level design of multi-beam satellite systems and wireless networks.

*Contributions on system-level design*

The proposed SD+NC scheme contributes to the system-level design of the multi-beam satellite systems uplink by proposing a design methodology for deriving the optimal number of GWs and code-rate to achieve a certain target system outage probability. The technique shows systematically better performance than classical schemes based on standalone SD both in SSS and DSS scenarios. In the latter, novel cognitive elements are also proposed.

*Contributions on wireless networks designs*

The contributions addressing this objective assess a general scenario with a variable number of sources, one or two relays and a single receiver; therefore, the technique and methodology are not only valid for the forward uplink of multi-beam satellite systems but also to any other scenario with the same shape as the associated paper and book chapter contributions and posterior publications show.

## 6.2 FUTURE LINES OF RESEARCH

This thesis has covered soundly the objectives listed in Chapter 1. Observing the current trends in multi-beam satellite systems, the work presented could be expanded as follows:

*Addressing mobile UTs performance*

Mobile terminals are already one of the major solicitors of high throughput services. This type of users experience most of the times serious difficulties to receive satellite signals under urban and suburban scenarios where multi-path and deep fading effects are common. Multicasting according to the channel conditions of the worst UT is even more inefficient in this scenario since a significant number of UTs may face harsh reception conditions. Using a multi-beam system model accounting for mobile UTs the presented NC techniques can be adapted so that important throughput improvements can be also obtained in this scenario. There are a number of challenges to be addressed for such adaptation such as obtaining timely and accurate CSI feedback from the UTs and averaging this feedback an optimal number of time-slots before scheduling a certain MODCOD.

*Development of a system model covering mobile UTs*

Addressing the performance of the proposed NC techniques for mobile UTs is one of the identified future lines of research. However, the unified multi-beam satellite system model developed in this thesis reflects only UTs under an Additive White Gaussian Noise (AWGN) channel. A new multi-beam satellite system model, or a modification of the present one, accounting for the Land

Mobile Satellite (LMS) channel would have to be developed such that results can be extracted for mobile UTs.

*Addressing BH Performance with NC*

Recent studies suggest that BH-based satellites could become a reality in the coming years. Whereas the introduced NC technique is, in principle, valid for any type of multi-beam system featuring an adaptive physical layer performance results are only extracted for the CONV type. Given the trends on the satellite throughput demand, it would be desirable to address the performance of the proposed techniques under a BH scenario while taking into account the particularities of this type of system such as the non-continuous illumination of beams.

*Optimization for DSS*

As already discussed, DSS are becoming every time more common due to the co-existence of old satellites with the new generation of HTS during the operational and replacement cycles. The design methodology deriving the optimal number of GWs and code rate applies only to SSS and should be in the future expanded to DSS.

*Emphasis on CR Techniques*

DSS systems will certainly require more intelligent ground systems in order to effectively share, the sometimes scarce, available resources. Such intelligence can be achieved by employing CR techniques. This thesis proposes a concept showing that CR and NC could not only improve the DSS system availability but also the effectiveness of SS. Such concept would need to be analyzed in more detail to fully understand its potential.

# BIBLIOGRAPHY


[ACDB+10] X. Alberti, J.M. Cebrian, A. Del Bianco, Z. Katona, J. Lei, M.A. Vazquez-Castro, A. Zanus, L. Gilbert, and N. Alagha. System capacity optimization in time and frequency for multibeam multimedia satellite systems. In *ASMA Conf. and SPSC Workshop*, pages 226–233, Sept 2010.

[ACG+10] J. Anzalchi, A. Couchman, P. Gabellini, G. Gallinaro, L. D'Agristina, N. Alagha, and P. Angeletti. Beam hopping in multi-beam broadband satellite systems: System simulation and performance comparison with non-hopped systems. In *ASMA Conf. and SPSC Workshop*, pages 248–255, Sept 2010.

[ACLY00] R. Ahlswede, Ning Cai, S.-Y.R. Li, and R.W. Yeung. Network information flow. *Information Theory, IEEE Transactions on*, 46(4):1204–1216, Jul 2000.

[ADI+12] B. Ahlgren, C. Dannewitz, C. Imbrenda, D. Kutscher, and B. Ohlman. A survey of information-centric networking. *IEEE Commun. Magazine*, 50(7):26–36, 2012.

[AGAVC11] R. Alegre-Godoy, N. Alagha, and M.A. Vazquez-Castro. Heuristic algorithms for flexible resource allocation in beam hopping multi-beam satellite systems. In *29th AIAA International Communications Satellite Systems Conference*, 2011.

[AGS14] R. Alegre-Godoy and I. Stojkovic. Improving the availability of the sar/galileo return link service via network coding. In *Satellite Navigation Technologies and European Workshop on GNSS Signals and Signal Processing (NAVITEC), 2014 7th ESA Workshop on*, pages 1–6, Dec 2014.

[AGVCJ11] Ricard Alegre-Godoy, Maria Angeles Vázquez-Castro, and Lei Jiang. Unified multibeam satellite system model for payload performance analysis. In *PSATS*, volume 71, pages 365–377, 2011.

[AKO15] Z. Gao Z. Han A. Kalantari, G. Zheng and B. Ottersten. Secrecy analysis on network coding in bidirectional multibeam satellite communications. *IEEE Transactions on Information Forensics & Security*, accepted, May 2015.

[BM08] I. Bisio and Mario Marchese. Efficient satellite-based sensor networks for information retrieval. *Systems Journal, IEEE*, 2(4):464–475, Dec 2008.

[CCO13] D. Christopoulos, S. Chatzinotas, and B. Ottersten. User scheduling for coordinated dual satellite systems with linear precoding. In *Communications (ICC), IEEE International Conference on*, pages 4498–4503, June 2013.

[CG07] M. A. Vázquez-Castro Castro and G. S. Granados. Cross-layer packet scheduler design of a multibeam broadband satellite system with adaptive coding and modulation. *IEEE Transactions on Wireless Communications*, 6(1):248–258, 2007.

[CODG15] Symeon Chatzinotas, Bjorn Ottersten, and Riccardo De Gaudenzi. *Cooperative and Cognitive Satellite Systems*. Academic Press, 1st edition, 2015.

[FATS13] H. Fenech, Amos, Tomatis, and Soumpholphkakdy. Ka-sat and future hts systems. In *Vacuum Electronics Conference (IVEC), 2013 IEEE 14th International*, pages 1–2, May 2013.

[FS07] Christina Fragouli and Emina Soljanin. Network coding fundamentals. In *Foundations and Trends in Netowrking*, 2007.

[FTA+16] H. Fenech, A. Tomatis, S. Amos, V. Soumpholphakdy, and J. L. Serrano Merino. Eutelsat HTS systems. *Int. J. Satell. Commun. Network.*, pages n/a–n/a, 2016.

[FyLBW06] Christina Fragouli, Jean yves Le Boudec, and Jörg Widmer. Network coding: An instant primer. *ACM SIGCOMM Computer Communication Review*, 2006.

[HMK+06] Tracey Ho, M. Medard, R. Koetter, D.R. Karger, M. Effros, Jun Shi, and B. Leong. A random linear network coding approach to multicast. *Information Theory, IEEE Transactions on*, 52(10):4413–4430, Oct 2006.

[KETJ12] A. Kyrgiazos, B. Evans, P. Thompson, and N. Jeannin. Gateway diversity scheme for a future broadband satellite system. In *ASMS Conf. and SPSC Workshop*, pages 363–370, Sept 2012.

[KK06] Chung Ha Koh and Young Yong Kim. A proportional fair scheduling for multicast services in wireless cellular networks. In *IEEE VTC Fall*, pages 1–5, 2006.

[LVC10] J. Lei and M.A. Vazquez-Castro. Joint power and carrier allocation for the multibeam satellite downlink with individual SINR constraints. In *Communications (ICC), IEEE International Conference on*, pages 1–5, May 2010.

[LVC11] J. Lei and M.A. Vazquez-Castro. Multibeam satellite frequency/time duality study and capacity optimization. *Communications and Networks, Journal of*, 13(5):472–480, Oct 2011.

[MGdC14] M. Muhammad, G. Giambene, and T. de Cola. Channel prediction and network coding for smart gateway diversity in terabit satellite networks. In *Global Communications Conference (GLOBECOM), 2014 IEEE*, pages 3549–3554, Dec 2014.

[MMA13] Tomaso de Cola Matteo Berioli Muhammad Muhammad, Giovani Giambene and Nader Alagha. Network-coding-based gateway handover scheme for terabit satellite networks. In *31th AIAA International Communications Satellite Systems Conference*, 2013.

[PVC09a] D. Pradas and M. A. Vázquez-Castro. Cross-layer rate allocation of multicast transmission over hybrid DVB-SH. In *IWCLD*, pages 1–5, 2009.

[PVC09b] D. Pradas and M. A. Vázquez-Castro. Multicast transmission optimization over hybrid DVB-SH systems. In *IEEE VTC Spring*, pages 1–5, 2009.

[PVC11] D. Pradas and M. A. Vázquez-Castro. NUM-based fair rate-delay balancing for layered video multicasting over adaptive satellite networks. *IEEE J. Sel. Areas Commun.*, 29(5):969–978, 2011.

[SAEG09] A. Sali, G. Acar, B. Evans, and G. Giambene. A comparison of multicast adaptive techniques in reliable delivery over geo satellite networks. In *IEEE VTC Spring*, pages 1–5, 2009.

[SCH] scholar.google.com.

[SCI] http://www.scimagojr.com/.

[SCO14] Shree Krishna Sharma, Symeon Chatzinotas, and Björn Ottersten. Cognitive beamhopping for spectral coexistence of multibeam satellites. *Int. J. Satell. Commun. Network.*, pages 69–91, 2014.

[VB09] F. Vieira and J. Barros. Network coding multicast in satellite networks. In *Next Generation Internet Networks (NGI)*, pages 1–6, July 2009.

[VC13] M.A. Vazquez-Castro. Graph model and network coding gain of multibeam satellite communications. In *Communications (ICC), IEEE International Conference on*, pages 4293–4297, June 2013.

[VCA12] M.-A. Vazquez-Castro and N. Alagha. Multi-link reception multibeam satellite system model. In *ASMS Conf. and SPSC Workshop*, pages 132–138, Sept 2012.

[VCAAG11] M. A. Vázquez-Castro, Pimentel-Niño M. A., and R. Alegre-Godoy. *Tecnologías de la Información y las Comunicaciones para zonas rurales. Aplicación a la atención de salud en países en desarrollo*, chapter Las redes de telecomunicación basadas en satélite, pages 149–162. CYTED, 2011.

[VLA12a] F. Vieira, D.E. Lucani, and N. Alagha. Codes and balances: Multibeam satellite load balancing with coded packets. In *Communications (ICC), IEEE International Conference on*, pages 3316–3321, 2012.

[VLA12b] F. Vieira, D.E. Lucani, and N. Alagha. Load-aware soft-handovers for multibeam satellites: A network coding perspective. In *ASMS Conf. and SPSC Workshop*, pages 189–196, 2012.

[VSB10] F. Vieira, S. Shintre, and J. Barros. How feasible is network coding in current satellite systems? In *ASMA Conf. and SPSC Workshop*, pages 31–37, 2010.

[VVCSG06] F. Vieira, M. A. Vázquez Castro, and G. Seco Granados. A tunable-fairness cross-layer scheduler for dvb-s2. *International Journal of Satellite Communications and Networking*, 24(5):437–450, 2006.

[WSZL11] Shanshan Wang, Yalin E. Sagduyu, Junshan Zhang, and Jason H. Li. Spectrum shaping via network coding in cognitive radio networks. *IEEE INFOCOM*, pages 396–400, 2011.

[ZDL+13] Changliang Zheng, Eryk Dutkiewicz, Ren Ping Liu, Rein Vesilo, and Zheng Zhou. Efficient data transmission with random linear coding in multi-channel cognitive radio networks. *IEEE Wireless Communications and Networking Conference*, pages 77–82, 2013.

Part II

# JOURNAL PUBLICATIONS (MAIN ANNEX)

# A

# NETWORK CODED MULTICAST OVER MULTI-BEAM SATELLITE SYSTEMS

**R. Alegre Godoy and M. Á. Vázquez-Castro***

*Mathematical Problems in Engineering*, 2015

ABSTRACT

We propose a multicast scheme for multi-beam satellite systems exploiting both the multi-user and spatial diversity inherent in this type of systems while taking into account realistic physical distributions of User Terminals (UTs) over the coverage. Our proposed scheme makes use of the well known Adaptive Coding and Modulation (ACM) feature in Digital Video Broadcasting over satellite, 2nd Generation (DVB-S2) and Extension (DVB-S2X) standards but also incorporates a set of innovative features. First, multi-link reception, i.e. receivers that can syntonize different frequencies and/or polarizations, together with Network Coding (NC) is used to enable decoding of signals from adjacent beams (spatial diversity). Second, efficient and fair allocation of resources is achieved through Proportionally Fair Multicast (PFM) scheduling. Our results, obtained over realistic non-uniform UTs distributions, show average system multicast throughput gains up to 88% with regard to state of the art multicast schemes. Furthermore, a complete cross-layer architecture is proposed, fully compliant with the standard providing Quality of Service (QoS) guarantees.

## A.1 INTRODUCTION

Recent studies are showing an increasing demand for the efficient distribution of personalized contents in Internet based networks [2]. This has led to the deployment of satellite platforms delivering high throughputs (HTS systems) such as Ka-SAT [11] or constellations of communication satellites such

* The authors are with the department of Telecommunications and Systems Engineering, Universitat Autònoma de Barcelona.

as the O3b system [5]. Recent works even consider collocating two satellites covering the same region in order to cope with the user needs [7, 29]. Beyond the aforementioned satellite physical aspects, it is also possible to satisfy the user needs by improving the logical mechanisms delivering multimedia contents. Multicasting is one of the cornerstones for the effective dissemination and distribution of personalized multi-media contents in broadband networks and the focus of this paper. Applications such as audio/video streaming, online gaming, file distribution and file downloading are based on multicast-like transmissions.

In wireless networks, including multi-beam satellite networks, the main challenge when multicasting is how to address the heterogeneous channels conditions of the User Terminals (UTs), i.e. the presence of multi-user diversity. In clear-sky conditions the difference in Signal to Interference plus Noise Ration (SINR) between a UT located at the center of the beam and a UT located at the edge is typically 2-3dB. When Adaptive Coding and Modulation (ACM) is adopted at the physical layer as in Digital Video Broadcasting over Satellite-2nd generation (DVB-S2) [9] and DVB-S2 extension (DVB-S2X) [8] standards, this difference in SINR is translated into a spectral efficiency difference of 11%-25% [9, 32]. The differences in spectral efficiency can be much higher if we consider a beam partially affected by a rain event.

Traditional colouring schemes in multi-beam systems allow many opportunities for exploiting spatial diversity. A UT can potentially access to a number of orthogonal transmissions from the adjacent beams [32]. In that case UTs in the border of the beam would be more advantaged than those in the center of the beam. Since current UTs are syntonized at a single frequency, orthogonal transmissions are not exploited. A multi-link receiver, i.e. a receiver able to syntonize different frequencies and polarizations, could access and decode the signal meant for adjacent beams. As mentioned in [32] the design of this type of receivers is perfectly possible with the current technology. UTs distribution also plays a fundamental role. In real life users are not uniformly distributed but concentrated in specific areas such as cities. The concentration of terminals in specific areas of the coverage also affects the performance of cellular based systems [30, 25].

In this paper we take into account these three aspects, multi-user and spatial diversity and UTs distribution to design a multicasting scheme for the efficient delivery of broadband contents.

### A.1.1 *Related works on satellite multicast*

Multicast in multi-beam satellite systems has been little investigated from the scheduling and resources allocation point of view. The authors in [31] propose to choose a fixed Reed Solomon code and a fixed rate out of a set of possible rates in order to accomplish a certain degree of reliability. Following a similar approach to [31], works in [23, 22] propose to choose a modulation and codification (MODCOD) which ensures reception to a subset of the UTs in the multicast group. The rest could only decode with a certain probability. In

[28] a traditional approach is adopted and information is multicasted according to the channel conditions of the worst UT in the multicast group. With respect to these works our approach takes advantage of multi-user diversity in order to select in each time-slot the optimal MODCOD rather than assuming a fixed scheme. To the best of our knowledge, the authors in [24] provide the most similar approach to our work since the scheme they propose is based on ACM. In particular, authors propose a Network Utility Maximization (NUM) to trade delay and rate also accounting for Quality of Service (QoS) and multi-user diversity. With respect to this work we introduce the novelty of multi-link reception UTs together with Network Coding (NC) which enables decoding orthogonal transmissions.

Furthermore, our paper breaks the traditional approach of assuming uniform UTs distributions and provides results and analysis for non-uniform distributions which are close to reality.

### A.1.2 *Related works on NC for multi-beam satellite systems*

In the past few years a number of works have studied the implementation of NC in multi-beam satellite systems. In [36] an overview of possible satellite scenarios where NC can be applied is provided. For the particular case of multi-beam satellite systems, NC is proposed as a mechanism to reduce retransmissions. Works in [35, 34] take advantage of the orthogonal transmissions available using multi-link reception. However, the focus is on unicast transmissions and NC is used to provide enhanced reliability and flexibility rather than increasing the throughput. Our previous works in [3, 4] assessed the feasibility of using NC for multicasting in multi-beam satellite systems. As a result, it was identified that the multi-link reception approach together with NC coding could bring important benefits subject to the location of the UTs. These papers describe a preliminary concept and lack of a:

- Method to decide when to use the multi-link reception with NC feature.
- Scheduling policy selecting the optimal MODCOD for the multicast service.

### A.1.3 *Contributions of the paper*

This paper proposes a full multicasting scheme, i.e. scheduling policy, packet scheduling architecture and algorithm to decide if the multi-link reception with NC feature must be used or not. Our work presents the following novel results with respect to use of NC technology:

- A technique for the joint use of multi-link reception, NC and Proportionally Fair Multicast (PFM).

And the following novel results in the field of satellite multicasting:

- Introduce and adapt the PFM scheduling concept in [15]. More specifically, we provide MODCOD selection and use of the multi-link reception with NC feature when suitable.
- Its associated cross-layer packet scheduling architecture with respect to the Internet Engineering Task Force (IETF) differentiated services at IP level model (Diffserv).
- A scheme providing multicast throughput gains employing the same resources as a traditional multicast scheme demonstrated via analysis and simulations over theoretical and realistic non-uniform UTs distributions.

The rest of the paper is organized as follows: Section A.2 introduces the multi-beam satellite system model. Section A.3 describes the proposed multicast scheme. The packet scheduling architecture is introduced in Section A.4. Finally, Section A.5 provides numerical evaluation of the system performance and Section A.6 draws conclusions on the work done.

## A.2 SYSTEM MODEL

### A.2.1 *Multi-Beam Satellite System Model*

We assume a multi-beam and multi-gateway satellite system with $N_b$ beams, $P$ polarizations and frequency re-use factor $f_r$. The number of colours of the system is $N_c = Pf_r$. Forward link transmissions are based on DVB-S2/DVB-S2X with ACM. Each gateway (GW) is associated to a subset of the overall number of beams (or cluster). GWs receive channel state information (CSI) messages from the UTs through a feedback channel.

Let a GW of the system serve the subset of beams $\mathcal{C} = \{b_1, b_2, ..., b_{|\mathcal{C}|}\}$. Each beam $b_j \subset \mathcal{C}$ has assigned a number of UTs $u_j$ requesting the same multicast service. Let us derive the SINR for a UT $i$ in $b_j$, $1 \leq i \leq u_j$. First, let the number of co-channel beams of the overall system be $K = N_b/N_c$. Now, we define $\mathbf{H} \in \mathbb{C}^{K\times K}$ as the forward link channel matrix which can be decomposed as $\mathbf{H} = \mathbf{BG}$. Matrix $\mathbf{B} \in \mathbb{C}^{K\times K}$ accounts for the atmospheric, propagation, space and ground system effects and is defined as

$$\mathbf{B} = diag(\sqrt{\beta_1}, \sqrt{\beta_2}, ..., \sqrt{\beta_K}) \tag{1}$$

where $\beta_j = OBO_{HPA} L_{sat} L_{prop} G_{UT}$, being $OBO_{HPA}$ the output back-off of the satellite high power amplifier, $L_{sat}$ the satellite repeater losses, $L_{prop}$ the propagation losses and $G_{UT}$ the UT antenna gain. Matrix $\mathbf{G} \in \mathbb{C}^{K\times K}$ accounts for the square root of the satellite antennas gains towards the concrete position of the UT and is defined as

$$\mathbf{G} = \begin{pmatrix} \sqrt{g_{11}} & \cdots & \sqrt{g_{1K}} \\ \vdots & \ddots & \vdots \\ \sqrt{g_{K1}} & \cdots & \sqrt{g_{KK}} \end{pmatrix} \tag{2}$$

where $\sqrt{g_{vw}}$ stands for the square root of antenna gain for antenna $v$ towards the location of the UT at beam $w$. Therefore, each element $h_{vw} \in \mathbf{H}$ accounts for all the gains and losses from satellite antenna $v$ towards UT location at beam $w$. The received signal $y_{i,j}$ at UT $i \in b_j$ can be expressed as

$$y_{i,j}(x,y) = \sqrt{P_{sat}} h_{jj}(x,y) s_j + \sqrt{P_{sat}} \sum_{l \neq j} h_{lj}(x,y) s_l + n_i \tag{3}$$

where $P_{sat}$ is the satellite transmitted power, $n_i$ is the Gaussian noise (zero mean complex circular noise of variance $N_i$) and $s_j$ and $s_l$ are the transmitted and interfering symbols respectively. Assuming constant transmitting power the SINR can be extracted directly from Eq. (3) and is given by

$$\Gamma_{i,j}(x,y) = \frac{P_{sat}|h_{jj}(x,y)|^2}{P_{sat}\sum_{l \neq j}|h_{lj}|^2 + N_i} \tag{4}$$

Under the ACM specification of DVB-S2 and DVB-S2X, SINR values are mapped to spectral efficiencies (or equivalently MODCODs) as follows

$$\begin{aligned} \eta_{i,j} &= f_{DVB-S2}(\Gamma_{i,j}) \\ \eta_{i,j} &= f_{DVB-S2X}(\Gamma_{i,j}) \end{aligned} \tag{5}$$

where $\eta_{i,j}$ is the spectral efficiency for UT $i$ in $b_j$ and $f_{DVB-S2}$, $f_{DVB-S2X}$ are mapping functions that relate SINRs and spectral efficiencies for DVB-S2 and DVB-S2X standards respectively.

### A.2.2 *Multi-Link Reception System Model*

The work in [32] introduces and models multi-link multi-beam systems. Such systems assume the use of multi-link receivers, i.e. receivers which can syntonize different frequencies or polarizations to simultaneously decode orthogonal transmissions from adjacent beams.

The main concept is as follows. In a multi-beam system with $N_c$ colours, UTs can potentially decode up to $N_c$ transmissions, 1 transmission from the own beam and $N_c - 1$ transmissions from adjacent beams in orthogonal frequencies and/or polarizations. This effect is produced because the antenna gain of each spot-beam is so high, that even UTs outside of the beam observe values of SINR that lie within the range of available MODCODs and can decode the signal. To do so:

- UTs must have multi-link reception capabilities, e.g. a terminal with a single antenna, one Low Noise Block down-converter (LNB) and multiple reception chains to detect and decode different polarizations and bands.
- UTs must observe a value of SINR higher or equal than the one required to decode the MODCOD transmitted in the orthogonal beam. Conversely, the GW can lower the MODCOD transmitted in a beam to let a number of UTs outside of the beam decode the signal.

In our multicasting scheme we assume UTs can decode their own transmission and one out of the $N_c - 1$ orthogonal transmissions. More specifically, the transmission with strongest SINR or equivalently the transmission from the closest adjacent beam. This enables and extra path to reach each UT and the opportunity to exploit spatial diversity. Let subscript $a$ denote the adjacent beam whose signal intends to decode UT $i$ in $b_j$ and let $\Gamma^a_{i,j}(x,y)$ be the SINR observed from this adjacent beam. $\Gamma^a_{i,j}(x,y)$ is obtained particularizing Eq. (4) with beam $a$, i.e. substituting $h_{jj}$ with $h_{aj}$ and computing the interference power from the co-channel beams of $a$. The spectral efficiency achievable from such adjacent beam is denoted as $\eta^a_{i,j}$ and obtained particularizing Eq. (5) with $\Gamma^a_{i,j}(x,y)$.

Figure 1 shows the MODCODs achievable for different locations (in U/V coordinates [37]) within a beam of a 70-beam system. More specifically, the top plot shows, per each location, the adjacent beam providing better SINR (the location and the adjacent beam with strongest SINR are plotted in the same color, dashed lines separate the different areas). The mid and bottom plots show the achievable MODCODs from the own and determined adjacent beam transmissions respectively. It can be observed that any point of the beam can decode an orthogonal transmission and that locations close to the edge of the beam and in the beam overlapping areas can decode it with a high order MODCOD. Locations in the center of the beam could only decode signals employing low spectral efficiency MODCODs.

### A.2.3 *Network Coding Model*

In our multicast scheme UTs can simultaneously decode their own transmission and one orthogonal transmission. The objective of NC is to avoid receiving duplicated versions of the same packet and ease the scheduling at the GW side. Therefore, whenever our proposed scheme sends packets over two paths, those packets will be coded employing NC. We perform NC at the IP layer for the following reasons:

- Our objective is to increase the average multicast throughput in a single multicast service. IP allows to identify the content of the packets and classify them into different multicast services such that NC is performed in a intra-service manner. Working at lower layers would not allow this classification.
- IP headers can be easily modified to include the encoding coefficients necessary for decoding [14].

In particular we adopt Random Linear Network Coding (RLNC) due to its simplicity and capacity-achieving performance, although any other network code would be, in principle, applicable. The scheme generates a random linear coded packet from $N_p$ native packets as follows. Let $L$ denote the length in bits of a native IP packet. Then, the payload of each packet $p_t$ is split into blocks of $\epsilon$ bits. Let $d_{tk}$ denote the $k$-th block of $t$-th packet, with $1 \leq k \leq L/\epsilon$. Next, we

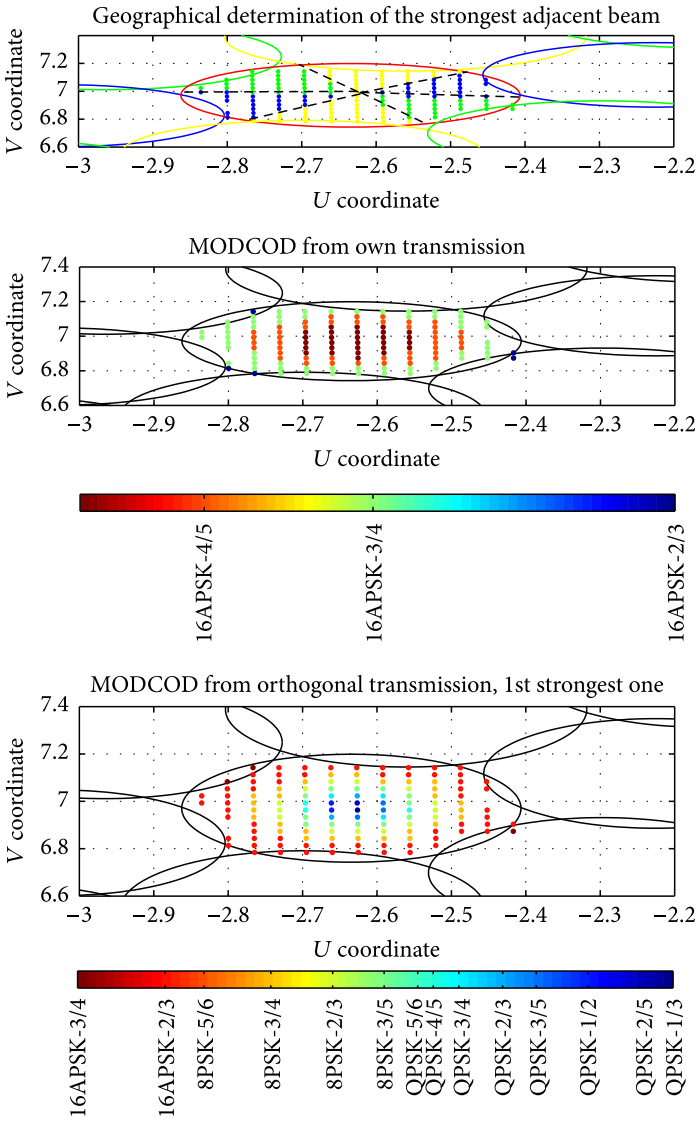


Figure 1: Example of achievable MODCODs for locations within a beam of interest. Results extracted from a 70 beam, 4 coloured system under DVB-S2.

choose $N_p$ random coefficients $c_t$ from $\mathbb{F}_q$, with $q = 2^\epsilon$ . The $k$-th coded block of a coded packet is given by

$$C_k = \sum_{t=1}^{N_p} c_t d_{tk},\ 1 \leq k \leq L/\epsilon \tag{6}$$

The encoding coefficients $c_1, ..., c_{N_p}$ are added in the header of the packet unless pseudo-random codes are used and then only the seed needs to be sent. In the receiver side, at least $N_p$ coded packets must be received to retrieve the original packets. The parameter $\epsilon$ is the size of the finite field and should be big enough to ensure that the probability of generating two linearly dependent (l.d.) coded packets is negligible. Section A.3 and A.4 introduce the specific parameters and architectural details necessary to perform RLNC.

### A.2.4 *User Terminals Distribution*

We employ the method in [20] to generate the non-uniform distributions of UTs. Specifically, we break the area of interest, i.e. the cluster of beams $\mathcal{C}$, in a number of bins $N_z$. Each bin $z$ is assigned a different probability $P_z$ of containing a UT according to a function $\phi_z$. In this case, $\phi_z$ is a function of the coordinates $x_z, y_z$ of the bin and given by a symmetrical 2-D truncated Gaussian function [30]

$$\phi_z(x_z, y_z) = \alpha \frac{\exp\left(-\alpha\left[(x_z - x_0)^2 + (y_z - y_0)^2\right]\right)}{\pi[1 - \exp(-\alpha R_0^2)]} \tag{7}$$

where $x_0, y_0$ is the UTs distribution center, $R_0$ is the radius and $\alpha$ is the location index. To express $\phi_z$ as a probability it must be normalized by the total sum of $\phi_z$ over all the $N_z$ bins considered

$$P_z(x_z, y_z) = \frac{\phi_z(x_z, y_z)}{\sum_{z=1}^{N_z} \phi_z(x_z, y_z)} \tag{8}$$

Then, we can model UTs distribution in a cluster $\mathcal{C}$ by the quadruple $(\alpha, R_0, x_0, y_0)$ and analyze average multicast throughput results varying these parameters. Negative values of $\alpha$ concentrate UTs towards the edge of the cluster whilst positive values of $\alpha$ concentrate UTs around $x_0, y_0$. $\alpha = 0$ provides a uniform distribution.

## A.3 MULTICAST PROPORTIONAL FAIRNESS FOR MULTI-BEAM SATELLITE SYSTEMS

Figure 2 shows a functional diagram of the proposed multicast scheme based on a cross-layer architecture. Novel blocks, at GW and UT side, are shadowed in green. We define multicast as the transmission of a data flow (or multicast service) from the GW to a number of UTs in the cluster $\mathcal{C}$ controlled by the GW. The UTs requesting the service are known as the multicast group. The scheme we propose applies to each multicast service individually (intra-service), hence explanations of the multicast policies assume a single multicast service. Scheduling is performed on a slot-by-slot basis, i.e. in the current slot we choose how packets are to be transmitted in the next slot. The scheme has been designed such that if follows the coherence time of the channel (i.e. time-windows in the scheduling are not required because the satellite channel for fixed UTs shows only medium/long term variations even under rain conditions).

On the GW side we introduce 3 novel blocks which carry out the Link Layer (LL) scheduling and substitute classical scheduling policies. Let us assume a system with ACM at the physical layer and let $M$ be the number of MODCODs of the system. We denote by $\eta^m$ the spectral efficiency of the $m$-th MODCOD, with $1 \leq m \leq M$. The bitrate provided by $\eta^m$ is given by

$$r^m = R_s \eta^m \tag{9}$$

where $R_s$ denotes the system symbol rate. The objective of LL scheduling, formed by the 3 green blocks, is two fold: 1) Choose the most appropriate transmission mode in each time-slot, i.e. decide whether the multi-link reception capabilities of the UTs have to be exploited or not. 2) Choose the appropriate value of spectral efficiency (i.e. MODCOD) for the next time-slot according to the transmission mode selected and the CSI reports received from the UTs in the current slot. This is equivalent to say the multicast policy is scheduling a certain number of UTs (those able to decode the selected MODCOD).

In particular:

- The block Proportionally Fair Multicast (PFM) computes per each beam of the cluster $\mathcal{C}$ (and per multicast service) which is the most suitable MODCOD according to the proportionally fair rule. Hence, it exploits multi-user diversity.
- The block PFM with NC (PFM-NC) computes for the entire cluster $\mathcal{C}$ a common MODCOD for all the beams of the cluster delivering that service. Data is sent network coded using RLNC and UTs use its multi-link reception capabilities to attempt decoding the signal from its own beam and its adjacent beam with higher SINR.
- The block combined PFM (C-PFM) selects the most appropriate transmission mode, PFM (non use of multi-link reception capabilities) or PFM-NC (use of multi-link reception capabilities) in each time-slot by computing the mode obtaining the highest multicast rate.
- The inputs required for the PFM, PFM-NC and C-PFM blocks are the MODCODs achievable by the UTs in base to their CSI feedback. The LL Resource Manager (LLRM) provides this information to these 3 blocks.

PFM, PFM-NC and C-PFM blocks are described in detail in subsections A.3.1, A.3.2 and A.3.3, respectively. The rest of the GW follows a traditional approach such that our proposed scheme can be implemented via software modifications with minimal intrusion. Incoming multicast traffic is classified per beam, per QoS following the IETF Diffserv model and per multicast service before forwarded to the LL schedulers. The specific packet scheduling architecture of the GW is described in detail in Section A.4.

The membership management of the multicast groups is supported by the Internet Group Management Protocol (IGMP) [13]. The LLRM collects information of the multicast groups available at the IGMP block and the CSI of the UTs. UTs not only send the CSI with respect to its own beam but also the CSI with respect to all its adjacent beams. The collaboration between the IGMP block and the LLRM provides the following information: 1) Which beams are involved in the transmission of a certain multicast service. 2) The number of UTs per beam and its SINR with respect to the own and adjacent beams. 3) Combining 1) and 2), identifying the orthogonal transmission with strongest SINR.

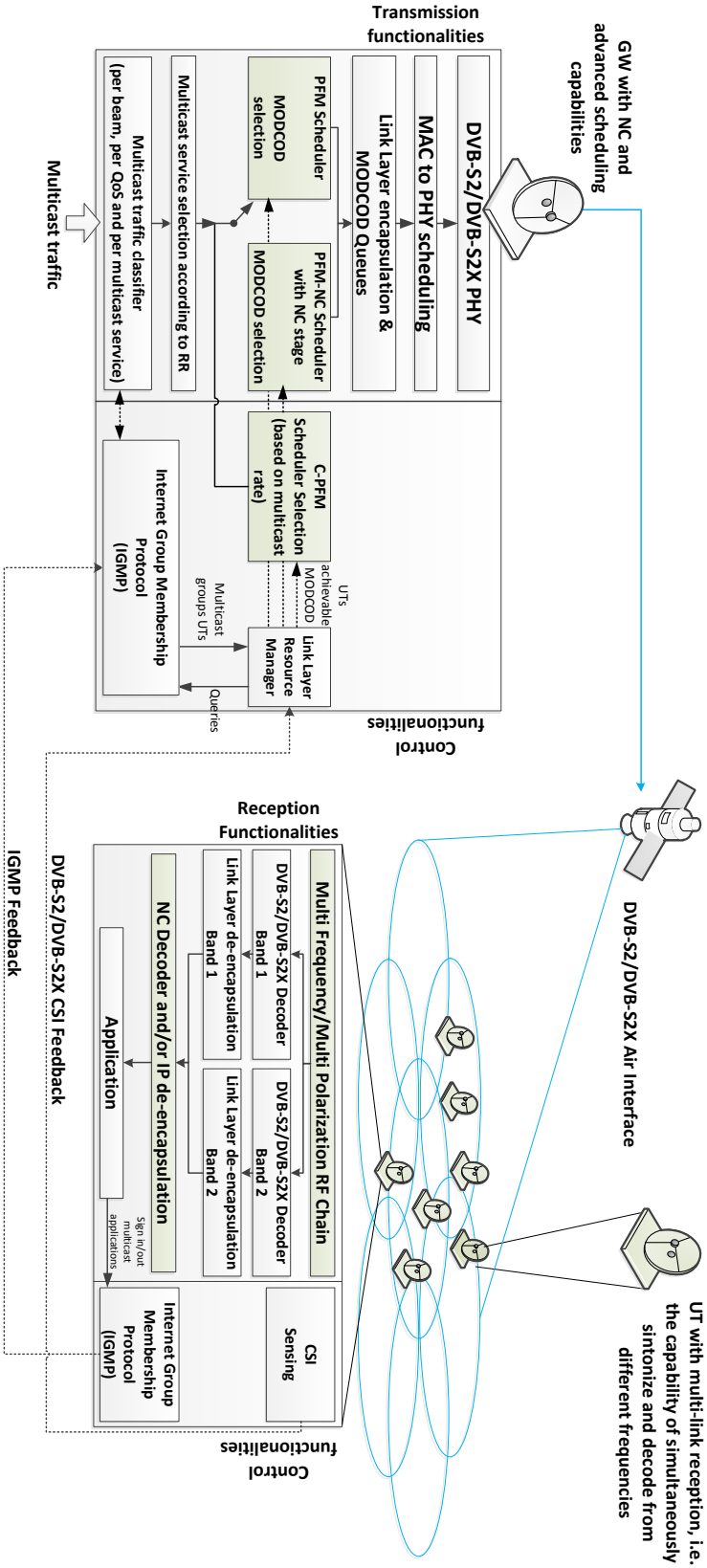


Figure 2: Functional diagram of the proposed multicast scheme based on a cross-layer architecture.

On the UT side, the RF chain must be able to syntonize two different bands (frequencies and/or polarizations) in order to obtain the packets from the own beam and from the strongest adjacent beam. Physical layer and link layer packets are de-encapsulated in both bands up to the IP layer. At the IP layer, the UT checks if packets are network coded by looking at the IP headers:

- If not, packets from the adjacent beam are discarded and the packets from the own beam are de-encapsulated as usual and forwarded to the upper layers.
- If yes, decoding of the network coded packets is performed before de-encapsulating and forwarding the packets to the upper layers.

Although this may appear as a complex receiver, the multi-link reception does only need a single antenna and a single LNB as explained in A.2.2. Even if multiple reception chains to detect and decode different bands are necessary, such kind of terminals already exist and are defined for instance in Digital Video Broadcasting Satellite to Handheld (DVB-SH) for mode B devices [10]. DVB-S2X also provides tools to implement transmission of a single stream through several physical satellite transponders and how to carry out its reception through several DVB-S2X decoders in the receiver (the so-called channel-bonding for multi-tune receivers [8]). With regard to the decoding of network coded packets, a number of works have successfully assessed the feasibility of the technology in broadband networks, see for instance [6, 21, 17].

### A.3.1 *Proportionally Fair Multicast (PFM)*

In this sub-section we introduce the PFM block in Figure 2. In a PF allocation UTs with better channel state are scheduled more often than UTs with worse channel states. To this aim the GW performs the scheduling in two steps. 1) Compute the optimal per-beam MODCOD for the next time-slot. 2) Update the scheduled rates of each UT according to the MODCOD selected in step 1 for the next iteration.

Step 1: The MODCOD chosen for the next time-slot at beam $b_j$ out of the $M$ available MODCODs is given by

$$m_j^{pf}(t+1) = \arg\max_m \left\{ \prod_{i|r_{i,j}(t) \geq R_s \eta^m} \left(1 + \frac{R_s \eta^m}{R_{i,j}(t)}\right) \right\} \quad \forall j \in [1, |\mathcal{C}|] \tag{10}$$

where $R_{i,j}(t)$ accumulates the scheduled rates of UT $i$ in $b_j$ and $r_{i,j}(t)$ is the achievable bitrate by UT $i$ in $b_j$ given by $r_{i,j}(t) = R_s \eta_{i,j}(t)$.

Step 2: Let $\mathcal{S}_j^{pf}(t+1)$ denote the set of UTs in $b_j$ which will be scheduled at $t+1$ and given by

$$\mathcal{S}_j^{pf}(t+1) = \left\{ i | r_{i,j}(t) \geq r^{m_j^{pf}}(t+1) \right\} \tag{11}$$

where $r^{m_j^{pf}}(t+1) = R_s \eta^{m_j^{pf}}(t+1)$ is the bitrate provided by spectral efficiency $\eta^{m_j^{pf}}(t+1)$ at beam $b_j$. Subsequently, $R_{i,j}$ is updated by

$$R_{i,j}(t+1) = \begin{cases} R_{i,j}(t) + r^{m_j^{pf}}(t+1) & , i \in S_j^{pf}(t+1) \\ R_{i,j}(t) & , elsewhere \end{cases} \tag{12}$$

The PFM scheme takes advantage of multi-user diversity because (10) selects the most appropriate MODCOD per time-slot according to the channel conditions across the UTs.

### A.3.2 *Proportionally Fair Multicast with Network Coding (PFM-NC)*

We now introduce the PF block employing NC (PFM-NC) in Figure 2 to take advantage of the extra path provided by orthogonal transmissions. To this aim, the GW considers the cluster as one entity with a number of UTs $U = \sum_{j=i}^{|\mathcal{C}|} u_j$ and performs the scheduling in 3 steps. 1) Select for each UT the orthogonal transmission with strongest SINR from which it will receive packets in addition to those sent through its own beam. 2) Compute the optimal MODCOD to use in the cluster for the next time-slot taking into account orthogonal transmissions. 3) Update the scheduled rates of each UT according to the MODCOD selected in step 2 for the next iteration.

Since UTs receive packets from two paths employing the same MODCOD, the min-cut/max-flow theorem states that up to 2 different packets can be received simultaneously. Due to the layout of the multi-beam network, the only way to ensure that all scheduled UTs will receive both packets is to send packets network coded. For instance, Figure 3a shows an example where one of the UTs would only receive one of the packets $p_1$, $p_2$ independently of the packets sent by each queue. Instead, if every queue generated a single coded packet all UTs would receive $p_1$ and $p_2$. Moreover, NC simplifies the scheduling because the system just transmits combined packets instead of looking at the topology of the network and decide which packets should be selected in each queue for transmission, e.g. Figure 3b shows that all UTs can obtain $p_1$ and $p_2$ but previous knowledge of the topology is necessary to decide which packet forwards each queue. Hence, under PFM-NC, the per-beam queues of a specific multicast service will generate a single coded packet from the same $N_p = 2$ native packets as explained in A.2.3. Then, all the UTs able to decode the chosen MODCOD will always get two different coded packets. Those UTs unable to decode orthogonal transmissions will get only one coded packet and will not be able to convey the original packets, i.e. they are considered as non scheduled UTs.

Step 1: Select for each UT an adjacent beam, i.e. the orthogonal transmission with strongest SINR, in order to decode simultaneously from two different paths. Such adjacent beam is chosen as follows. Let $\mathcal{A}_j = \{a_1, ..., a_{|\mathcal{A}_j|}\}$ be the set of adjacent beams to $b_j$ and let $\Gamma_{i,j}^{a_e}$ be the SINR of UT $i$ in $b_j$ with respect the adjacent beam $a_e$. UT $i$ in $b_j$ selects the adjacent beam $a$ such that

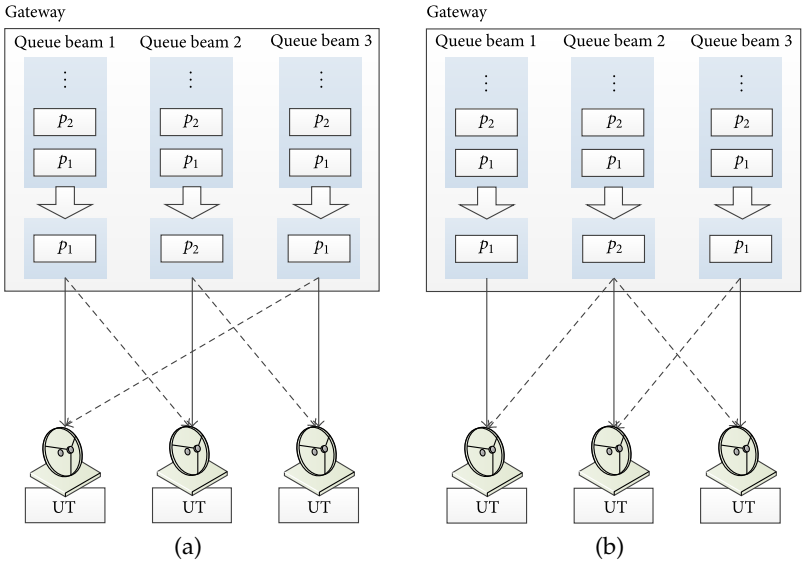


Figure 3: Two examples of inefficient multicasting from a GW transmitting uncoded packets to three UTs in three beams. Continuous and dashed arrows represent transmissions from the own and best best adjacent beam respectively.

$$e^* = \arg\max_{e} \left\{ \Gamma_{i,j}^{a_e} | a_e \in \mathcal{A}_j, a_e \in \mathcal{C}, u_e \neq 0 \right\} \tag{13}$$

The related spectral efficiency of $\Gamma_{i,j}^{a_{e^*}}$, $\eta_{i,j}^{a_{e^*}}$, is obtained from Eq. (5). The conditions in the argmax in Eq. (13) restrict the selection of $a_e$ to those adjacent beams that belong to $\mathcal{C}$ and have at least one UT subscribed to the multicast service. Note that this differentiates our scheme from load balancing techniques since we do not use sparing resources from an adjacent beam but we take advantage of the resources already in use in the adjacent beam. If none of the adjacent beams accomplish the conditions in Eq. (13) or the SINR from the chosen adjacent beam lies without the MODCOD range, then $\eta_{i,j}^{a_{e^*}} = 0$.

Step 2: The optimal MODCOD in the PFM-NC scheme is given by

$$m^{nc}(t+1) = \arg\max_{m} \left\{ \prod_{i | r_{i,j}^{a_{e^*}}(t) \geq R_s \eta^m} \left( 1 + \frac{2R_s \eta^m}{R_{i,j}(t)} \right) \right\} \tag{14}$$

where $r_{i,j}^{a_{e^*}}(t) = R_s \eta_{i,j}^{a_{e^*}}$. Thus, given a value of $R_s \eta^m$, the product in (14) takes into account only those UTs that can decode at such rate from the orthogonal transmission. Implicitly, this means the UT can support that rate from the own transmission and therefore the factor 2 in the numerator of Eq. (14).

Step 3: Let $S^{nc}(t+1)$ denote the set of UTs in $\mathcal{C}$ scheduled at $t+1$ and given by

$$S^{nc}(t+1) = \left\{ i | r_{i,j}^{a_{e^*}}(t) \geq r^{m^{nc}}(t+1) \right\} \tag{15}$$

where $r^{m^{nc}}(t+1) = R_s \eta^{m^{nc}}(t+1)$ is the bitrate provided by spectral efficiency $\eta^{m^{nc}}$ in the cluster $\mathcal{C}$. Subsequently, $R_{i,j}$ is updated by

$$R_{i,j}(t+1) = \begin{cases} R_{i,j}(t) + 2r^{m^{nc}}(t+1) & , i \in S^{nc}(t+1) \\ R_{i,j}(t) & , elsewhere \end{cases} \tag{16}$$

When a UT is scheduled, we take into account that receives information from two paths by adding a factor of 2 in the second term of the scheduled rates.

### A.3.3 *Combined PFM/PFM-NC (C-PFM)*

In the two previous sub-sections we have introduced the two blocks of Figure 2 based on the PF rule, PFM and PFM-NC. In short: 1) PFM exploits multi-user diversity. Under clear-sky conditions tends to favour UTs in the center of the beam. 2) PFM-NC exploits multi-user and spatial diversity. Under clear-sky conditions tends to favour UTs in the edge of the beam. Following, we introduce the control block to select the most appropriate scheme for transmitting in each time-slot, i.e the selection block named C-PFM. Let $f_j^{pf}(\eta^m)$ denote the product in Eq. (10) and $f^{nc}(\eta^m)$ denote the product in Eq. (14). $f_j^{pf}(\eta^m)$ and $f^{nc}(\eta^m)$ evaluate the average multicast rates at a given $\eta^m$ for the PFM and PFM-NC schemes respectively. Hence, at a given time-slot we compute $m_j^{pf}(t+1)$ and $m^{nc}(t+1)$ and evaluate the scheme providing better average multicast rate by comparing the outputs of $f_j^{pf}\left(\eta^{m_j^{pf}}(t+1)\right)$ and $f^{nc}\left(\eta^{m^{nc}}(t+1)\right)$. Since the latter takes into account all the UTs in the cluster, we perform the comparison with the product of all $f_j^{pf}\left(\eta^{m_j^{pf}}(t+1)\right)$. Then, scheduled rates must be updated according to the scheme selected using Eq. (12) or Eq. (16). Algorithm in Table 1 shows the C-PFM multicasting scheme we propose.

## A.4 PACKET SCHEDULING ARCHITECTURE

In this section we describe the packet scheduling architecture for the proposed multicast scheme. Although our work focuses on how to improve the average multicast throughput of a single multicast service, we show how our scheme integrates with an architecture offering more services. We build upon the architecture provided in [33] for unicast transmissions and optimize it for multicast transmissions. Our scheme requires modifications only at the LL level of the scheduler and can be implemented by modifying the software/firmware of the GW. As in [33], QoS between the different multicast services is achieved adopting the IETF Diffserv model at IP level which is a well-known and prevailing satellite QoS provision model [27, 18]. Specifically 3 Classes of Service (CoS) are defined: Expedited Forward (EF) for premium class services, Assured Forward (AF) for less constrained traffic and Best Effort (BE) for services with very low or without QoS. Figure 4 shows the proposed packet scheduling ar-

Table 1: C-PFM

1: At time-slot $t$ obtain $m_j^{pf}(t+1)\ \forall j$ and $m^{nc}(t+1)$ based on Eq. (10) and Eq. (14) respectively.
2: Compute $f_j^{pf}\left(\eta^{m_j^{pf}}(t+1)\right)\ \forall j$ and $f^{nc}\left(\eta^{m^{nc}}(t+1)\right)$.
3: **if** $\prod_{j=1}^{|\mathcal{C}|} f_j^{pf}\left(\eta^{m_j^{pf}}(t+1)\right) \geq f^{nc}\left(\eta^{m^{nc}}(t+1)\right)$ **then**
4: Transmit in PFM mode with MODCOD $m_j^{pf}(t+1)\ \forall j$
5: Update rates according to Eq. (12)
6: **else**
7: Transmit in PFM-NC mode at MODCOD $m^{nc}(t+1)$
8: Update rates according to Eq. (16)
9: **end if**
10: Next time slot

chitecture for the EF CoS. The structure would be analogous for the AF and BE CoS. The cross-layer control functionalities introduced in Section A.3 (see Figure 2) are not shown in the figure to ease the understanding.

Let us assume the GW of cluster $C$ transmits $\sigma_{EF}$, $\sigma_{AF}$ and $\sigma_{BE}$ multicast services per EF, AF and BE CoS respectively. First of all, incoming multicast traffic is classified per beam, per QoS and per multicast service resulting in a number of IP queues $\sigma_{EF}$, $\sigma_{AF}$ and $\sigma_{BE}$ per CoS. After that, per each CoS, a coordinated Round Robin (RR) stage pulls packets from a specific service within each CoS. Without loss of generality, let us assume packets from EF CoS service 1 are pulled. At this point, C-PFM computes, from the UTs achievable MODCODs, which is the optimal transmission mode according to algorithm in Table 1:

- If PFM is selected, the optimal MODCOD per each beam of the cluster $\mathcal{C}$ is computed according to Eq. (10). Then, per each beam area a packet from service 1 is pulled, encapsulated using Generic Stream Encapsulation (GSE) or Multi Protocol Encapsulation (MPE) and forwarded to the appropriate MODCOD queue.
- If PFM-NC is selected, for the entire cluster $\mathcal{C}$ a single optimal MODCOD is computed according to Eq. (14). Now, per each beam area two packets from service 1 are pulled and coded into a single packet using RLNC. This packet is encapsulated using GSE or MPE and forwarded to the appropriate MODCOD queue.

GSE/MPE packets are buffered in the MODCOD queues. The Tuneable Fairness Weighted Round Robin (TF-WRR) scheduler in [33] is substituted by a simple First Come First Service (FCFS) packet selector. Whilst the TF-WRR in [33] allows unicast sessions within a CoS to be fairly treated, this concept

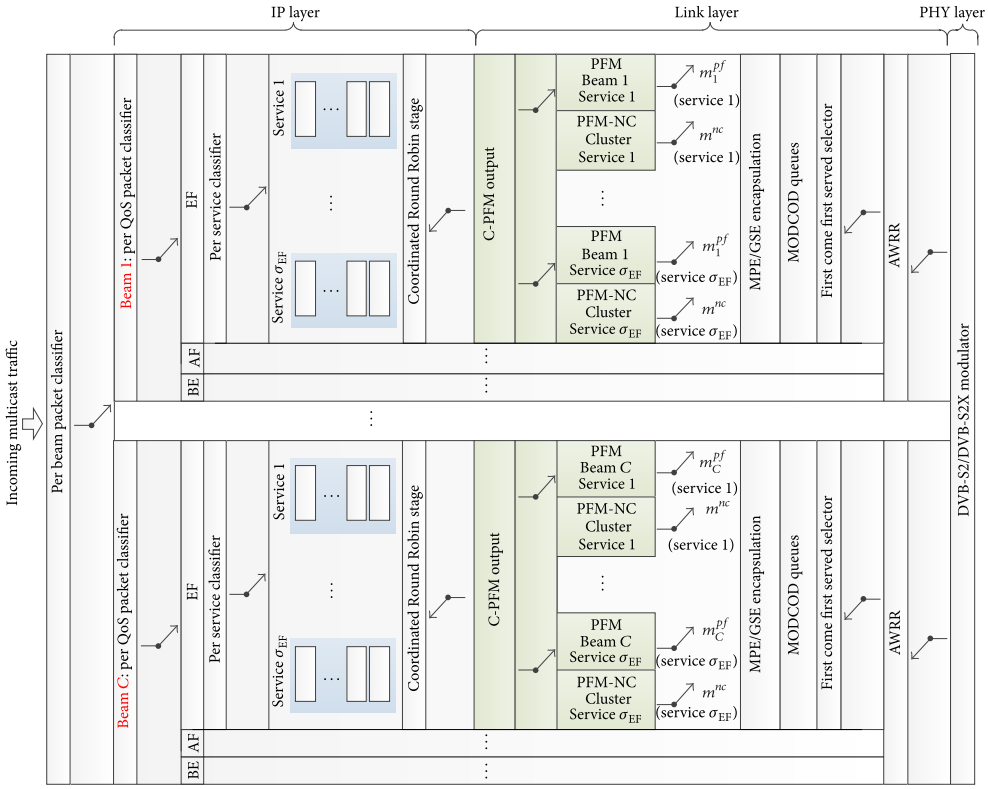


Figure 4: Proposed packet scheduling architecture according to IETF Diffserv model at IP level.

is already provided for each multicast session by our combination of PFM, PFM-NC and C-PFM blocks. In the last stage before the DVB-S2/DVB-S2X modulator, the Adaptive Weighted Round Robin (AWRR) scheduler provides the QoS guarantees among the different CoS.

## A.5 SIMULATION RESULTS

In order to show results for the proposed scheme, we focus on clusters of 6/7 beams under the control of a single GW within a system of the characteristics of Table 2. Note that this is a feasible approach since HTS systems require of several GW feeder links in order to provide UTs with the required throughputs for broadband and multimedia applications [12, 16]. The UTs distributions in the cluster are generated as detailed in subsection A.2.4 and for realistic case in Spain. The main figure of merit we analyze is the average system multicast throughput defined as the time average bitrate-sum offered to the UTs. Since our scheme applies to multicast services individually, and with the purpose of not masking the actual results of the proposed scheme, we focus on the performance of a single multicast performance. The performance of our proposed scheme is compared to the Worst Case Multicast (WCM) scheme [28] and compared to a scheme with only the PFM implementation (subsection A.3.1) such that the improvements of the multi-link reception with NC can be easily observed. In the following subsections, we justify the use of DVB-S2X for our

Table 2: System characteristics.

| Parameter | Value |
|---|---|
| $N_b$ | 70 |
| $N_c$ | 4 |
| Frequency | 19.95GHz |
| System symbol rate | 180Mbauds |
| PHY protocol | DVB-S2X |
| LL protocol | GSE |
| Network layer protocol | IP |
| IP packets size | 1344 Bytes |
| NC overhead | 10 Bytes |
| Number of services | 1 |

particular scheme, provide simulation results for clear-sky and rainy conditions and give practical insights on how to provide a Service Level Agreement (SLA) for UTs that are not so frequently scheduled.

### A.5.1 *DVB-S2 vs DVB-S2X*

In Figure 1 we have shown, per each location within a beam, the achievable MODCODs when decoding signals from the own and from the adjacent beam providing better SINR for a DVB-S2 based system. Figure 5 shows the equivalent information for a DVB-S2X based system. It can be observed that at the same locations the UTs under DVB-S2X can be assigned MODCODs with higher spectral efficiencies (a combination of higher modulation order and higher code-rate) from the own and adjacent beam providing better SINR and hence an improved throughput can be delivered.

Moreover, DVB-S2X incorporates natively the afore-mentioned channel-bonding tool for multi-tune receivers to split and uplink a single stream into several satellite transponders (i.e. different beams) and to receive it with a DVB-S2X receiver implementing several physical layers. Hence, DVB-S2X seems a more appropriate standard to support our scheme.

### A.5.2 *Clear-sky conditions*

Figure 6 and Figure 7 show the average multicast throughput for 6 relevant UTs distributions, generated as in subsection A.2.4, for a cluster $\mathcal{C}$ of 7 beams.

When UTs tend to be distributed over a large area, as in Figure 6, the proposed C-PFM scheme can achieve gains in average system multicast throughput up to the 27%. Such advantage is obtained when most of the UTs are located in, or around, the overlapping area of the beam because the scheme enables the transmission with multi-link reception and NC. Note that the PFM scheme, which does not incorporate multi-link reception, attains a sim-

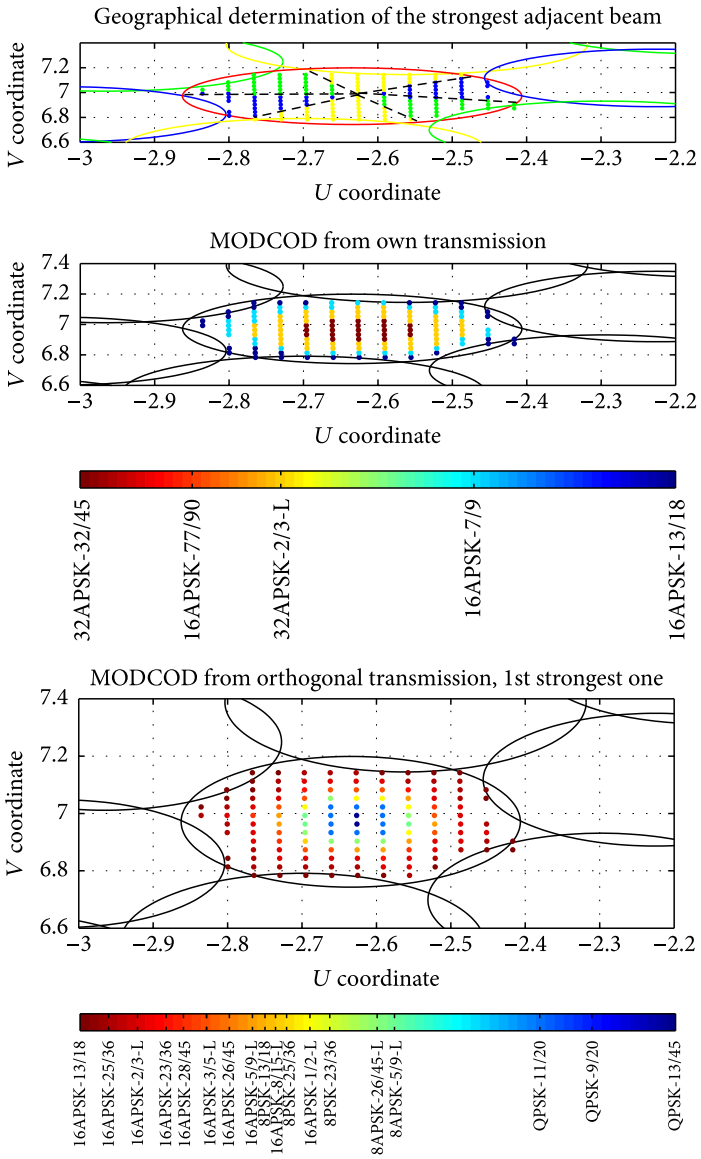


Figure 5: Example of achievable MODCODs for locations within a beam of interest. Results extracted from a 70 beam, 4 coloured system under DVB-S2X.

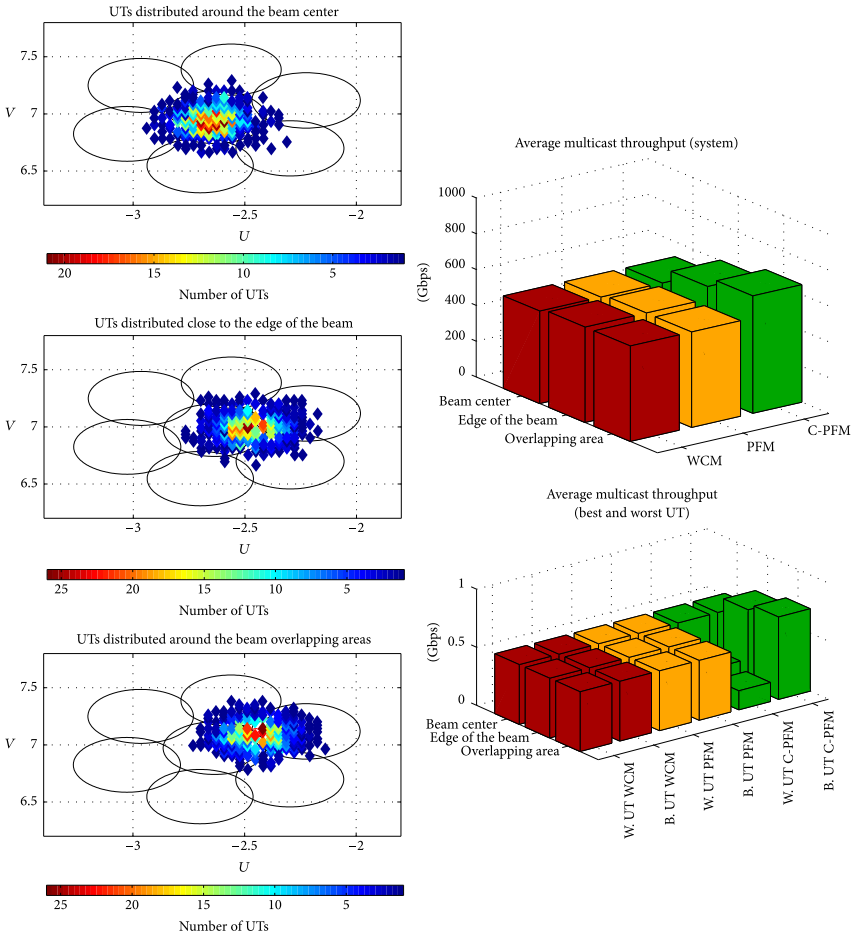


Figure 6: Average multicast throughput for 3 UTs distribution within a cluster of beams. $\alpha = 50, R_0 = R_C, x_0, y_0$ ={beam center, close to the edge, overlapping area}.

ilar throughput to the WCM scheme. As most of the UTs tend to be located further from the overlapping area, i.e. close to the beam edge or in the beam center, the gain obtained decreases to 16% and 3% respectively. This is mainly produced because the multi-link reception capability with NC is not activated that often since it is not favourable to the UTs located in the center of the beam. Even if some MODCOD balancing is achieved due to the PF rule, it is not high enough to provide significant average system multicast throughput gains.

When UTs are concentrated in smaller areas, as Figure 7 shows, the gains tend to be larger. If the UTs are located in the beam overlapping area the gain in average system multicast throughput is 88% and it gradually decreases to 64% and 5% when UTs are highly concentrated close to the edge of the beam or in the beam center respectively. Ideally, if all the UTs where located in the the beam overlapping area (e.g. in a regional satellite broadcast for a city) a 100% throughput gain could be achieved, except for the 10 bytes overhead introduced when including the encoding coefficients in the network coded IP packets.

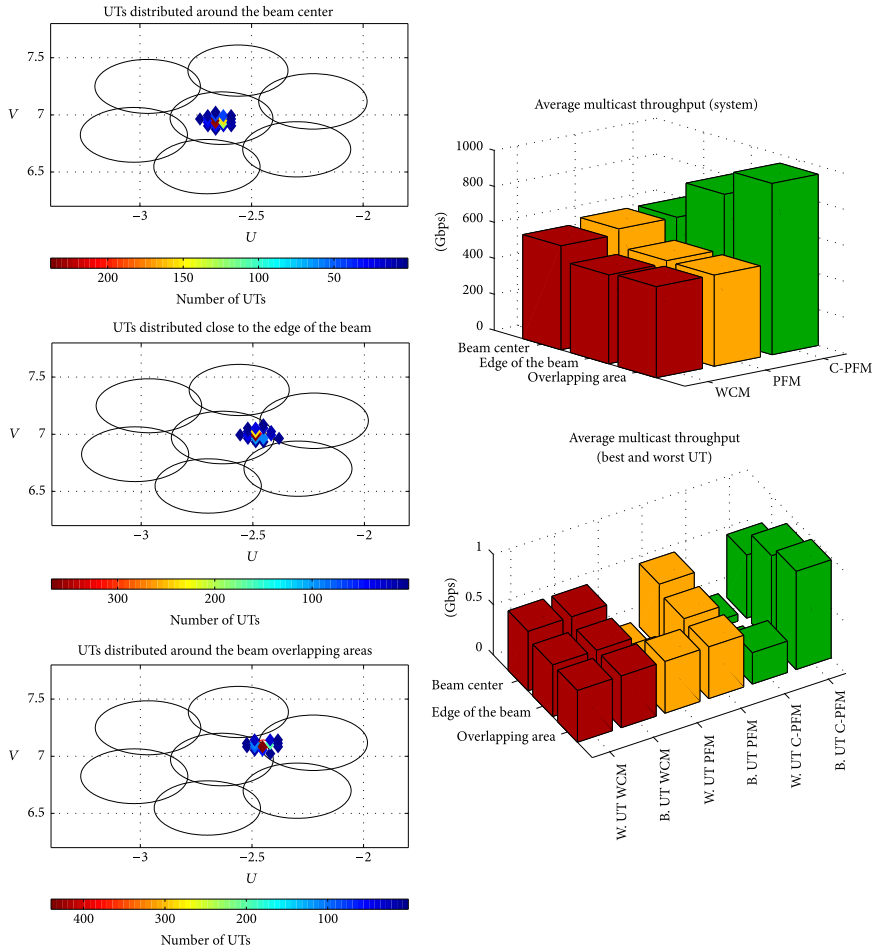


Figure 7: Average multicast throughput for 3 UTs distribution within a cluster of beams. $\alpha = 1000, R_0 = R_C, x_0, y_0$ ={beam center, close to the edge, overlapping area}.

Hence, the proposed C-PFM scheme provides higher gains when UTs are located in the beam overlapping area or close to the edge of the beam concentrated in small (64%-88%) or large areas (16%-27%). When UTs are located in the center of the beam the gain is marginal (3%-5%). Moreover, this gain is achieved without employing additional resources, by just enabling UTs accessing orthogonal transmissions already in place.

### A.5.3 *Service Level Agreement*

The proposed C-PFM scheme optimizes the average multicast throughput of the system according to the PF rule but it does not guarantee a minimum throughput to each individual UT. This side effect of the PF rule is reflected in the right bottom plot of Figure 7 where the worst UT is assigned a negligible throughput, i.e. an SLA is not guaranteed to the UT. Many multicast applications are based on the delivery of video and audio such as video streaming, audio streaming or online gaming. The SLA guarantees that a minimum amount of data is delivered to the UT such these services are delivered

properly in a similar way traditional Digital Subscriber Line (DSL) operators guarantee a minimum connection quality to users in disfavoured areas while users in better areas get better connection quality.

The results in Figure 8 consider a GW providing multicast services to Spain. The number of UTs subscribed to the multicast service is proportional to the number of inhabitants of the 5 largest Spanish metropolitan areas [1]. We consider a minimum SLA with the UT equivalent to a half of the throughput achieved with the highest common achievable MODCOD from the own beam (see top plot of Figure 5), i.e. in average each UT should be scheduled once every 2 slots with such MODCOD. As it can be observed in the right bottom plot of Figure 8, without an SLA mechanism such reference level is not reached (the blue bars mark the minimum throughput per UT and the worst UT under the C-PFM scheme does not overcome it). A simple mechanism to provide a minimum SLA consists in periodically introducing slots with a MODCOD decodable by all the UTs in the cluster. In particular, the throughput assigned to the worst UT is averaged for a past number of slots and in case it does not reach the proposed level a MODCOD decodable by such UT is imposed. As it can be observed, now the worst UT is guaranteed the SLA but the average multicast throughput of the cluster has been affected since at certain slots the optimal MODCODs are not scheduled. In the case under study, the provision of SLA has reduced the average system multicast throughput gain compared to WCM from 32% to 21.5%.

The fact that each transmission is decodable by a different number of UTs due to the use of ACM should not affect to the proper delivery of multicast services proved that proper techniques are employed at the application layer. For audio and video streaming and online gaming Scalable Video Coding (SVC) [19] and Scalable Audio Coding (SAC) [26] techniques can be used. For instance, Figure 9 shows the spectral efficiency of the scheduled MODCODs when the SLA is guaranteed. When the MODCOD decodable by all the UTs is transmitted a video/audio base layer (BL) could be send such that all the UTs retrieve it. When MODCODs decodable only by a subset of the UTs are transmitted different levels of video/audio enhancement layers (ELs) can be sent.

For other multicast applications like file distribution and downloading which are less time sensitive, UTs able to decode all the MODCODs would retrieve the files faster and then abandon the multicast group. Then, the scheme would adapt the transmitted MODCODs according to this new set of UTs which could complete the download of the file a little later in time.

### A.5.4 *Rain Conditions*

Finally, we show that our scheme is also advantageous under rainy conditions while it is capable to maintain the SLA guarantee to the UT. To this aim we assume that the south east coast of Spain within the dotted ellipse in the left bottom plot of Figure 8 is under a rain event. Such event produces a 5dB attenuation. As it can be observed in the right bottom plot of Figure 8, the

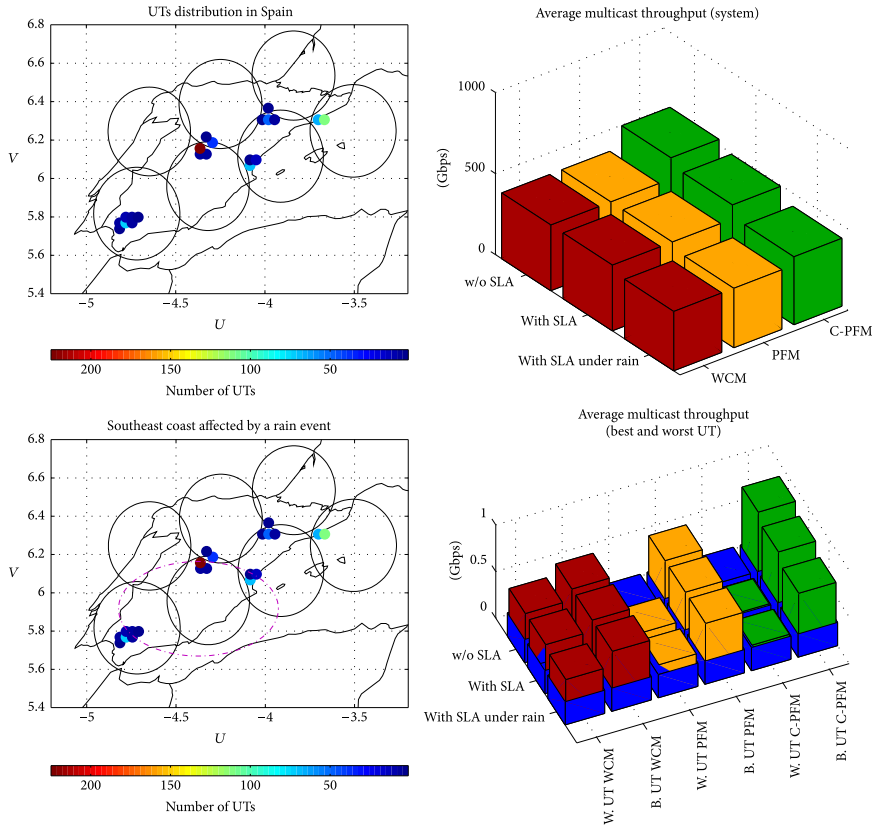


Figure 8: Average multicast throughput for a realistic UTs distribution in Spain.

C-PFM scheme still maintains a 15% gain in average multicast throughput compared to the WCM scheme while keeping the proposed SLA.

## A.6 CONCLUSIONS

In this paper we have proposed a full multicasting scheme for multi-beam satellite systems. Our scheme makes use of the ACM feature of DVB-S2 and DVB-S2X standards by employing a PF scheduling policy and opportunistically enables UTs, assumed to have multi-link reception capabilities and a NC decoder, to retrieve information from the adjacent beam providing better SINR. In particular, we have introduced the functional architecture logic in the GW, based on a cross-layer design, and UT side. We have also detailed the algorithms employed in the novel blocks in the GW and we have designed the packet scheduling architecture respecting the IETF Diffserv model at the IP level.

From the complexity point of view, the practical introduction of our scheme requires modifications at both the GW and the UT. While modifications in the GW can be implemented via software upgrades, the satellite UT requires further modifications. The RF chain must be able to syntonize two different bands in order to receive from the own and adjacent beam. Also, two separate decoding/de-encapsulating chains are necessary up to the IP level. Finally, the UTs need a NC decoder. Although these elements may build-up an apparent

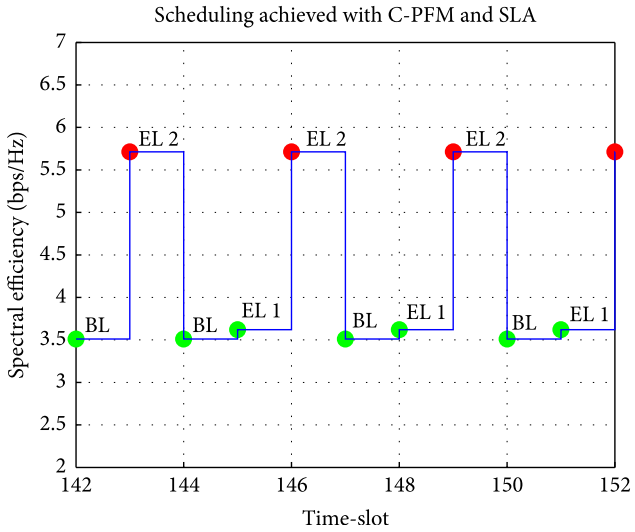


Figure 9: Spectral efficiency transmitted in each time-slot in the C-PFM scheme the for UTs distribution in Spain and considering a minimum SLA. Green dots signal time-slots where the multi-link with NC capability is not enabled. Red dots signal time-slots where the multi-link with NC capability is enabled.

complex receiver we have demonstrated that the standards and technology for its implementation are already in place.

From the results point of view, the average system multicast throughput gain provided by our scheme highly depends on the UTs distribution. With the aim of providing fair and realistic results, our simulations have been carried out over non-uniform theoretical and realistic distributions within clusters of few beams where transmissions employ the recently appeared DVB-S2X standard. The results obtained show the following. When the UTs tend to be located in the centers of the beams, the gain provided by our scheme is marginal, i.e. below 5%. However, when most of the UTs are located close to the edge of a beam or in the overlapping areas with another beam, even if the UTs spread over a large area of the cluster, the gain provided by our scheme can reach the 88%. This gain is mainly enabled by the multi-link reception and NC.

Moreover, a simple SLA mechanism has been introduced and simulated such that a minimum service is guaranteed to the UT while still providing significant gains (21%) even under rain conditions (15%). In addition, we have suggested, for some relevant multicast applications, proper techniques at the upper layers to deal with the different amounts of data delivered to each UT. Finally, the gains achieved by our scheme do not require the use of additional resources but only enabling UTs accessing orthogonal transmissions already in use by UTs in other beams.

As future line of research we would like to investigate and analyze the performance of the proposed scheme in a mobile environment where the election of a suitable modulation and codification becomes more challenging since UTs are subject to fast channel variations. Moreover, our intra-service policy could

be combined with inter-service policies in order to meet the different requirements demanded by multicast services.

## CONFLICT OF INTERESTS

The authors declare that there is no conflict of interests regarding the publication of this paper.

## REFERENCES

[1] Centro Nacional de Información Geográfica (CNIG). available at http://www.cnig.es/.

[2] B. Ahlgren, C. Dannewitz, C. Imbrenda, D. Kutscher, and B. Ohlman. A survey of information-centric networking. *IEEE Commun. Magazine*, 50(7):26–36, 2012.

[3] R. Alegre-Godoy, N. Alagha, and M. A. Vázquez-Castro. Offered capacity optimization mechanisms for multi-beam satellite systems. In *Communications (ICC), IEEE International Conference on*, pages 3180–3184, 2012.

[4] R. Alegre-Godoy, S. Gheorghiu, N. Alagha, and M. A. Vázquez-Castro. Multicasting optimization methods for multi-beam satellite systems using network coding. In *29th AIAA International Communications Satellite Systems Conference*, 2011.

[5] S.H. Blumenthal. Medium earth orbit ka band satellite communications system. In *Military Communications Conference (MILCOM), IEEE*, pages 273–277, 2013.

[6] N. Capela and S. Sargento. Optimizing network performance with multihoming and network coding. In *Globecom Workshops (GC Wkshps), IEEE*, pages 210–215, 2012.

[7] D. Christopoulos, S. Chatzinotas, and B. Ottersten. User scheduling for coordinated dual satellite systems with linear precoding. In *Communications (ICC), IEEE International Conference on*, pages 4498–4503, June 2013.

[8] DVB Document A83-2. *Digital Video Broadcasting (DVB); Second generation framing structure, channel coding and modulation systems for Broadcasting, Interactive Services, News Gathering and other broadband satellite applications. Part II: S2-Extensions (DVB-S2X) - (Optional)*. 2014.

[9] ETSI: EN 302 307. *Digital Video Broadcasting (DVB); Second generation framing structure, channel coding and modulation systems for Broadcasting, Interactive Services, News Gathering and other broadband satellite applications (DVB-S2)*. 2009.

[10] ETSI TS 102 585 V1.2.1 (2011-09). *Digital Video Broadcasting (DVB); System Specifications for Satellite services to Handheld devices (SH) below 3 GHz*. 2011.

[11] H. Fenech, Amos, Tomatis, and Soumpholphkakdy. Ka-sat and future hts systems. In *Vacuum Electronics Conference (IVEC), IEEE International*, pages 1–2, 2013.

[12] Mysore R. R. B. Arapoglou P. Gharanjik, A. and B. Ottersten. Multiple gateway transmit diversity in q/v band feeder links. *Communications, IEEE Transactions on*, PP(99):1–11, 2014.

[13] B. Cain H. Holbrook and B. Haberman. *Using Internet Group Management Protocol Version 3 (IGMPv3) and Multicast Listener Discovery Protocol Version 2 (MLDv2) for Source-Specific Multicast*. RFC 4604, 2006.

[14] Zheng Huang, Xunrui Yin, Xin Wang, Jin Zhao, and Xiangyang Xue. CODED IP: On the feasibility of IP-layer network coding. In *ICCCN*, pages 1–6, 2008.

[15] Chung Ha Koh and Young Yong Kim. A proportional fair scheduling for multicast services in wireless cellular networks. In *IEEE VTC Fall*, pages 1–5, 2006.

[16] A. Kyrgiazos and B. Evans. Gateway diversity for q/v feeder links: Requirements, characteristics, and challenges. In *ASMS Conf. and SPSC Workshop*, pages 323–330, 2014.

[17] S. Lee and W. W. Ro. Accelerated network coding with dynamic stream decomposition on graphics processing unit. *The Comp. J.*, 55(1):21–34, 2010.

[18] Heyu Liu and Fuchun Sun. A QoS-Oriented Congestion Control Mechanism for Satellite Networks. *Mathematical Problems in Engineering*, 2014:1–13, 2014.

[19] F.A. Mogus. Performance comparison of multiple description coding and scalable video coding. In *Communication Software and Networks (ICCSN), IEEE International Conference on*, pages 452–456, 2011.

[20] M. Newton and J. Thompson. Classification and generation of non-uniform user distributions for cellular multi-hop networks. In *Communications (ICC), IEEE International Conference on*, volume 10, pages 4549–4553, 2006.

[21] A Paramanathan, M.V. Pedersen, D.E. Lucani, F.H.P. Fitzek, and M. Katz. Lean and mean: network coding for commercial devices. *Wireless Communications, IEEE*, 20(5):54–61, 2013.

[22] D. Pradas and M. A. Vázquez-Castro. Cross-layer rate allocation of multicast transmission over hybrid DVB-SH. In *IWCLD*, pages 1–5, 2009.

[23] D. Pradas and M. A. Vázquez-Castro. Multicast transmission optimization over hybrid DVB-SH systems. In *IEEE VTC Spring*, pages 1–5, 2009.

[24] D. Pradas and M. A. Vázquez-Castro. NUM-based fair rate-delay balancing for layered video multicasting over adaptive satellite networks. *IEEE J. Sel. Areas Commun.*, 29(5):969–978, 2011.

[25] Cen Qian, Sihai Zhang, and Wuyang Zhou. Traffic-based dynamic beam coverage adjustment in satellite mobile communication. In *Wireless Communications and Signal Processing (WCSP), International Conference on*, pages 1–6, 2014.

[26] E. Ravelli, V. Melkote, T. Nanjundaswamy, and K. Rose. Joint optimization of the perceptual core and lossless compression layers in scalable audio coding. In *Acoustics Speech and Signal Processing (ICASSP), IEEE International Conference on*, pages 365–368, 2010.

[27] Elizabeth Rendon-Morales, Jorge Mata-Díaz, Juanjo Alins, Jose L. Muñoz, and Oscar Esparza. Cross-layer packet scheduler for qos support over digital video broadcasting-second generation broadband satellite systems. *Int. J. of Commun. Syst.*, 27(10):2063–2082, 2014.

[28] A. Sali, G. Acar, B. Evans, and G. Giambene. A comparison of multicast adaptive techniques in reliable delivery over geo satellite networks. In *IEEE VTC Spring*, pages 1–5, 2009.

[29] Shree Krishna Sharma, Symeon Chatzinotas, and Bjorn Ottersten. Cognitive beamhopping for spectral coexistence of multibeam satellites. *Int. J. Satell. Commun. Network.*, pages 69–91, 2014.

[30] Xue Tang and Hongwen Yang. Effect of user distribution on the capacity of cellular networks. In *National Conf. on Inf. Tech. and Computer Science*, pages 370–373, 2012.

[31] A. Tunpan and M.S. Corson. Bulk data multicast rate scheduling for hybrid heterogeneous satellite-terrestrial networks. In *IEEE ISCC*, pages 238–244, 2000.

[32] M. A. Vázquez-Castro and N. Alagha. Multi-link reception multibeam satellite system model. In *ASMS Conf. and SPSC Workshop*, pages 132–138, 2012.

[33] M. A. Vázquez-Castro and F. Vieira. DVB-S2 full cross-layer design for QoS provision. *IEEE Commun. Magazine*, 50(1):128–135, 2012.

[34] F. Vieira, D.E. Lucani, and N. Alagha. Codes and balances: Multibeam satellite load balancing with coded packets. In *Communications (ICC), IEEE International Conference on*, pages 3316–3321, 2012.

[35] F. Vieira, D.E. Lucani, and N. Alagha. Load-aware soft-handovers for multibeam satellites: A network coding perspective. In *ASMS Conf. and SPSC Workshop*, pages 189–196, 2012.

[36] F. Vieira, S. Shintre, and J. Barros. How feasible is network coding in current satellite systems? In *ASMA Conf. ans SPSC Workshop*, pages 31–37, 2010.

[37] D.D. Opiedun W.L. Cook and L.R. Karl. Generation and display of satellite antenna patterns. *Comsat Technical Review*, 19(2):259–297, 1989.

# B

# SPATIAL DIVERSITY WITH NETWORK CODING FOR ON/OFF SATELLITE CHANNELS

**R. Alegre Godoy and M. Á. Vázquez-Castro***

*IEEE Comm. Letters*, 17(8), pages 1612-1615, 2013

ABSTRACT

In this letter, we investigate the advantages of network coding (NC) combined with spatial diversity (SD) in scenarios with multiple sources, a single satellite and a single receiver. Each link source - satellite is modeled as an ON/OFF channel. We show that our system matches a wide number of realistic scenarios, from Wireless Sensor Networks (WSN) to Delay Tolerant Networks (DTN). We propose employing random linear network coding (RLNC) together with SD to reduce the system outage probability with respect to traditional SD scheme. The theoretical expressions we derive and the simulations performed show that the proposed scheme significantly reduces the system outage probability for a wide range of channel conditions. Moreover, we also propose a method for obtaining the optimal code rate constrained to a maximum system outage probability, which can serve as system design methodology.

## B.1 INTRODUCTION

Spatial diversity (SD) has been recognized as an effective technique to overcome losses in wireless fading channels [10]. More recent works have studied how to introduce physical layer Network Coding (NC) along with SD in terrestrial scenarios such as Distributed Antenna Systems (DAS) to reduce the system outage probability [4]. SD has also been applied to other type of relay scenarios where multiple sources cooperate and communicate with a single destination through a relay in presence of deep fadings. Typical examples are the uplink of satellite systems [7, 2, 5].

* The authors are with the department of Telecommunications and Systems Engineering, Universitat Autònoma de Barcelona.

In this work, we propose to implement packet-level NC together with SD in multiple source/single receiver satellite based scenarios to reduce the system outage probability, i.e. the probability that the receiver is unable to collect all the information packets sent by the source. In order to model deep fadings produced due to randomness of the surrounding environment each link source-satellite is modeled as an ON/OFF channel using a two state Markov chain. We assume the set of sources have exchanged their packets and can perform linear combinations of them to send network coded versions of the packets. More specifically, we show a method to select the optimal code rate in terms of expected rate providing a system outage probability below a maximum value. To the best of our knowledge, the implementation of NC in this type of satellite scenarios is yet unexplored. We compare our proposed scheme with traditional SD scheme. System outage probability results are obtained through analysis of the theoretical expressions we derive and validated through simulation of the scenario under study. Moreover, we also show results for the optimal code rate selection and provide network design criteria based on this results.

The paper is organized as follows: Section B.2 introduces the multiple sources/single receiver system model and channel model. Section B.3 describes the traditional SD scheme and the NC scheme we propose. We also derive the theoretical expressions for the system outage probability in this section. Finally, Section B.4 provides numerical evaluation of the system performance and on Section B.5 conclusions drawn from the work are presented.

## B.2 SYSTEM MODEL

We assume a single relay (satellite) network with a multiple source/single receiver configuration. We assume $|S|$ sources and each link source-satellite is modeled as an ON/OFF channel. The link between the satellite and the receiver is assumed reliable. During the ON states, the satellite receives packets from the sources correctly and during OFF states packets from the sources are lost. We use a two state Markov chain to model the transitions between ON and OFF states [8]. Let $E_G$ and $E_B$ be the expected durations in seconds of the good and bad states respectively. For a mean transmission rate of $R$ packets per second, the mean durations in packets of the good ($D_G$) and bad ($D_B$) states are derived in [8] and given by $D_G = R \cdot E_G$, $D_B = R \cdot E_B$ respectively. The equilibrium state probabilities are given by $p_G = \frac{D_G}{D_G+D_B}$ and $p_B = \frac{D_B}{D_G+D_B}$, where $p_G$ and $p_B$ correspond to the time share of ON and OFF states respectively [8]. In this letter we assume uncorrelated channels but with identical channel statistics. Identical statistics means identical $E_G$, $E_B$, $D_G$, $D_B$ and consequently $p_G$, $p_B$. Finally, we also assume the set of sources have already exchanged their packets and can coordinate to select a subset of the packets to be sent using SD.

A number of scenarios match the described system, especially in satellite systems. For instance in WSN for environmental monitoring, sensors transmit the sensed information to a reduced group of sinks. These sinks can cooperate

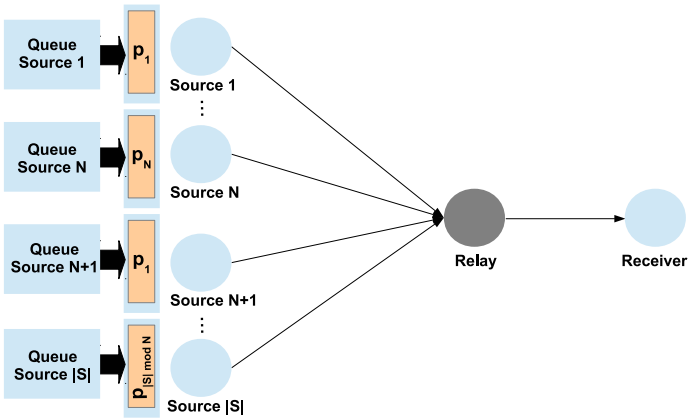


Figure 1: SD scheme. Sources have already exchanged their packets and coordinate to select the packets each source sends. $s_i$ sends packet $p_{i \bmod N}$.

before sending the information to a remote host through satellite [2]. Due to the nature of the information sensed (hurricanes, sandstorms etc.), the channel suffers of deep fadings and can be modeled as an ON/OFF channel. In scenarios involving smart gateways and satellite DTNs, earth sites also communicate and cooperate through a wired network [7, 3]. The channel between the earth sites and the satellite is also subject to deep fadings or intermittent connections and can be modeled as an ON/OFF channel [6].

## B.3 PROPOSED NETWORK CODING SCHEME FOR SPATIAL DIVERSITY

In this section we introduce the traditional SD scheme and the scheme with SD and NC we propose (SD+NC).

### B.3.1 *System outage probability with SD for ON/OFF channel scenarios*

We focus on the transmission of $N$ different packets. Let the set of packets to be transmitted be $P = \{p_1, p_2, \ldots, p_N\}$. We assume $|S|$ sources in total. The set of sources is $S = \{s_1, s_2, \ldots, s_{|S|}\}$. Let $s_1$ to $s_N$, $N \leq |S|$, transmit each a different packet $p_1$ to $p_N$. The SD scheme is such that sources $s_{N+1}, s_{N+2}, \ldots, s_{|S|}$ will correspondingly transmit packets $p_1, p_2, \ldots, p_{|S| \bmod N}$. Figure 1 shows the SD scheme. Let $n_{p_j}$ denote the number of sources sending the packet $p_j$ with $1 \leq j \leq N$. A system outage occurs when any of the $N$ packets sent is not received. We use $P_{out}^{SD}$ to denote this probability, given by

$$P_{out}^{SD}(N, |S|) = 1 - \sum_{i=N}^{|S|} p_G^i p_B^{(|S|-i)} T_{i,N} \tag{1}$$

where $T_{i,N}$ denotes the number of combinations of $i$ elements with $N$ different elements that can be built from the multiset $\mathcal{P} = (P, f)$ with $f(p_i) = n_{p_i}$ [11]. The second term in Eq. (1) evaluates the probability of receiving $N$ packets. The term $p_G^i p_B^{(|S|-i)}$ evaluates the probability of having $i$ source-satellite links

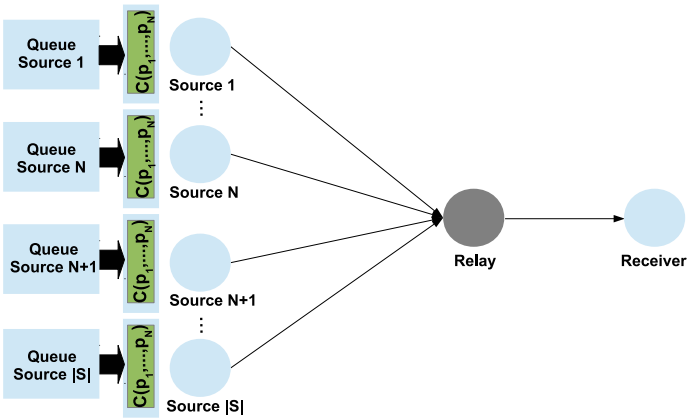


Figure 2: Proposed SD+NC scheme. Each source sends a random linear combination of the same $p_1$ to $p_N$ packets.

in good state and $T_{i,N}$ computes the number of ways of getting $N$ different packets taking into account the cases where repeated versions of the same packet would be received. In order to compute $T_{i,N}$, first the integer solutions of the following equation must be found

$$x_{p_1} + ... + x_{p_N} = i,\ 1 \leq x_{p_j} \leq n_{p_j},\ j = 1, ..., N \tag{2}$$

Eq. (2) can be easily transformed into a standard form with the change of variable $y_{p_j} = x_{p_j} - 1$ where each $y_{p_j}$ ranges from 0 to $n_{p_j} - 1$. Then, Eq. (2) can be solved through standard algorithms [1]. Let $x^*_{l,p_j}, \ldots, x^*_{l,p_N}$ be one of the $N_s$ solutions of Eq. (2), then $T_{i,N}$ can be obtained as

$$T_{i,N} = \sum_{l=1}^{N_s} \left( \prod_{j=1}^{N} \binom{n_{p_j}}{x^*_{l,p_j}} \right) \tag{3}$$

### B.3.2 *System outage probability with SD+NC for ON/OFF channel scenarios*

Under this scheme each of the $|S|$ sources employ SD to send a single coded packet. Specifically, each source employs Random Linear Network Coding (RLNC) to generate a single coded packet from the same $N$ native packets, where we assume $N \geq 1$. Let $L$ denote the length in bits of a native packet. Then, the payload of each packet $p_j$ is split into blocks of $m$ bits. Let $b_{jk}$ denote the $k$-th block of $j$-th packet, with $1 \leq k \leq L/m$. Next, we choose $N$ random coefficients $c_j$ from $\mathbb{F}_q$, with $q = 2^m$. The $k$-th coded block of a coded packet is given by

$$C_k = \sum_{j=1}^{N} c_j b_{jk},\ \forall k = \{1, \ldots, L/m\} \tag{4}$$

The encoding coefficients, $c_1, ..., c_N$, are added in the header of the packet. In the receiver side, at least $N$ coded packets must be received to retrieve the

original packets. The parameter $m$ is the size of the finite field and should be big enough to ensure that the probability of generating two linearly dependent (l.d.) coded packets is negligible. Figure 2 shows the SD+NC scheme we propose where coded packets are indicated as C(·). A system outage occurs, when less than $N$ coded packets are received. We use $P_{out}^{NC}$ to denote this probability, given by

$$P_{out}^{NC}(N,|S|) = 1 - \sum_{i=N}^{|S|} p_G^i p_B^{(|S|-i)} \binom{|S|}{i} \tag{5}$$

The second term in Eq. (5) evaluates the probability of receiving $N$ coded packets. Since the probability of receiving l.d. coded packets is very low for a large enough field size, any $N$ coded packets in the receiver side suffice to recover the original $p_1, ..., p_N$ packets. Hence, for a given $i \geq N$, the term $p_G^i p_B^{(|S|-i)}$ evaluates the probability of having $i$ source-satellite links in good state and $\binom{|S|}{i}$ computes the number of distinct $i$-source-satellite link subsets from the $|S|$ source-satellite links.

The reason for the better behavior of SD+NC scheme is two-fold. First, NC avoids that duplicated versions of the same packet are received. Second, NC provides fair protection of the packets. Each coded packet stores information from $N$ original packets, then if one source-satellite link is in bad state it equally affects to all the $N$ packets and not to a single packet as in the SD case. Hence, that for a large enough number of sources all the $N$ packets are likely to be received whilst for the SD scheme it completely depends on which specific links are in good or bad state. The main disadvantages of the proposed SD+NC scheme are: 1) At least $N$ packets must be received to get useful information. 2) Packets suffer from an extra delay due to the coding overhead. Both disadvantages can be mitigated employing Systematic RLNC (SRLNC) where the first $N$ sources send uncoded packets and the last $|S| - N$ would be coded packets.

### B.3.3 *Optimal code rate selection for SD+NC scheme*

The SD+NC scheme described in the previous section can be seen as a packet level coding scheme of rate $r = N/|S|$. Let $E_R$ be the expected packet rate in reception, given by

$$E_R = r \cdot P_{suc}^{NC} \tag{6}$$

where $P_{suc}^{NC}$ corresponds to the term $\sum_{i=N}^{|S|} p_G^i p_B^{(|S|-i)} \binom{|S|}{i}$ in Eq. (5). Our objective is to obtain the value of $r$ maximizing $E_R$ but constrained to a maximum value of system outage probability $P_{out}^*$. Let $z_i$ be $p_G^i p_B^{(|S|-i)} \binom{|S|}{i}$. According to [9], $z_i \sim \mathcal{N}(\mu_{z_i}, \sigma_{z_i}^2)$ where $\mu_{z_i} = |S| p_G$ and $\sigma_{z_i}^2 = |S| p_G p_B$. Since the summation in $P_{suc}^{NC}$ can be approximated by an integral a first approximation of $P_{suc}^{NC}$ is given by $P\{N \leq z_i \leq |S|\}$. A better approximation is obtained computing $P\{N - \frac{1}{2} \leq z_i \leq |S| + \frac{1}{2}\}$ [9]. The solution can be obtained by introducing the $\text{erf}(\cdot)$ function and it is given by

$$\hat{P}_{suc}^{NC}(r) = \frac{1}{2}\left[1 + \mathrm{erf}\left(\Delta_r\right)\right] \tag{7}$$

where:

$$\Delta_r = \frac{\mu_{z_i} - |S|r + \frac{1}{2}}{\sqrt{2\sigma_{z_i}^2}} \tag{8}$$

Now, we can write the optimization problem as

$$\begin{aligned} \max_{r} \quad & \hat{E}_R(r) = r \cdot \hat{P}_{suc}^{NC}(r) \\ \text{s.t.} \quad & P_{out}^{NC} \leq P_{out}^{*} \\ & \frac{1}{|S|} \leq r \leq 1 \end{aligned} \tag{9}$$

where $\hat{E}_R$ is a continuous function with a local maxima in the interval $[\frac{1}{|S|}, 1]$. Let $r^*$ be the optimal solution to the problem in Eq. (9). In the SD+NC scheme we propose, the code rate must be obtained as a fraction of $N/|S|$, with $N \in \mathbb{Z}^+$, $N \leq |S|$. Hence, there exist two candidate values of $N$ leading to the optimal rate selection

$$N_1 = \lfloor r^*|S| \rfloor, N_2 = \lceil r^*|S| \rceil \tag{10}$$

where $\lceil y \rceil / \lfloor y \rfloor$ indicates the smallest/greatest integer greater/smaller or equal than $y$. The optimal value $N_{opt}$ is given by evaluating $E_R(\frac{N_1}{|S|})$, $E_R(\frac{N_2}{|S|})$ and choosing the one providing the higher $E_R$, proved that $P_{out}^{NC}(N_2, |S|) \leq P_{out}^{*}$. In case the latter is not accomplished $N_{opt} = N_1$. Finally, the optimal code rate is given by

$$r_{opt} = \frac{N_{opt}}{|S|} \tag{11}$$

### B.4 SIMULATION RESULTS

In order to evaluate the performance of our proposed scheme we built a ns2 simulator implementing the SD and SD+NC schemes. Specifically, we simulate the two scenarios in Table 1. First, a WSN scenario where sensors cooperate and transmit sensed data to a remote host through a satellite. Packet sizes and transmission rates are low according to this type of networks. We consider a fast variable channel, i.e. fast transitions of the ON and OFF states, modeling a developing hurricane or sandstorm. The second scenario is a DTN where several earth stations cooperate and send information to a spacecraft through a relay satellite. Packet size is set to 1500 bytes, a typical value for the IP protocol included in Consultative Committee for Space Data Systems (CCSDS) protocol architecture. Transmission rate is very low since the uplink for this scenario is typically used for sending command messages. Mean durations of the good and bad states are 20 and 10 minutes respectively, modeling intermit-

Table 1: Simulated scenarios.

| **Parameters** | **WSN [2]** | **DTN [5]** |
|---|---|---|
| Packet size (bytes) | 200 | 1500 |
| Rate (kbps) | 200 | 10 |
| Propagation delay (s) | 0.250 | 6.6 |
| Number of sources | 1-10 | 1-10 |
| $E_G$ (s) | 4 | 1200 |
| $E_B$ (s) | 4 | 600 |
| $N$ | 2 | 2 |
| $m$ (Only in SD+NC) | 8 | 8 |
| Simulation time (s) | 100 | 10000 |
| Rounds | 10 | 10 |

tent periods of rain. For both scenarios we run 10 simulations long enough to let several changes of states and then average results. We compare simulated results with the theoretical expressions in Eq. (1) and Eq. (5).

Figure 3 shows the system outage probability for SD and SD+NC schemes in both scenarios. Both theoretical (Th.) and simulated (Sim.) results are shown in the figure. It can be observed that theoretical and simulated curves match validating the theoretical expressions in Eq. (1) and Eq. (5). It can also be observed that the SD+NC scheme achieves lower system outage probability than SD in both scenarios. The performance of the SD+NC scheme improves when the number of sources increases. If we focus on the WSN case, we expect to have a large number of sensors deployed in the area of interest. The figure shows that for 10 sensors the system outage probability is reduced in one order of magnitude approximately, from $10^{-1}$ to $10^{-2}$. In the DTN case the decrease in the system outage probability is even bigger, however we expect to have a fewer number of earth stations collaborating. If we consider the case of 5 earth stations, the system outage probability is reduced in 58%. Under the traditional SD scheme, 7 earth stations collaborating would be required to achieve that value of system outage probability as Figure 3 shows. This brings an additional advantage since the SD+NC scheme can achieve a target system outage probability with a fewer number of sources. This means an important reduction of deployment costs, especially in scenarios involving costly earth stations.

In the upper sub-figure of Figure 4 we show the value of $N_{opt}$ for the DTN scenario after the optimization process proposed in Section IV-C. The optimization problem in Eq. (9) is solved using *fmincon* Matlab function. It can be observed that $N_{opt}$ increases with increasing values of $|S|$ and $P^*_{out}$. However, the most important observation of this figure is the fact that for a fixed value of $N_{opt}$ there exist several values of $|S|$ accomplishing the restriction of $P^{NC}_{out} \leq P^*_{out}$. For instance, with $N_{opt} = 2$, a $P^{NC}_{out} \leq 10^{-1}$ can be achieved with 5 and 6 sources because both code rates $2/5$ and $2/6$ achieve a system outage probability lower than $10^{-1}$. Hence, in the bottom sub-figure we show the min-

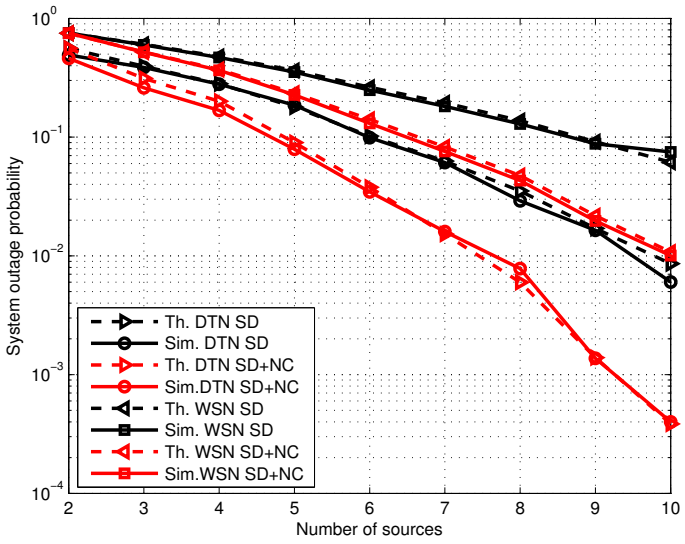


Figure 3: Simulation results and respective theoretical curves for the System outage probability in WSN and DTN scenarios.

imum number of sources $|S|_{min}$ to accomplish a certain $P^*_{out}$ given a value of $N$. Consequently, a design methodology can be derived from these results. 1) If $|S|$ is fixed, the optimal code rate can be obtained maximizing the expected rate for a given system outage probability. 2) If $N$ is fixed, the minimum number of sources can be obtained for a given system outage probability.

## B.5 CONCLUSIONS

In this letter we have presented a NC scheme to be applied in scenarios where multiple sources cooperate and employ SD to reach a receiver through a single satellite. Our scheme is meant for scenarios where the links source-satellite can be modeled as an ON/OFF channel due to deep fadings produced by the randomness of the surrounding environment. We have analyzed the performance of the system outage probability, i.e. the probability that the receiver is unable to decode all the information packets sent by the sources, for these two schemes. Simulation results and the theoretical expressions we have derived show that the SD+NC scheme provides lower outage probability. For the specific case of a WSN with 10 sensors the system outage probability is reduced in one order of magnitude approximately. In the case of DTN networks the outage probability is also reduced, but what is more important a target system outage probability can be achieved with fewer earth stations reducing significantly deployment costs. We have also presented a method to obtain the optimal code rate constrained to a maximum system outage probability in the SD+NC scheme. This result has rendered itself as a design methodology for the optimal use of the proposed scheme.

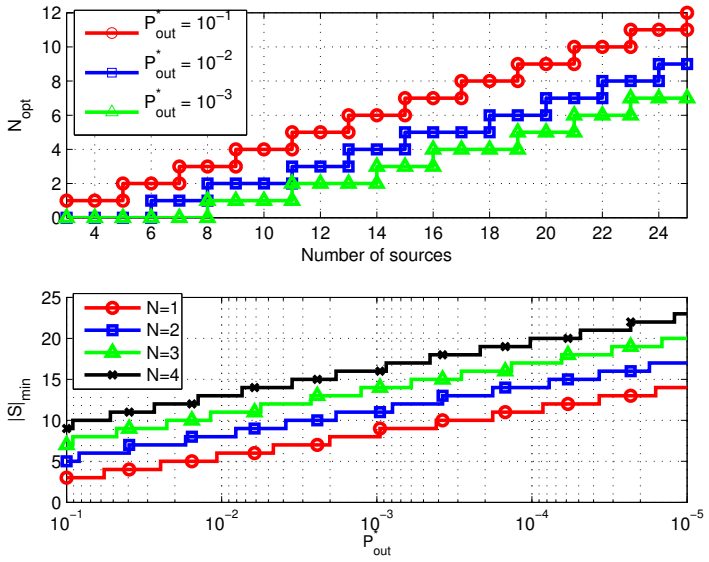


Figure 4: Upper sub-figure: Optimal value of $N$ for DTN scenario. Bottom sub-figure: Minimum value of $|S|$ to accomplish $P^*_{out}$ given $N$.

## REFERENCES


[1] G.E. Andrews. *The Theory of Partitions*. Number v. 2 in Computers & Typesetting. Addison-Wesley Publishing Company, Advanced Book Program, 1976.

[2] I. Bisio and Mario Marchese. Efficient satellite-based sensor networks for information retrieval. *Systems Journal, IEEE*, 2(4):464–475, Dec 2008.

[3] C. Caini and V. Fiore. Moon to earth dtn communications through lunar relay satellites. In *ASMS Conf. and SPSC Workshop*, pages 89–95, Sept 2012.

[4] Yingda Chen, S. Kishore, and Jing Li. Wireless diversity through network coding. In *Wireless Communications and Networking Conference (WCNC), IEEE*, volume 3, pages 1681–1686, April 2006.

[5] T. de Cola and Mario Marchese. Reliable data delivery over deep space networks: Benefits of long erasure codes over arq strategies. *Wireless Communications, IEEE*, 17(2):57–65, April 2010.

[6] D. Divsalar and S. Dolinar. Long erasure correcting codes. In *CCSDS Spring Meeting*, March 2008.

[7] A. Kyrgiazos, B. Evans, P. Thompson, and N. Jeannin. Gateway diversity scheme for a future broadband satellite system. In *ASMS Conf. and SPSC Workshop*, pages 363–370, Sept 2012.

[8] Erich Lutz. A markov model for correlated land mobile satellite channel. *International Journal of Satellite Communications*, 14(4):333–339, 1996.

[9] A. Papoulis. *Probability, Random Variables, and Stochastic Processes*. McGraw Hill, 1984.

[10] A. Sendonaris, E. Erkip, and B. Aazhang. User cooperation diversity. part i and part ii. *Communications, IEEE Transactions on*, 51(11):1927–1948, Nov 2003.

[11] Apostolos Syropoulos. Mathematics of multisets. In *Multiset Processing*, volume 2235 of *Lecture Notes in Computer Science*, pages 347–358. Springer, 2001.

Part III

# CONFERENCE PUBLICATIONS (COMPLEMENTARY ANNEX)

# C

# UNIFIED MULTIBEAM SATELLITE SYSTEM MODEL FOR PAYLOAD PERFORMANCE ANALYSIS

**R. Alegre Godoy, M. Á. Vázquez-Castro and Jiang Lei***

*PSATS*, volume 71, pages 365–377, 2011

ABSTRACT

This paper presents a novel unified multibeam satellite system model for the performance analysis of different satellite payloads. The model allows the analysis in terms of Signal to Interference plus Noise Ratio (SINR) and Co- Channel Interference (CCI). Specifically we formulate the SINR as a function of the multibeam geometry for a given user location granularity. Furthermore, we apply our model to analyze the performance of two novel satellite payloads with respect to current conventional (CONV) ones using fixed frequency reuse and per-beam frequency/time assignment: the so-called "flexible" (FLEX) payload and the "beam-hopping" (BH) which allow a flexible per-beam frequency assignment and a flexible per-beam time assignment respectively. Our results show that CONV payloads achieve higher SINR values than BH and FLEX payloads at the expense of lower bandwidth assignment to the beams. Leading, therefore, to a trade-off, between received signal quality and resource management flexibility.

## C.1 INTRODUCTION

Current trends of multibeam satellite systems focus on the design of more efficient systems in order to achieve not only larger throughputs but also flexible resource management. There already exists an amount of work corresponding to this topic, such as the implementation of new techniques, e.g. power control [5], Forward Error Correction (FEC) codes at physical or link layer [7] and

* The authors are with the department of Telecommunications and Systems Engineering, Universitat Autònoma de Barcelona.

Adaptive Coding and Modulation (ACM) techniques [7]. In addition, another way to achieve larger throughputs is by increasing the number of beams. However, this leads to an increment of the CCI since the same frequency is reused by a subset of beams.

This effect was noticed in reference [3] where pre-coding schemes were used in order to overcome the CCI. Also references [5] and [6] focus on algorithms for satisfying user requirements and performing the multiple access respectively taking into account the minimization of the CCI. Therefore, studying the CCI is of relevant importance in satellite systems in order to validate new multibeam satellite payload models.

The aim of this paper is to formulate the unified expressions for multibeam satellite systems in order to compare the performances of any payload models. Based on the general expressions we compare the performance of three different satellite payloads, a conventional payload model (CONV) and two novel payload models named flexible (FLEX) and beam-hopping (BH). All three models are designed for the multimedia broadband satellite services. This comparison is carried out in terms of SINR and CCI.

The remainder of the paper is organized as follows: Section C.2 introduces the derivation of the general system model. In Section C.3 we introduce three payload models which are designed for the broadband multimedia and IP services. Finally in Section C.4 we evaluate the performance of the payload models. Section C.5 draws the conclusions.

## C.2 DERIVATION OF A UNIFIED SYSTEM MODEL

In this section, we first depict preliminary issues for the general system model derivation, i.e. the multibeam geometry and chosen antenna models. Subsequently, we express the steps to model the system in a general and unified way.

### C.2.1 *Multibeam Satellite Geometry*

The multibeam satellite geometry interested in this paper is shown in Figure 1, without loss of generality we focus on an example with two beams. Assuming that the position of a specific user (*e.g. P*) in a beam i, a beam center BC j and the satellite SL is known, we can compute the distances ($P$,$BC_j$), ($P$,$SL$) and ($SL$,$BC_j$). Therefore, we can derive the angle $\theta_{ij}$ between the link ($P$,$SL$) and ($SL$,$BC_j$ ) by applying the cosine law.

$$\theta_{ij} = \arccos\left(\frac{(P,BC_j)^2 - (SL,BC_j)^2 - (SL,P)^2}{-(SL,BC_j)(SL,P)}\right) \tag{1}$$

where $\theta_{ij}$ is the angle between the user location inside the beam $i$ and the corresponding beam center $BC_j$ (*e.g.* $\theta_{12}$ shown in Figure 1). Note that we can also obtain $\theta_{ii}$ (e.g. $\theta_{11}$ in Figure 1) in the same way.

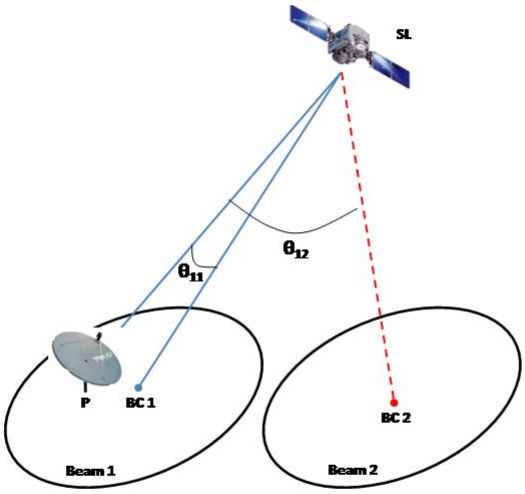


Figure 1: Considered geometry.

### C.2.2 *Analytical Antenna Models*

We now present the two analytical antenna models that generate the multi-beam coverage. The first one is the Single Feed per Beam Network (SFBN) antenna model with combined transmission and reception antennas, i.*e.* each of the beams has a dedicated feed element to generate the beam and the same antennas are used for signal transmission and reception. In the analyzed payload models, both CONV and BH structures implement SFBN antenna model which is analytically expressed as in [3]:

$$G(\theta) = G_{max}\left(\frac{J_1(u)}{2u} + 36\frac{J_3(u)}{u^3}\right)^2 \tag{2}$$

where $u = 2.07123\frac{\sin\theta}{\sin\theta_{-3dB}}$, being $\theta_{-3dB}$ the half angle power bandwidth, $G_{max}$ the antenna boresight gain and $J_1$ and $J_3$ are the Bessel functions of first and third kind respectively. The other one is the Array Fed Reflector (AFR) antenna model using separated transmission and reception antennas, *i.e.* we have fewer antenna elements than beams, and the beams are generated through a Digital Beam Forming Network (DBFN). Different antennas are used for transmission and reception of the signal. FLEX payload structure implement the AFR model which can be modeled as in [8]:

$$G(\theta,\phi) = \sum_{i=1}^{N} c_i g_i(\theta,\phi) \quad for \quad \sum_{i=1}^{N} |c_i|^2 \tag{3}$$

where $N$ are the number of elements in the AFR antenna, $c_i$ is a complex excitation coefficient and $g_i(\theta,\phi)$ is the secondary component beam directivity.

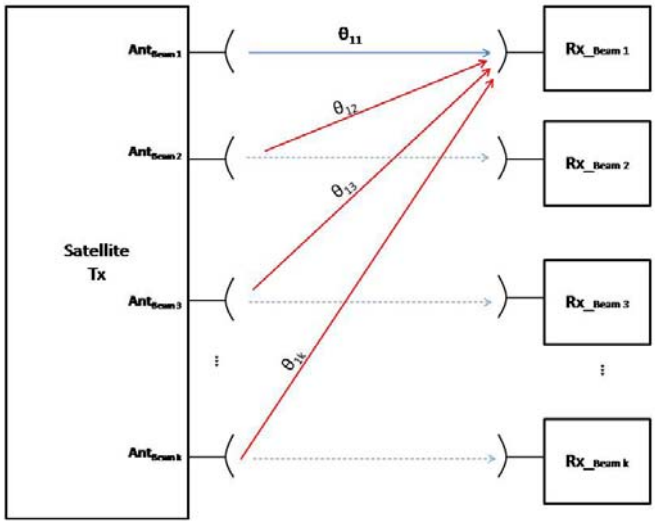


Figure 2: Considered scenario.

### C.2.3 *SINR Derivations*

In this subsection we introduce the formulation of the general multibeam satellite system model. We first define the overall channel matrix $\mathbf{H} \in \mathbb{C}^{k \times k}$ which is composed of two terms: (1) the satellite antenna gains matrix $\mathbf{G} \in \mathbb{C}^{k \times k}$ which depends on the angle $\theta$, (2) the link budget matrix $\mathbf{A} \in \mathbb{C}^{k \times k}$ . Subsequently, the received signal model and SINR can be formulated to study the CCI.

We adopt following notations:

- Vectors are set in bold lowercase letters.
- Matrixes are set in bold uppercase letters.
- Superscript $(.)^T$ denotes the transpose of a vector or matrix in $(.)^T$.
- $diag(\mathbf{x})$ stands for a diagonal matrix with the elements of $\mathbf{x}$ on its main diagonal.

The scenario is shown in Figure 2, where a user in the interested beam $i$ (*e.g.* beam 1 in the figure) is being interfered by any number of beams, *e.g.* $k$. The desired signal power level depends on the angle, $\theta_{ij}$, where $i = j$ ($\theta_{11}$ in the figure), of the user with its beam center. The interference signal power level depends on the $\theta_{ij}$'s where $i \neq j$ ($\theta_{12}$ to $\theta_{1k}$ in the figure).

Let the symbols transmitted to user $i$ inside the coverage of beam $i$ be defined as $\mathbf{x}_i = [x_{i1}, x_{i12}, ..., x_{iM}]$. Let also define the link budget matrix $\mathbf{A} \in \mathbb{C}^{k \times k}$ and the channel matrix gain $\mathbf{G} \in \mathbb{C}^{k \times k}$ which includes the satellite antennas gains as:

$$A = diag(\sqrt{\beta_1}, \sqrt{\beta_2}, ..., \sqrt{\beta_k}) \tag{4}$$

$$G = \begin{pmatrix} g_{11} & g_{12} & \cdots & g_{1k} \\ g_{21} & g_{22} & \cdots & g_{2k} \\ \vdots & \vdots & \ddots & \vdots \\ g_{k1} & g_{k2} & \cdots & g_{kk} \end{pmatrix} \tag{5}$$

where:

- $\beta_i = OBO_{hpa} L_{sat} L_{down} G_{gt}$ where the parameters show the gain and losses which is the gain and losses terms that do not depend on the angle $\theta$, $OBO_{hpa}$ is the Output Back-Off of the High Power Amplifier (HPA), $L_{sat}$ is the satellite repeater output losses, $L_{down}$ is the free space losses and the additional rain, polarization, atmospheric and scintillation losses of the FWD downlink, and $G_{gt}$ is the ground terminal antenna gain.
- $g_{ij} = \sqrt{g(\theta_{ij})}$ is the square root of the antenna gain between the satellite transmitter antenna for beam $j$ and beam $i$, being $\theta_{ij}$ the angle that forms the receiver in beam $i$ towards the spot-beam center $j$ as seen from the satellite. Hence, we can formulate the overall channel matrix $\mathbf{H}$ as:

$$\mathbf{H} = \mathbf{AG} = \begin{pmatrix} h_{11} & h_{12} & \cdots & h_{1k} \\ h_{21} & h_{22} & \cdots & h_{2k} \\ \vdots & \vdots & \ddots & \vdots \\ h_{k1} & h_{k2} & \cdots & h_{kk} \end{pmatrix} \tag{6}$$

where the element of $\mathbf{H}$, *e.g.* $h_{ij}$ is defined as $h_{ij} = \sqrt{\beta_i g(\theta_{ij})}$. Note that the definition of matrix $\mathbf{A}$ and matrix $\mathbf{G}$ can help us to separate the overall channel matrix into two terms, one does not depend on the $\theta$ (*i.e.* $\beta_i$) whilst the other one depends on $\theta$ (*i.e.* $g(\theta_{ij})$). The reason being, we can evaluate the CCI at beam level as a function of the angle $\theta$. Subsequently we can express the received symbols $\mathbf{y}_i(\theta) \in \mathbb{C}^{M \times 1}$ for a user in a beam $i$ by separating the received signal from non-desired signal as in Eq. (7).

$$\mathbf{y}_i(\theta) = \sqrt{P_{sat}} h_{ii} \mathbf{x}_i + \sum_{j=1, j \neq i}^{j=k} \sqrt{P_{sat}} h_{ij} \mathbf{x}_j + \mathbf{n}_i \tag{7}$$

where the term $\sqrt{P_{sat}} h_{ii} \mathbf{x}_i$ is our desired signal, the term $\sum_{j=1, j \neq i}^{j=k} \sqrt{P_{sat}} h_{ij} \mathbf{x}_j$ is the co-channel interference and the term $\mathbf{n}_i$ is a column vector of zero mean and complex circular noise with variance $N$. By replacing $h_{ij}$ with $\sqrt{P_{sat} \beta_i g(\theta_{ij})}$ we can obtain the following expression:

$$\mathbf{y}_i(\theta) = \sqrt{P_{sat} \beta_i g(\theta_{ii})} \mathbf{x}_i + \sum_{j=1, j \neq i}^{j=k} \sqrt{P_{sat} \beta_i g(\theta_{ij})} \mathbf{x}_j + \mathbf{n}_i \tag{8}$$

The SINR can be derived from Eq. (7) for a specific user in beam $i$ by assuming that the power of the transmitted symbols is normalized, $\mathrm{E}[|\mathbf{x}_i|^2] = 1$.

$$SINR_i(\theta) = \frac{P_{sat}|h_{ii}(\theta)|^2}{\sum_{j=1, j\neq i}^{j=k} \left(P_{sat}|h_{ij}(\theta)|^2\right) + N_i} \tag{9}$$

By replacing $h_{ij}$ with $h_{ij} = \sqrt{\beta_i g(\theta_{ij})}$, Eq. (9) can be reformulated as:

$$SINR_i(\theta) = \frac{P_{sat}\beta_i g(\theta_{ii})}{\sum_{j=1, j\neq i}^{j=k} \left(P_{sat}\beta_i g(\theta_{ij})\right) + N_i} \tag{10}$$

Regarding the obtained expressions in Eq. (9) and Eq. (10) we have to note that:

- The expression of the received signal, *i.e.* $\mathbf{y}_i(\theta)$, and the signal to interference plus noise ratio, *i.e.* $SINR_i(\theta)$, depend not only on the $\theta_{ii}$ where $i = j$ (*i.e.* the angle between user $i$ and its beam center $i$) but also on the $\theta_{ij}$ where $i \neq j$ (*i.e.* the angle between user $i$ and each of the interferers $j$). Thus, we have expressed the received signal and the SINR as a function of $\theta$, which is the objective of this subsection.
- $\beta_i = OBO_{hpa} L_{sat} L_{down} G_{gt}$ depends on the system payload design. We can extract specific SINR expressions for each of the payloads, $SINR_i^{CONV}(\theta)$, $SINR_i^{FLEX}(\theta)$ and $SINR_i^{BH}(\theta)$, by replacing $\beta_i$ with $\beta_i^{CONV}$, $\beta_i^{FLEX}$ and $\beta_i^{BH}$ respectively where the superscripts CONV, FLEX and BH stand for the acronym of each of the payloads we will present in Section C.3.

## C.3 PAYLOAD MODELS

The aim of this section is to describe three different payloads models which are designed for the multimedia and IP broadcasting services in a multi-star access network, using Digital Video Broadcasting over Satellite second generation (DVB- S2) in the FWD link and Digital Video Broadcasting Return Channel over Satellite (DVB-RCS) in the return (RTN) link. We first study the current operating payloads in multibeam satellite systems (Conventional payload or CONV in the equations) in order to have reference for the comparison with the other two payloads. Subsequently, we study the flexible payload model where the carrier allocation is fully flexible for each beam (Flexible Payload or FLEX in the equations). Finally we introduce the beam-hopping payload model, in which a subset of beams can be illuminated simultaneously during each timeslot (Beam-hopping payload or BH in the equations). Regarding to the satellite payloads configuration and performance evaluation, more results can be found in [1].

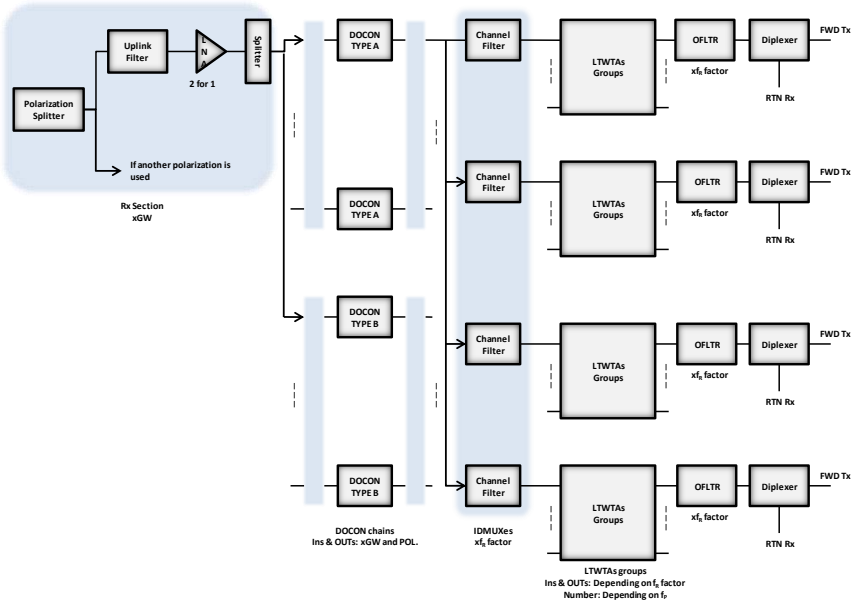


Figure 3: Conventional payload.

### C.3.1 *Conventional Payload*

Conventional payload, abbreviated CONV, is used for the classical MF-TDM transmission schemes where the total bandwidth is divided into a fixed number of portions. Each beam can be assigned one of the portions. Portions of the bandwidth (carrier slots) can be reused or not. The elements forming part of the conventional FWD link payload can be seen in Figure 3.

After the uplink signal filtering of each polarization output, the antenna elements are connected to a 2 for 1 redundant Low Noise Amplifier (LNA). Depending on the frequency plan, more than one type of Down Converter (DOCON) could be needed, so the splitter performs the action of sending the signal to the correct DOCON. Then, the DOCONs down-convert each of the frequency segments. Depending on the number of gateways and the number of polarizations, the number of inputs and outputs of the DOCONs could change. Then Input Demultiplexers (IDMUXes) separate the channels assigned to each user link beam, the needed number of IDMUXes is at least the same as the frequency reuse factor. A group of Linear Traveling Wave Tube Amplifiers (LTWTAs) are used to provide the final amplification of the channels and Output Filters (OFLTRs) are used to limit the inter-modulation and harmonics high amplification effects.

### C.3.2 *Flexible Payload*

Flexible payload, or just FLEX, is used in Non Orthogonal Frequency Reuse (NOFR) air interfaces where a ground cell can allocate a variable number of carriers depending on the traffic requirement. The elements constituting the flexible FWD link payload can be seen in Figure 4.

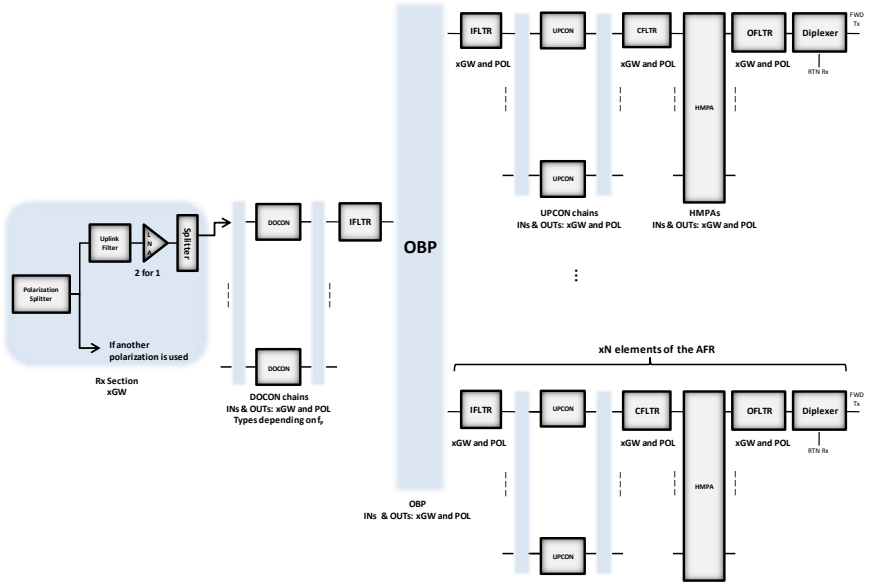


Figure 4: Flexible payload.

In the FWD link, firstly each polarization output signal is amplified by a LNA, then the DOCONS down-convert the received signals to the C-band frequency, consequently the On Board Processor (OBP) can process the converted signals. The Intermediate Filters (IFLTRs) are applied to limit the out of band spurious emissions. The OBP performs the following actions:

- Spectral isolation of the individual modulated user channels that compose each Frequency Division Multiplexing (FDM) multiplexed, multicarrier, gateway signal.
- Routing and steering of the complex samples that compose the uplink carriers signals received on FWD uplink to the destined FWD downlink Digital Beam Forming Network (DBFN) in order to generate the subsequent FWD downlink signals.
- Spatial filtering of the complex samples that compose the uplink carriers signals to generate the subsequent constituent beam signals to be applied to the antenna elements.
- Frequency synthesis of the spatially filtered element beam signals to generate the FDM multiplexed, multicarrier element signal to be applied to each of the antenna elements that compose the transmission antenna array.

The signals from the output of the OBP are then up-converted to the downlink frequencies by the Up Converters (UPCONs) and filtered by the Chanel Filters (CFLTRs) to limit the out of band spurious emissions. Hybrid Matrix Power Amplifiers (HMPAs) composed of LTWTAs are used to amplify the signals that feed the antenna elements. Signals are filtered with OFLTRs before

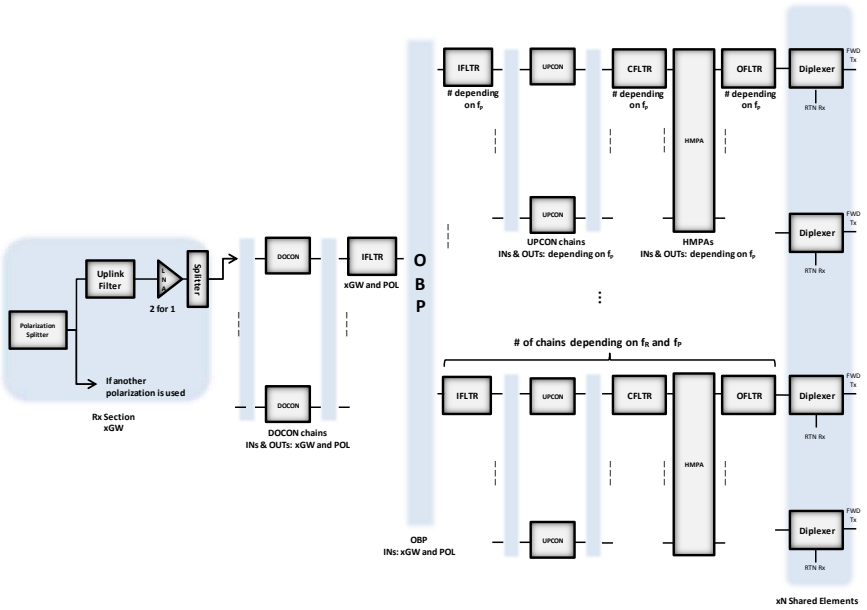


Figure 5: Beam-hopping payload.

transmitted to limit the noise in the receive frequency band and to limit the spurious emissions.

### C.3.3 *Beam-hopping Payload*

Beam-hopping payload, abbreviated BH, is used in air interfaces where the total bandwidth is used in some specific beams during a timeslot. The elements in the beam-hopping FWD link payload can be seen in Figure 5.

In the FWD link the signals go through the 2 for 1 LNAs, then are down-converted to the OBP C-band and processed by the IFLTRs to limit the out of band spurious emissions. The OBP performs the following actions:

- Spectral isolation of the individual, phase modulated carriers signals that constitute each FDM multiplexed, multicarrier gateway signal.
- Grouping the carriers received on the FWD uplink into FWD downlink sets.
- Frequency synthesis of the FWD downlink carrier sets to generate the sub-sequent FDM multiplexed, multicarrier signals. These synthesized multicarrier signals are identified as beam-hopping signals.
- Application of the beam-hopping signals to the antenna elements.

The signal at the output of the OBP is up-converted from the OBP C-band to the FWD downlink frequency by the UPCON, filtered and amplified by HMPAs. The signal is filtered with OFLTRs before sending to the antenna feed elements to limit noise and harmonic distortion.

Table 1: System parameters for the simulations.

| Parameter | Value |
|---|---|
| Orbit | GEO |
| Satellite position | 0°,0° |
| Frequency band | 19.50GHz |
| Modulation | 8PSK |
| System bandwidth | 500MHz |
| Frequency re-use factor | 17.5 |
| $\theta_{-3dB}$ | 0.249° |

## C.4 NUMERICAL RESULTS

In order to evaluate and compare performance of the payload models presented above, in a realistic multibeam scenario, we will study the CCI and the $SINR(\theta)$. Note that, given space constraints, herein we only discuss the comparative performance evaluation of CONV and BH payloads. However, we note that the authors in [4] have shown that the flexible payload and beam-hopping payload are dual of each other. We assume a 70-beam multi-star access system scenario. For each of the beams we analyze:

- The effect of the interference in the received SINR with respect to the number of adjacent interfering beams.
- The effect of the interference in the SINR with respect to all non-adjacent beams.

The system parameters are shown in Table 1 and the payload parameters of the CONV and BH payload parameters are extracted from [1].

### C.4.1 *Effect of Adjacent Interfering Beams*

Figure 6 shows the average received SINR for the conventional CONV and BH payload as a function of the number of adjacent interfering beams. Figure 7 shows the improvement of the average SINR in percentage in the conventional payload with respect to the BH payload for a user located inside the coverage of the beam with coordinates 14.25° Latitude and 50.75° Longitude.

From the figures above it can be observed:

- Case with 0 interferers is equivalent to the received SNR in the beam of interest.
- Adjacent interfering beams cause a fast decrease of the received SINR for both payloads; however, differences are lower as the number of adjacent beams increase.
- For any number of adjacent interfering beams CONV payload is less affected by CCI than BH payload and hence by results obtained in [4]

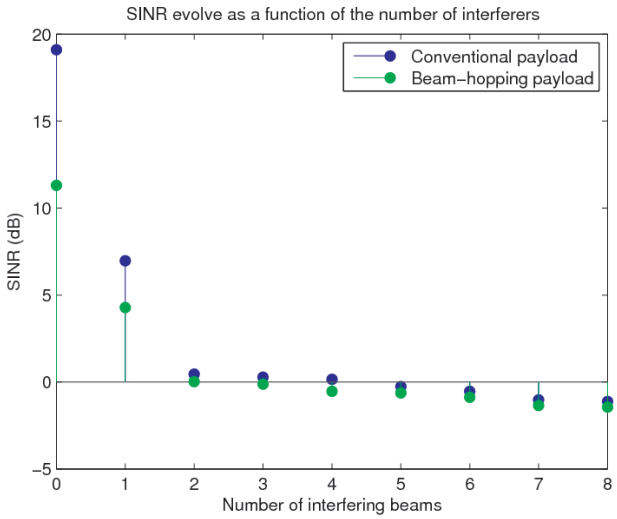


Figure 6: Average SINR as a function of the number of interferers.

than FLEX payload since the bandwidth assigned to beams is higher in BH and FLEX schemes.

Therefore, it should be avoided to assign the same frequency band to adjacent beams in the CONV payload, and to illuminate at the same time adjacent beams in the BH payload. Besides we can note that CONV payload achieves higher SINR's basically because the amount of bandwidth assigned to each beam is lower than in the BH payload where we assign all the bandwidth to each beam. This bandwidth assignment is done in order to satisfy user requirements in a more efficient and flexible way rather the fixed conventional way used in CONV model. Hence there is a clear trade-off between bandwidth assignment and signal strength and by extension between throughput and signal strength. This means, if we want to achieve larger throughputs, we have to assign more bandwidth to each beam, in order to deal with broadband traffic, but received signal power will be lower because of the noise bandwidth. It is worth mentioning that this trade-off is not a bad feature for the novel payloads, as a uniform quality throughout the coverage might not be necessary.

### C.4.2 *Effect of non-adjacent interfering beams*

In this subsection we show the effect on the SINR in the beam of interest when we set non-adjacent beams following a typical 4 colored frequency reuse scheme in the conventional payload (for 70 beam frequency reuse factor 17.5). In order to obtain comparison we will illuminate the same beams in the beam-hopping payload and compare the obtained results. Obtained SINR for CONV payload can be seen in Figure 8.

In the Figure 8, the grey line indicates the original contour of the beam when there are no interferers (3dB loss). Note that within the original contour of the beam, now the SINR values can differ in 10dB as show the contours. However the SINR levels received in zones close to the center of the beam are big enough

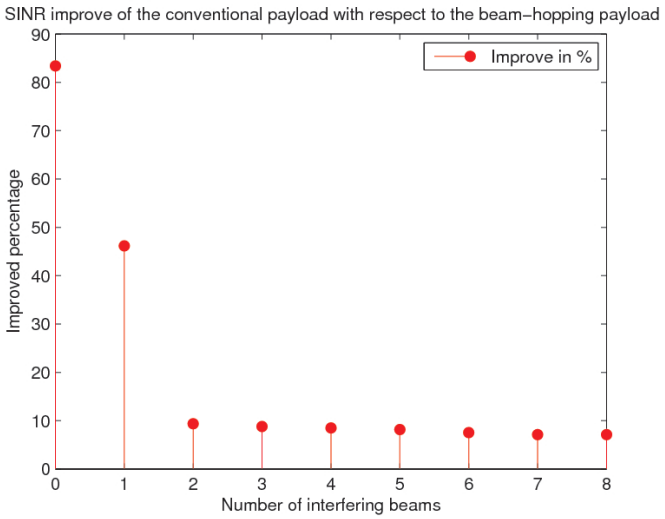


Figure 7: SINR increase of the conventional payload with respect to the beam-hopping payload.

to ensure the correct reception of the signal. Simulations results (not shown here for matter of lack of space) let us draw the same conclusions for the BH payload, a similar interference pattern is obtained. Nevertheless, when illuminating the same set of beams assigning all the bandwidth to each of them, the SINR value obtained in the center of the beam is 6dB under the value of the conventional payload, i.e. as in the adjacent interfering beams case, BH payload is more affected by the CCI than CONV payload. As explained before, this is produced because BH and FLEX schemes assign larger bandwidth to each beam, hence the noise bandwidth is bigger. So, under this scenario we also find the bandwidth signal strength throughput trade-off only that the SINR decrease is not produced in such a drastic way as the interfering beams are now further.

## C.5 CONCLUSIONS

In this paper we have presented a unified system model for multibeam satellite systems. The model allows the performance analysis of different payloads in terms of received signal strength and co-channel interference. The model is easy to use as itidentifies the key parameters of the payloads to be analyzed and how they should be included in the model.

We have applied our model for the performance analysis of two novel satellite payloads with respect to current conventional (CONV) ones: the so-called "flexible" (FLEX) payload and the "beam-hopping" (BH), both described in the paper. The first one allows a flexible per-beam frequency assignment while the second one allows a flexible per-beam time assignment. This flexibility is lacking in current CONV payloads, with fixed frequency reuse and per-beam frequency/time assignment.

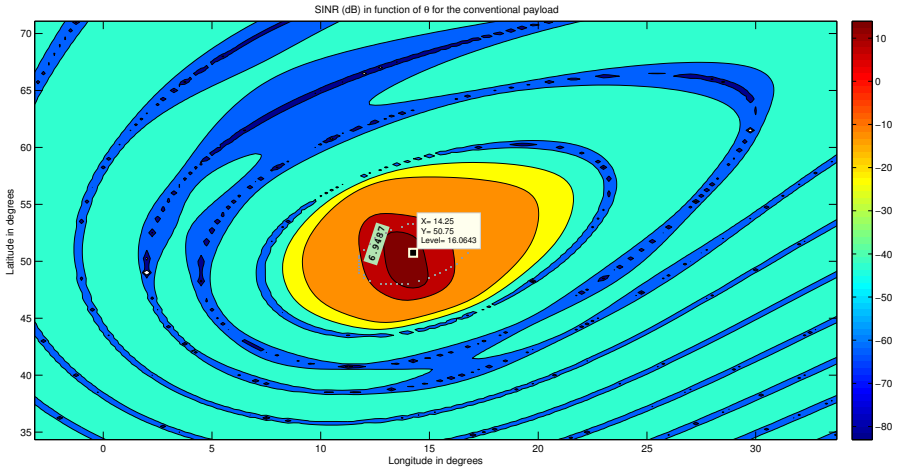


Figure 8: SINR in the beam of interest for a set of non-adjacent interfering beams using a four colored frequency reuse scheme.

The numerical results we have obtained with our developed unified model indicate that the CONV payload achieves better received signal strength and co-channel interference management throughout the coverage than the BH novel payload. This means that a trade-off exists between received signal quality and resource management flexibility. The reason for this is that the new payloads can accommodate larger bandwidths per beam, which is an advantageous feature for handling broadband traffic. This trade-off is actually not a bad feature for the novel payloads as a uniform quality throughout the coverage might not be necessary. For lack of space we have not included the numerical results for the FLEX payload, which show the same trend as the BH and it can be further justified by the duality between both payloads [4].

Our results are fully in line with the results in the related papers [5] and [4], which focus on the resource management algorithms of the proposed payloads.

## REFERENCES

[1] X. Alberti, J.M. Cebrian, A. Del Bianco, Z. Katona, J. Lei, M.A. Vazquez-Castro, A. Zanus, L. Gilbert, and N. Alagha. System capacity optimization in time and frequency for multibeam multi-media satellite systems. In *ASMA Conf. and SPSC Workshop*, pages 226–233, Sept 2010.

[2] Thomas M. Cover and Joy A. Thomas. *Elements of Information Theory*. Wiley-Interscience, 1991.

[3] M.A. Diaz, N. Courville, C. Mosquera, Gianluigi Liva, and G.E. Corazza. Non-linear interference mitigation for broadband multimedia satellite systems. In *Satellite and Space Communications (IWSSC), International Workshop on*, pages 61–65, Sept 2007.

[4] J. Lei and M.A.V. Castro. Frequency and time-space duality study for multibeam satellite communications. In *Communications (ICC), IEEE International Conference on*, pages 1–5, May 2010.

[5] J. Lei and M.A. Vazquez-Castro. Joint power and carrier allocation for the multibeam satellite downlink with individual SINR constraints. In *Communications (ICC), IEEE International Conference on*, pages 1–5, May 2010.

[6] Qingchong Liu and Jia Li. Multiple access in broadband satellite networks. In *Communications (ICC), IEEE International Conference on*, volume 1, pages 417–421 vol.1, May 2003.

[7] Gerard Maral and Michel Bousquet. *Satellite communications systems : systems, techniques and technology*. Wiley, 1998.

[8] K. Ueno. Multibeam antenna using a phased array fed reflector. In *Antennas and Propagation Society International Symposium, IEEE*, volume 2, pages 840–843, July 1997.

# D

# HEURISTIC ALGORITHMS FOR FLEXIBLE RESOURCE ALLOCATION IN BEAM HOPPING MULTI-BEAM SATELLITE SYSTEMS

**R. Alegre Godoy*, N. Alagha† and M. Á. Vázquez-Castro***

*AIAA ICSSC*, 2011

ABSTRACT

In this paper we study capacity optimization algorithms for flexible resource allocation in the forward downlink of beam hopping (BH) multi-beam satellite systems. In particular, we propose two heuristic algorithms which allocate capacity resources based on the per- beam traffic requests. Since traffic requests throughout the coverage are not uniformly distributed, each beam demands a different amount of capacity. The algorithms we propose allocate beams to a certain number of time-slots within a predefined window length such that per-beam required capacity matches as much as possible the offered capacity. Our algorithms are based on one reviewed algorithm in the literature but introducing a set of heuristic modifications which allow to improve the performance, mainly in terms of capacity. Simulations are carried out over a 70 beam reference system operating at Ka band, using different traffic distributions and employing a unified analysis tool in order to obtain fair comparisons. Results show that the algorithms we propose achieve improvements up to 15% in terms of usable capacity with respect to a conventional system. Moreover, our algorithms are built on a realistic BH payload model. The paper also provides a brief discussion on BH capacity boundaries.

* The authors are with the department of Telecommunications and Systems Engineering, Universitat Autònoma de Barcelona.

† The author is with the TEC-ETC section at ESA-ESTEC.

## D.1 INTRODUCTION

Current trends in multi-beam satellite systems focus on the design of more efficient systems in order to achieve not only larger throughputs but also provide flexible resource management at the beam level. The latter appears from the observation that traffic demand throughout the system coverage is not uniform leading to asymmetric traffic requests per beam.

Resource management flexibility in multi-beam satellite systems has been widely studied the past few years. Power allocation policies that stabilize the system based on the amount of unfinished work in the queue and on the channel state in order to maximize the total throughput have been proposed [7]. J. P. Choi *et. al.* proposed a trade-off optimization of the power and the carriers allocated to the beams taking into account the traffic distribution and the channel conditions [4, 3]. However, co-channel interference (CCI) is obviated in the study.

Our work studies algorithms for providing time and spatial flexibility in the forward downlink of BH multi-beam satellite systems. In this type of systems, a window of several time-slots is defined and within each of them a different subset of all the beams is illuminated such that offered capacity per beam is as close as possible to the required. Algorithms used for performing the beam to time-slot allocations are of paramount importance since the system performance is derived from them. There already exists an amount of work corresponding to this topic. Convex optimization algorithms under Binary Power Allocation (BPA) assumption have been proposed, applicable not only to BH schemes but also to schemes providing frequency and space flexibility [6]. J. Anzalchi *et. al.* address the problem by jointly applying Genetic Algorithm (GA), Neighborhood Search (NS) and Iterative Local Search (ILS) [2]. In this paper we propose two algorithms based on the convex optimization algorithm [6, 1] but introducing a set of heuristic modifications. In particular, we introduce a pre-allocation stage, add a new degree of freedom in the optimization process allowing to optimize through Output Back-Off (OBO) values and let beam dual polarization for hot spot-beams. The simplicity of our algorithms results into very fast optimizations.

The reminder of the paper is organized as follows. Section D.2 introduces the assumed system and payload model for BH schemes. Section D.3 introduces the optimization problem and describes in details the proposed algorithms. Section D.4 shows the simulation results and discusses on the capacity bounds of BH systems. Finally, Section D.5 draws conclusions on the work done.

## D.2 BH SYSTEM AND PAYLOAD MODEL

Throughout the paper we assume a dual-polarized multi-beam system with $N_b$ beams. The beam to time-slot allocation takes place over $W$ time-slots. Illuminated beams are assigned the entire bandwidth in one or both polarizations. User Terminals (UTs) within a beam are multiplexed using Time Division Mul-

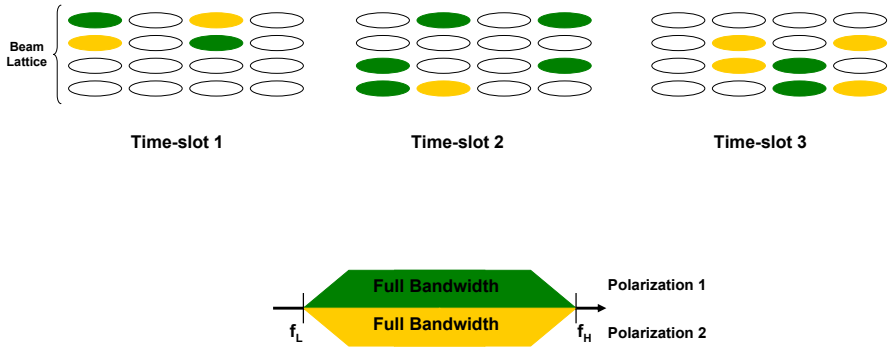


Figure 1: BH payload model.

tiplexing (TDM). Figure 1 illustrates such transmission scheme for a 16 beam lattice.

The BH satellite payload model assumed is shown in Figure 2. The reception front-end processes signals coming from the gateways (GWs). Those are filtered and amplified before being sent to the downconverters (DOCONs). DOCONs adequate the signals to the intermediate band used by the On Board Processor (OBP) which performs the following actions:

- Grouping of the carriers received on the forward uplink into the forward downlink sets.
- Frequency synthesis of the forward downlink carriers sets to generate the sub-sequent Frequency Division Multiplexing (FDM) multi-carrier signals. These synthesized multi-carrier signals are identified as beam-hopping signals.
- Application of the beam-hopping signals to the antenna elements.

The signal at the output of the OBP is up-converted to the downlink frequency by the up-converters (UPCONs) for a posterior high power amplification carried out by the chain of channel filters (CFLTRs), Traveling Wave Tube Amplifiers (TWTAs) and Output Filterts (OFLTRs). Note that in this payload model the number of CFLTRs-TWTAs-OFLTRs chains is lower than the number of beams as opposite to conventional payload models where the number of amplification chains matches the number of beams. Therefore, a routing block controlled by the OBP is added in order to match the output signal of each of the chains to the correct antenna element. The objective for reducing the number of amplification chains is two fold. First the payload mass of the satellite is reduced which leads to cheaper satellite launchers. Second, the DC Power Consumption of the satellite is reduced due to the fewer number of TWTAs. It is worth mentioning that the BH payload model can also be implemented through a transparent payload (without OBP) where the GW and the payload synchronize to switch the appropriate amplification chains according to the beams to be the illuminated in each time-slot.

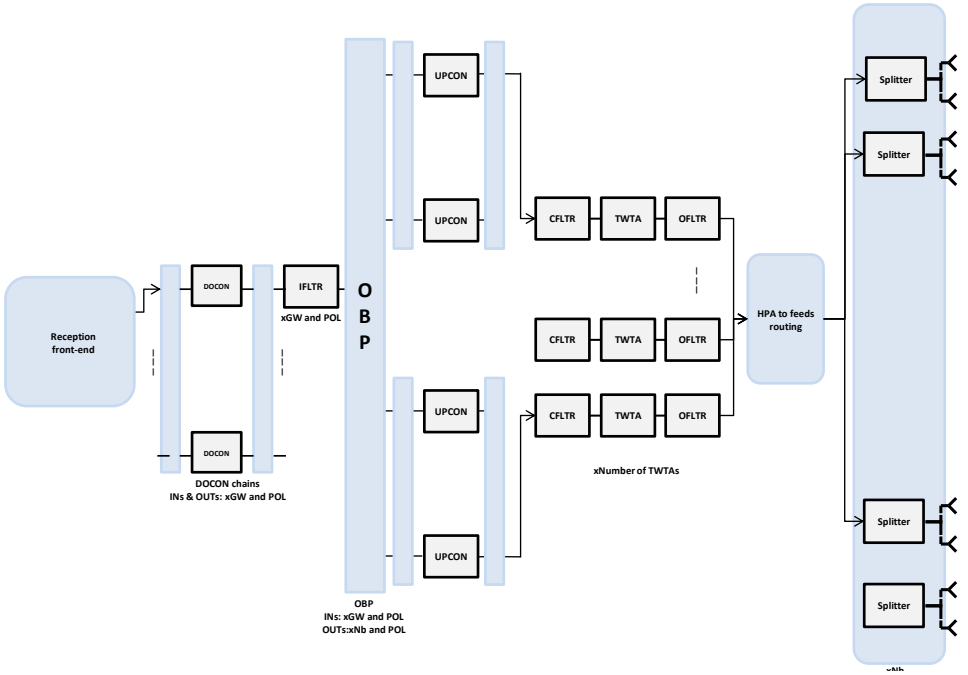


Figure 2: BH payload model.

According to this description we define the following parameters to characterize the payload:

- $P_{tot}$ denotes the available RF power.
- $N_{max}$ denotes the total number of beams that can be illuminated simultaneously.
- $P_{twta}$ denotes the saturation TWTA power.
- TWTAs can be back-offed applying different Output Back-Off (OBO) values out of set $\Omega = \{m_1, ..., m_n\}$ OBO values.

## D.3 ALGORITHMS FOR FLEXIBLE RESOURCE ALLOCATION

### D.3.1 *Optimization Problem*

The objective of the optimization is accommodating beams to time-slots such that each beam $i$ is offered a capacity value $R_i$ as close as possible to the required capacity $\hat{R}_i$. This can be mathematically expressed as:

$$\max \frac{\sum_{i=1}^{N_b} (\min R_i(N_i, P_{i,j}, \hat{R}_i))}{\sum_{i=1}^{N_b} \hat{R}_i} \tag{1}$$

$$\text{s. t.} \quad \sum_{i=1}^{N_b}\sum_{j=1}^{W} P_{i,j} \leq P_{tot}$$
$$P_{i,j} \leq P_{twta}$$
$$\sum_{i=1}^{N_b} T_{i,j} \leq N_{max}$$

where $N_i$ is the number of times a beam is illuminated throughout the entire window length $W$, $P_{i,j}$ is the power allocated to beam $i$ in time-slot $j$ and $T_{i,j} = \{0,1\}$ is a flag indicating if time-slot $j$ is allocated to beam $i$ ($T_{i,j} = 1$) or not ($T_{i,j} = 0$). $R_i$ in Eq. (1) can be obtained by:

$$R_i = \frac{BW}{W}\sum_{j=1}^{W} T_{i,j} log_2(1 + SINR_i^j) \tag{2}$$

where $BW$ denotes the bandwidth of the system and $SINR_i^j$ denotes the Signal to Interference plus Noise Ratio (SINR) of beam $i$ at time-slot $j$. Assuming Digital Video Broadcasting over Satellite second generation (DVB-S2) is used, Eq. (2) can be re-written as:

$$R_i = \frac{R_s}{W}\sum_{j=1}^{W} T_{i,j} f_{DVB-S2}(SINR_i^j) \tag{3}$$

where $R_s$ is the system symbol rate and $f_{DVB-S2}$ is a function which relates the SINR with a corresponding spectral efficiency value according to DVB-S2 physical layer capabilities. Note that forward link SINR thresholds do not need to be linked to DVB-S2 standards. It is possible to use standards relating SINR values to higher spectral efficiencies, i.e. to higher order modulation and codification pairs (MODCODs). SINR for the $i$-th beam at $j$-time-slot can be retrieved by:

$$SINR_i^j = \frac{A_i P_{i,j}}{N_0 + \sum_{r \in \phi_{cc}} A_r P_{r,j}} \tag{4}$$

where $N_0$ is the spectral noise density, $A_i$ denotes the channel and propagation attenuation at beam $i$ and $\phi_{cc}$ is the set of beams simultaneously illuminated except for beam $i$.

The optimization problem in Eq. (1) is not convex [6]. An amount heuristic iterative/combinatorial algorithms have been proposed in the literature. Usually, the proposed approach is based on filling a frequency and power plan matrices, $\mathbf{F}_p \in \{0,1\}^{N_b,2W}$ and $\mathbf{P}_p \in \mathbf{R}^{N_b,2W}$ respectively. $\mathbf{F}_p$ indicates the time-slots each beams is allocated to whilst $\mathbf{P}_p$ indicates the power assigned to the allocated beams. Both matrices are divided in two blocks, first 1 to $W$ columns indicate illuminations in one polarization while $W+1$ to $2W$ columns indicate illuminations in the alternate polarization.

### D.3.2 *State of the Art*

To the best of our knowledge current optimization algorithms are based either on convex [6, 1] or combinatorial [2] approaches.

#### D.3.2.1 *Convex Algorithm*

This algorithm is based on the individual SINR maximization of the beams, i.e. in each iteration all non-satisfied beams are assigned to the time-slot that maximize its individual SINR. After that, the capacity offered to each beam is updated and the set containing all non-satisfied beams is re-calculated to proceed with the next iteration. The process finishes when no more time-slots can be allocated. The advantage of this algorithm is that performs very fast optimizations with reasonably good results. However, it assumes Binary Power Allocation (BPA) and the sharing of the amplification chains is not implemented.

#### D.3.2.2 *Combinatorial Algorithm*

The optimization process for the combinatorial algorithm is based on a sequential application of the Genetic Algorithm (GA), Neighborhood Search (NS) and Iterative Local Search (ILS) algorithms. Each of these steps provides a more refined set of solutions based on the figure of merit to optimize. Although this algorithm implements the sharing of the amplification chains and also performs an optimization through different OBO values, its combinatorial nature makes it very slow. Moreover, obtained results are not as good as expected and the implementation of the TWTA sharing can lead to some beams not being illuminated throughout the window length, i.e. not accomplish the 100% of spatial availability.

### D.3.3 *Heuristic Algorithms*

In order to deal with the drawbacks of the algorithms in the literature, we propose two algorithms based on the *Convex* one. The novelty of our proposals lie on a set of heuristic modifications which not only improve the system performance in terms of usable capacity but also ensure the 100% of spatial availability while maintaining a similar power consumption level. Specifically:

- We design a pre-allocation stage in order to ensure that each beam is illuminated at least once.
- We introduce a new degree of freedom in the optimization process, i.e. optimization through different OBO values.
- We allow hot spot-beams dual-polarization in order to highly increase the offered capacity to these beams.

#### D.3.3.1 *Iterative Minimal Co-Channel Interference Algorithm (minCCI)*

*MinCCI* algorithm appears from the observation that is possible to illuminate beams far from each other in a way that the CCI is almost negligible [6]. Therefore, the problem becomes convex and the optimal number of time-slots that each beam is allocated to can be computed through cost-functions. Several practical issues appear from treating the problem with cost functions even under the assumption that CCI can be neglected:

- It is possible to retrieve the optimal number of time-slots that each beam is allocated to, nevertheless any illumination pattern procedure to place the time-slots in $\mathbf{F}_p$ and $\mathbf{P}_p$ matrices is described.
- In order to formulate the optimization through cost functions BPA is assumed. However, it is possible to back-off the TWTAs differently among time-slots such that the transmitted power by the satellite is reduced. It is well-known that under some CCI patterns reducing the transmitted power can not only increase the SINR, and therefore the offered capacity, but also bring a reduction in the power consumption.

In order to solve these issues, we propose a new algorithm that allocates beams to time-slots such that CCI is minimized. To this aim the following parameters are defined:

- $\Lambda_L$ and $\Lambda_R$ are two complementary sets of left and right polarized beams respectively.
- $\psi_{i,j}$ denotes the set of beams adjacent to beam $i$ which are illuminated at time-slot $j$.
- $\chi_{i,j}$ is a flag indicating whether TWTA assigned to beam $i$ is in use in time-slot $j$ ($\chi_{i,j} = 0$) or not ($\chi_{i,j} = 1$).
- $Th_j$ denotes the capacity generated by all active beam in time-slot $j$.

The first stage of the algorithm is the pre-allocation which is shown in table 1 in pseudo-code with indentation. During this stage first the offered capacity to each beam is set to 0. After that, each beam is assigned to the first time-slot possible taking into account not to exceed the maximum number of illuminated beams per time-slot and that no adjacent beams or beams using the same TWTA are illuminated simultaneously. Note that a tri-dimensional $\mathbf{P}_p$ matrix is defined such that for a given beam and time-slot all the $P_{twta} - m_l$ values are stored. Subsequently, a loop for calculating the optimal OBO value starts in step 4. For each time-slot is chosen the $m_l$ value that generates the higher capacity, i.e. that maximizes $Th_j$. Finally $R_i$ is computed as in Eq. (3) and stored.

Note that the pre-allocation stage ensures that each beam is illuminated at least once, providing the 100% of spatial availability.

The second stage of the algorithm performing the optimization process is shown in Table 2. It takes the $R_i$ values from the pre-allocation phase and

Table 1: Pre-allocation stage

1. **Initialize** $R_i \Leftarrow 0 \quad \forall i$
2. **for** $i = 1 : N_b$
3. **for** $j = 1 : W$

**if** $\sum_{i=1}^{N_b} \chi_{i,j} < N_{max}$ **then**

**if** $i \in \Lambda_L$ **and** $\psi_{i,j} = 0$ **and** $\chi_{i,j} = 0$ **then**

$\mathbf{F}_p(i,j) \Leftarrow 1$, $\mathbf{P}_p(i,j,:) \Leftarrow P_{twta} - m_l$,

**for all** $m_l \in \Omega$

**goto 2**

**if** $i \in \Lambda_R$ **and** $\psi_{i,j} = 0$ **and** $\chi_{i,j} = 0$ **then**

$\mathbf{F}_p(i,W+j) \Leftarrow 1$, $\mathbf{P}_p(i,W+j,:) \Leftarrow P_{twta} - m_l$,

**for all** $m_l \in \Omega$

**goto 2**

4. **for** $j = 1 : 2W$

**Compute** $Th_j = \sum_{i=1}^{N_b} \frac{T_{i,j} R_s}{W} f_{DVB-S2}(SINR_i^j)$ **for all** $m_l \in \Omega$

**Choose** $m_l$ **such that** $\max\{Th_j(m_1), ..., Th_j(m_l)\}$

5. **Update** $R_i$

builds the set $A_s$. Posteriorly the set is sorted such that places less satisfied beams first. After that, the optimization process starts. Per each time-slot a beam belonging to a certain polarization is allocated to it if accomplishes the following conditions: 1) the maximum number of beams to be illuminated in a given time-slot has not been reached, 2) any adjacent beams have been illuminated in that time-slot and 3) any beam using the same TWTA has already been illuminated in that time-slot. As in the pre-allocation, a tri-dimensional $\mathbf{P}_p$ matrix is used for storing all the $P_{twta} - m_l$ values. Once a time-slot has been completely allocated, the $m_l$ value that maximizes the capacity generated in that time-slot is chosen. Finally, the $R_i$ values are updated and the $A_s$ set is built and sorted again for the next loop. The process finishes whenever $A_s$ is empty, the power budget has been reached or the window length has been attained. From the described algorithm note the following:

- Illuminating adjacent beams is not allowed which means that a low CCI is expected and hence a good performance of the algorithm.
- Implements a realistic payload model since the TWTA sharing is introduced. This is done by defining the $\chi_{i,j}$. The fact that groups of beams share the same TWTA can cause that during the optimization process a beam is never illuminated. To solve this issue the pre-allocation stage is designed such that each beam is illuminated at least once during the optimization process.

Table 2: *minCCI* Optimization stage

1. **Build set** $A_s$ **with** $(R_i/\hat{R}_i) < 1$
2. **Sort set** $A_s = \{b_1, b_2, ..., b_k\} | 0 \leq \hat{R}_{b_n} - R_{b_n} < \hat{R}_{b_{n-1}} - R_{b_{n-1}}$
3. **while** $A_s \neq 0$ **and** $\sum_{i=1}^{N_b} \sum_{j=1}^{W} P_{i,j} < P_{tot}$ **and** $j < W$

**for** $j = 1 : W$

**for each** $i \in A_s = \{b_1, b_2, ..., b_k\}$

**if** $\sum_{i=1}^{N_b} \chi_{i,j} < N_{max}$ **then**

**if** $i \in \Lambda_L$ **and** $\psi_{i,j} = 0$ **and** $\chi_{i,j} = 0$ **then**

$\mathbf{F}_p(i,j) \Leftarrow 1$, $\mathbf{P}_p(i,j,:) \Leftarrow P_{twta} - m_l$,

**for all** $m_l \in \Omega$

**if** $i \in \Lambda_R$ **and** $\psi_{i,j} = 0$ **and** $\chi_{i,j} = 0$ **then**

$\mathbf{F}_p(i, W+j) \Leftarrow 1$, $\mathbf{P}_p(i, W+j, :) \Leftarrow P_{twta} - m_l$,

**for all** $m_l \in \Omega$

**Compute** $Th_j = \sum_{i=1}^{N_b} \frac{T_{i,j} R_s}{W} f_{DVB-S2}(SINR_i^j)$ **for all** $m_l \in \Omega$

**Choose** $m_l$ **such that** $\max\{Th_j(m_1), ..., Th_j(m_l)\}$

**Update** $R_i$

**Build set** $A_s$ **with** $(R_i/\hat{R}_i) < 1$

**Sort set** $A_s = \{b_1, b_2, ..., b_k\} | 0 \leq \hat{R}_{b_n} - R_{b_n} < \hat{R}_{b_{n-1}} - R_{b_{n-1}}$

**end**

- A new degree of freedom for the optimization process is introduced since also an optimization through different OBO values is performed.

#### D.3.3.2 *Iterative SINR Maximization Algorithm (maxSINR)*

This algorithm gathers the principles of the *Convex* algorithm in the literature but introducing our proposed heuristic modifications. The algorithm also runs in two stages, the pre-allocation stage already shown in Table 1 and the optimization stage which is shown in Table 3.

In the first step of the optimization, the $R_i$ values obtained in the pre-allocation stage are collected in order to build and sort the set $A_s$. Then, beams are separated into either left or right polarization and the algorithm seeks the time-slot that maximizes the individual SINR of that beam. In the search is taken into account that the maximum number of beams that can be illuminated in a time-slot has not been reached and that beams using the TWTA are not illuminated together in the same time-slot. Once the accommodation has been performed for all the beams in $A_s$, $R_i$ values are updated and the set is built and sorted again to proceed with another iteration. The process ends when $A_s$ is empty or the power budget has been reached. Finally, per each time-slot, the optimal $m_l$ value of OBO maximizing $Th_j$ is computed.

Table 3: *maxSINR* Optimization stage

1. **Build set** $A_s$ **with** $(R_i/\hat{R}_i) < 1$
2. **Sort set** $A_s = \{b_1, b_2, ..., b_k\} | 0 \leq \hat{R}_{b_n} - R_{b_n} < \hat{R}_{b_{n-1}} - R_{b_{n-1}}$
3. **while** $A_s \neq 0$ **and** $\sum_{i=1}^{N_b} \sum_{j=1}^{W} P_{i,j} < P_{tot}$

   **for each** $i \in A_s = \{b_1, b_2, ..., b_k\}$

   **if** $i \in \Lambda_L$ **then**

   **find** $j | \max(SINR_i^1, ..., SINR_i^W)$, $j \in 1..W$,

   **s.t.** $\chi_{i,j} < N_{max}$, $\chi_{i,j} = 0$

   $\mathbf{F}_p(i,j) \Leftarrow 1$, $\mathbf{P}_p(i,j,:) \Leftarrow P_{twta} - m_l$, **for all** $m_l \in \Omega$

   **if** $i \in \Lambda_R$ **then**

   **find** $j | \max(SINR_i^{W+1}, ..., SINR_i^{2W})$, $j \in 1..W$,

   **s.t.** $\chi_{i,j} < N_{max}$, $\chi_{i,j} = 0$

   $\mathbf{F}_p(i, W+j) \Leftarrow 1$, $\mathbf{P}_p(i, W+j, :) \Leftarrow P_{twta} - m_l$,

   **for all** $m_l \in \Omega$

   **Update** $R_i$

   **Build set** $A_s$ **with** $(R_i/\hat{R}_i) < 1$

   **Sort set** $A_s = \{b_1, b_2, ..., b_k\} | 0 \leq \hat{R}_{b_n} - R_{b_n} < \hat{R}_{b_{n-1}} - R_{b_{n-1}}$
4. **for** $j = 1 : 2W$

   **Compute** $Th_j = \sum_{i=1}^{N_b} \frac{T_{i,j} R_s}{W} f_{DVB-S2}(SINR_i^j)$ **for all** $m_l \in \Omega$

   **Choose** $m_l$ **such that** $\max\{Th_j(m_1), ..., Th_j(m_l)\}$
5. **Update** $R_i$

**end**

Note that this algorithm keeps the characteristics of the *Convex* algorithm since the beam to time-slot accommodations are performed in the same way but introducing our heuristic modifications.

### D.4 RESULTS

In this section we show the simulation results of the optimizations performed by each of the studied algorithms, i.e. *Convex, Combinatorial, minCCI* and *maxSINR* algorithms. To this aim we evaluate three figures of merit, the Usable System Capacity (USC), the Satisfaction Factor (SF) and the satellite DC power consumption ($\beta_{DC}$). USC models the portion of offered capacity that is actually profited by the UTs, i.e.:

$$USC = \sum_{i=1}^{N_b} \min(R_i, \hat{R}_i) \tag{5}$$

Table 4: System characteristics

| **Parameter** | **Value** |
|---|---|
| Standard | DVB-S2 |
| Number of beams | 70 |
| Downlink Frequency | 19.50$GHz$ to 20$GHz$ |
| Polarization | Dual |
| Bandwidth | 360$Mbauds$ |
| Available DC Power | 7136$W$ |
| Minimum Spatial Availability | 100% |

The USC in Eq. (5) can be also understood as a satisfaction factor (SF) measure since indicates the percentage of capacity usable for the system, i.e.:

$$SF = \frac{USC}{\sum_{i=1}^{N_b} \hat{R}_i} \tag{6}$$

Additionally, we will also focus on the DC consumption power of the satellite as a secondary figure of merit. The latter is essential to evaluate which is the cost for a good USC performance since we expect that a higher USC leads to higher DC power consumption. The power consumption is modeled as follows:

$$\beta_{DC} = \beta_{on} + \beta_{off} \tag{7}$$

where the term $\beta_{on}$ models the consumption of the TWTAs that are active and the term $\beta_{off}$ models the consumption of the TWTAs that are inactive. Specifically:

$$\beta_{on} = \sum_{i=1}^{N_b} \sum_{j=1}^{2W} T_{i,j} \mathbf{P}_p(i,j) \eta_{RF2DC}(OBO) \tag{8}$$

$$\beta_{on} = \beta_{RF} \cdot \eta_{RF2DC}(OBO)$$

$$\beta_{off} = P_{off} \sum_{j=1}^{2W} \sum_{i=1}^{N_b} (\chi_{i,j} + 1) \quad \forall \chi_{i,j} = 0 \tag{9}$$

where $\eta_{RF2DC}(OBO)$ is the RF to DC efficiency of the TWTA which depends on the OBO value assigned and $P_{off}$ is the DC power consumed by the TWTA when is not active.

Moreover, we also show some other characteristics of the algorithms such as the offered vs required per-beam capacities and the MODCODs distributions.

Table 5: BH and conventional payload characteristics

| **Payload Type** | **BH** | **CONV** |
|---|---|---|
| $P_{twta}$ | $131W$ | $131W$ |
| Colouring | 2 | 4 |
| Number of carriers | $1(360Mbauds)$ | $8(45Mbauds)$ |
| Number of TWTAs | 35 | 70 |
| Post-Amplification Losses | $2.1dB$ | $2.1dB$ |
| OBO | To be optimized | $1.1dB$ |

#### D.4.1 *System Parameters*

We carry out simulations over a 70 beam satellite system with the characteristics shown in Table 4. Table 5 specifies the BH payload configuration and the conventional payload (CONV) used as benchmark.

The traffic distributions we adopt for our simulations correspond to the prediction of the Digital Divide Satellite Offer (DDSO) study [5]. In particular, we focus on the prediction for the 2020 year since is the most demanding. In order to prove the robustness of our algorithm we will also use predictions for years 2012 and 2015.

In order to establish fair comparisons between the optimizations performed by each of the algorithms the following simulation method is adopted:

1. Each algorithm receives as input a set of files defining the satellite system and payload.
2. Algorithms perform the optimization and generate as unique output the $\mathbf{F}_p$ and $\mathbf{P}_p$ matrices.
3. An analysis tool collects the $\mathbf{F}_p$ and $\mathbf{P}_p$ matrices and the set of input files used as input for the algorithms. Subsequently, an accurate analysis is performed to obtain results for the desired figures of merit.

Note that in this way, the analysis is always performed by the same tool. Moreover, both the algorithms and the tool use the same set of input files. Therefore, we ensure the consistency in the obtained results.

#### D.4.2 *Numerical Results*

##### D.4.2.1 *Capacity Results*

Figure 3, Figure 4 and Figure 5 show the offered vs required per beam capacity for the CONV system, *minCCI* and *maxSINR* algorithms respectively.

Note that the CONV system assigns the same amount of capacity ($R_i$) to each beam without taking into account the required capacity ($\hat{R}i$). Hence, that some beams are over-served whilst other beams lack of resources leading to a waste of capacity and power. However, proposed BH algorithms in Figure

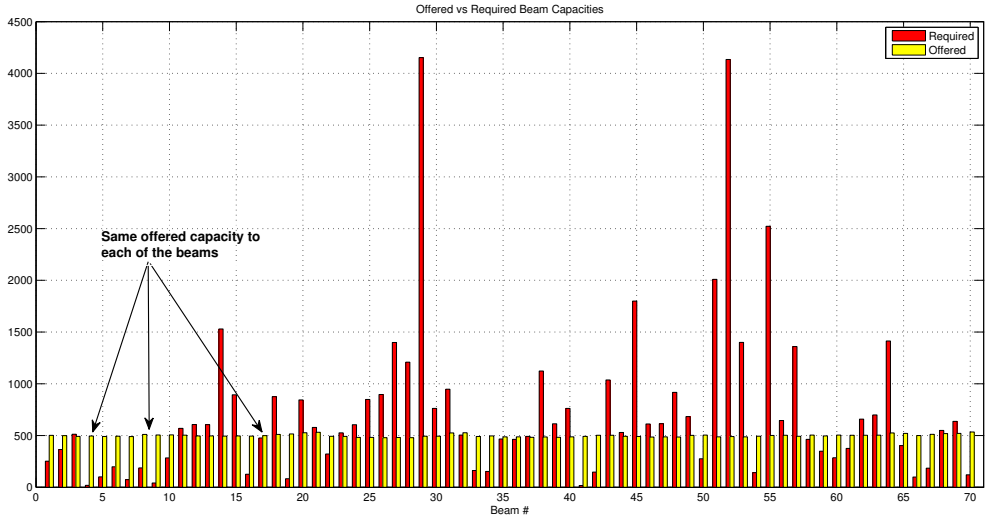


Figure 3: $R_i$ vs $\hat{R}_i$ for *CONV* system under 2020 traffic prediction.

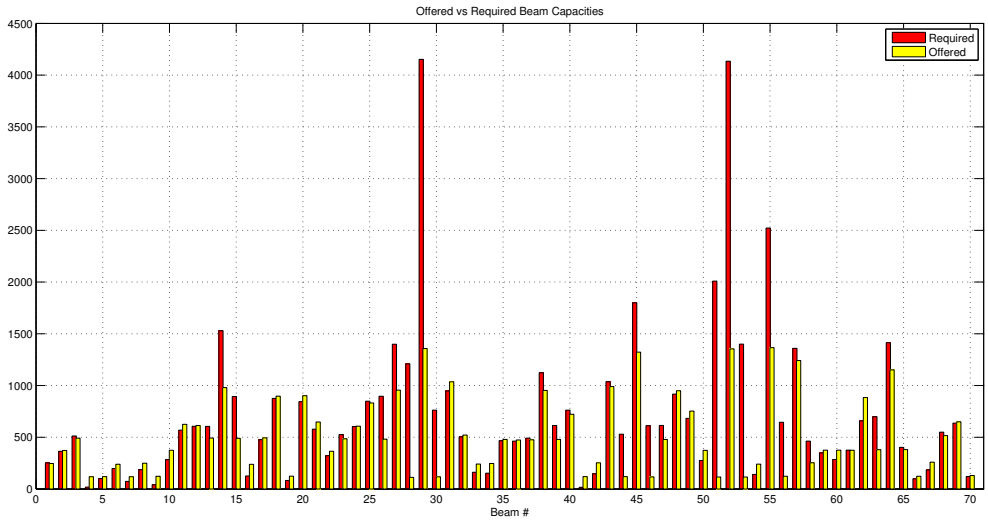


Figure 4: $R_i$ vs $\hat{R}_i$ for *minCCI* algorithm under 2020 traffic prediction.

4 and Figure 5 are able to offer per-beam capacity values very close to the demanded capacity, i.e. demonstrate flexibility in the resource assignments. Moreover, this implies power saving in the satellite.

As Figure 6 show, regardless of the traffic distribution, algorithms are able to adapt to the traffic shape and maximize the system usable capacity.

Note that in each of the traffic distributions shown, there are some beams which are demanding an important amount of traffic, e.g. beams 29 and 52 in Figure 5. In order to assign them more resources let introduce the following beam dual-polarization technique. Instead of illuminating these hot spot-beams using one polarization, we will illuminate them by assigning both polarizations simultaneously. Implementing this technique from the algorithm

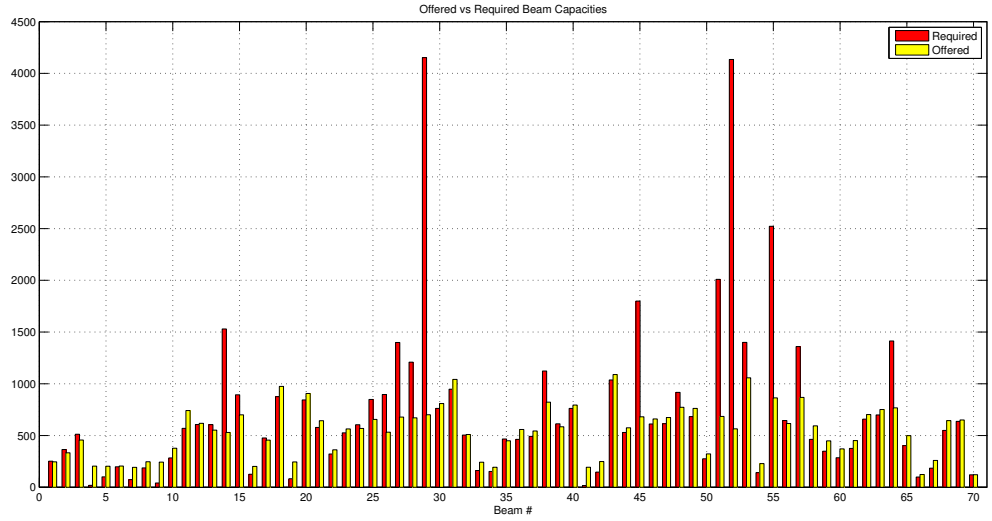


Figure 5: $R_i$ vs $\hat{R}_i$ for *maxSINR* algorithm under 2020 traffic prediction.

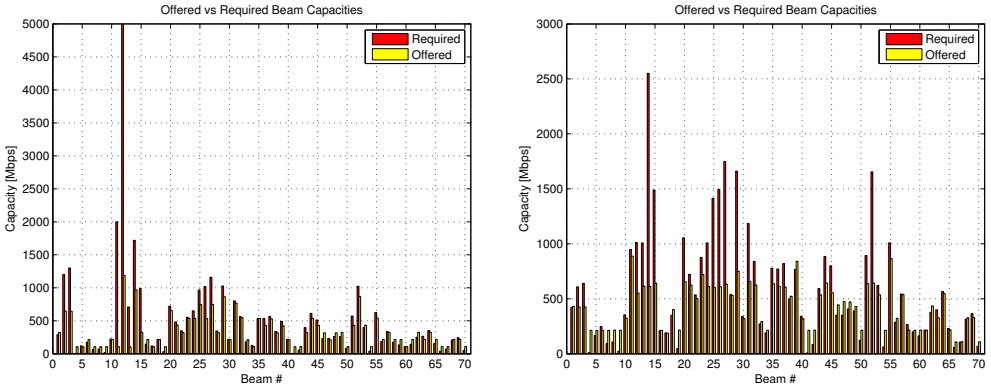


(a) $R_i$ vs $\hat{R}_i$ for *minCCI* algorithm under 2012 traffic prediction.

(b) $R_i$ vs $\hat{R}_i$ for *maxSINR* algorithm under 2015 traffic prediction.

Figure 6: Algorithm performance for other traffic distributions.

point of view is very simple since only requires to add the beams we want to dual-polarize in both sets $\Lambda_L$ and $\Lambda_R$. However, from the UT point of view implies a higher complexity since the terminal must be able to decode two polarizations simultaneously. Figure 7 and Figure 8 show the offered vs required capacity per beam by dual-polarizing some beams in contrast to the values in Figure 4 and Figure 6.

Note from the figures that the beams that are dual polarized experience a high increase in the offered capacity whilst the rest of the beams follow the shape of the traffic distribution normally. However, the dual polarization of the beams generates an additional interference that produces a slight decrease in the overall performance of the system. In spite of this drawback this is an interesting feature to satisfy beams that are requiring high capacity values,

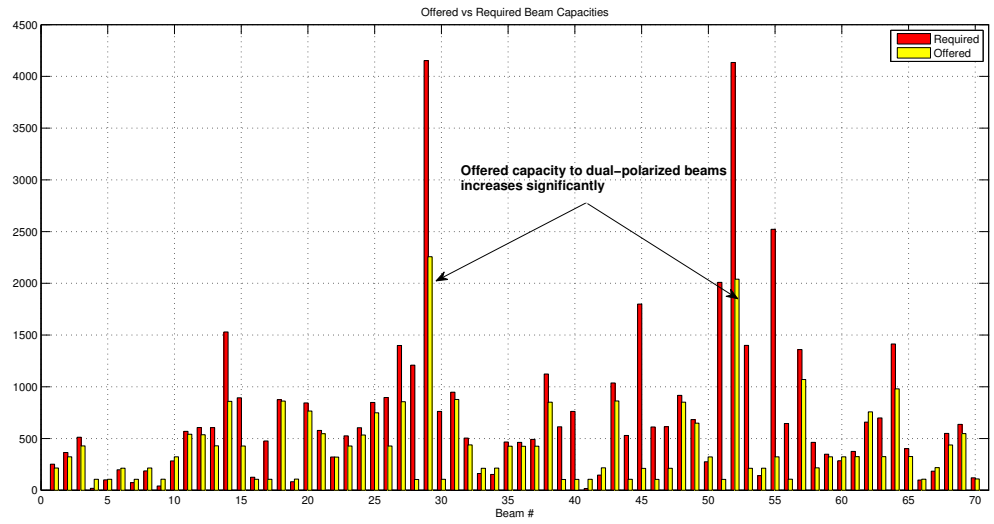


Figure 7: $R_i$ vs $\hat{R}_i$ for *minCCI* algorithm under 2020 traffic prediction (beam 29 and 52 dual-polarized).

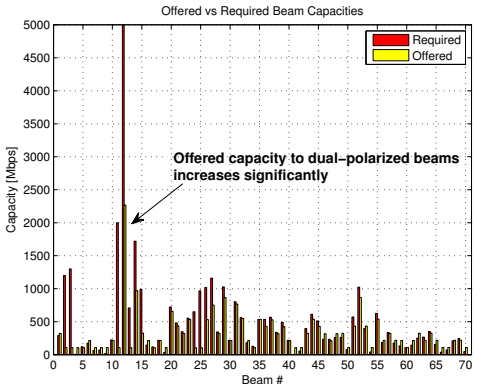


(a) $R_i$ vs $\hat{R}_i$ for *minCCI* algorithm under 2012 traffic prediction (beam 12 dual-polarized).

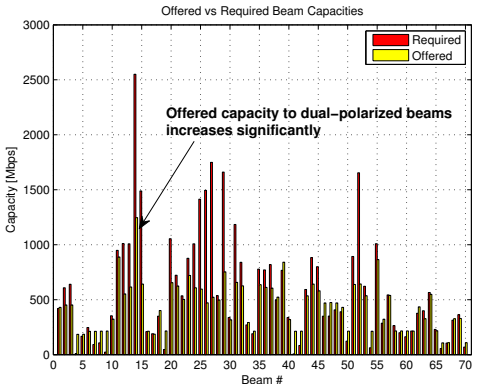


(b) $R_i$ vs $\hat{R}_i$ for *maxSINR* algorithm under 2015 traffic prediction (beam 14 dual-polarized).

Figure 8: Algorithm performance for other traffic distributions using beam dual-polarization.

moreover it can be applied in a temporary basis to cope with traffics peaks generated in some beams, e.g. Internet rush hours.

Table 6, Table 7 and Table 8 show a summary of the results obtained for each of the predicted traffic distributions, 2020, 2012 and 2015 respectively. For each distribution we evaluate the USC, SF and $\beta_{DC}$ performance for each studied BH algorithm and for a CONV system.

From the tables shown note that in general the performance of BH algorithms substantially improve the CONV system in terms of USC and $\beta_{DC}$ demonstrating the potential of BH systems. In particular, the algorithms we propose achieve an improvement with respect to the CONV system up to 15% in terms of USC and 30% reduction in terms of $\beta_{DC}$ Moreover, our proposals

Table 6: Simulation results under 2020 traffic distribution

| **Metric** | **CONV** | ***Convex*** | ***Genetic*** | ***minCCI*** | ***maxSINR*** |
|---|---|---|---|---|---|
| $USC$ (Mbps) | 26993.4 | 31884.3 | 30287.2 | 33629.2 | 34357.5 |
| $SF$ | 0.53 | 0.63 | 0.59 | 0.66 | 0.68 |
| $\beta_{DC}$ (W) | 6628.4 | 5758.1 | 4530.2 | 4693.4 | 4936.6 |

Table 7: Simulation results under 2012 traffic distribution

| **Metric** | **CONV** | ***Convex*** | ***Genetic*** | ***minCCI*** | ***maxSINR*** |
|---|---|---|---|---|---|
| $USC$ (Mbps) | 20756.3 | 23601.6 | 23805.4 | 24202.6 | 24873.4 |
| $SF$ | 0.60 | 0.69 | 0.70 | 0.71 | 0.72 |
| $\beta_{DC}$ (W) | 6628.4 | 5072.2 | 4084.2 | 4173.2 | 4281.2 |

Table 8: Simulation results under 2015 traffic distribution

| **Metric** | **CONV** | ***Convex*** | ***Genetic*** | ***minCCI*** | ***maxSINR*** |
|---|---|---|---|---|---|
| $USC$ (Mbps) | 24529.9 | 28203.8 | 28504.4 | 29302.7 | 30311.1 |
| $SF$ | 0.60 | 0.69 | 0.70 | 0.72 | 0.74 |
| $\beta_{DC}$ (W) | 6628.4 | 5429.7 | 4445.4 | 4871.2 | 4928.9 |

perform better than state of the art algorithms, achieving improvements up to 9% while maintaining a similar power consumption performance, ensuring the 100% of spatial availability and describing a more realistic payload model. Besides, we have presented a dual-polarization technique which allows hot spot-beams being assigned resources in both polarization such that capacity assigned to these particular beams is highly increased.

#### D.4.2.2 *MODCOD distribution*

Besides of evaluating the usable capacity and power performance of our algorithms we also focus on the obtained MODCOD distributions throughout the coverage. Figure 9 shows the classical MODCOD distribution for a CONV system, i.e. all users are highly concentrated in few high-order MODCODs allowing to runn into lower-order ones in case of deep fading events such as rain.

Under *minCCI* algorithm and we obtain the MODCOD distribution shown in the left of Figure 10 whilst for the rest of algorithms, *Convex*, *Combinatorial* and *maxSINR*, we obtain MODCOD distributions with a similar to to the right image in Figure 10.

Observe that the MODCOD distribution for *minCCI* algorithm is concentrated in few high-order MODCODs as in the CONV system ensuring that in case of rain events all UTs would be able to switch to low-order MODCOD. The reason for this behavior is the fact that the algorithm does not allow adjacent beams being illuminated simultaneously, reducing in this way the CCI.

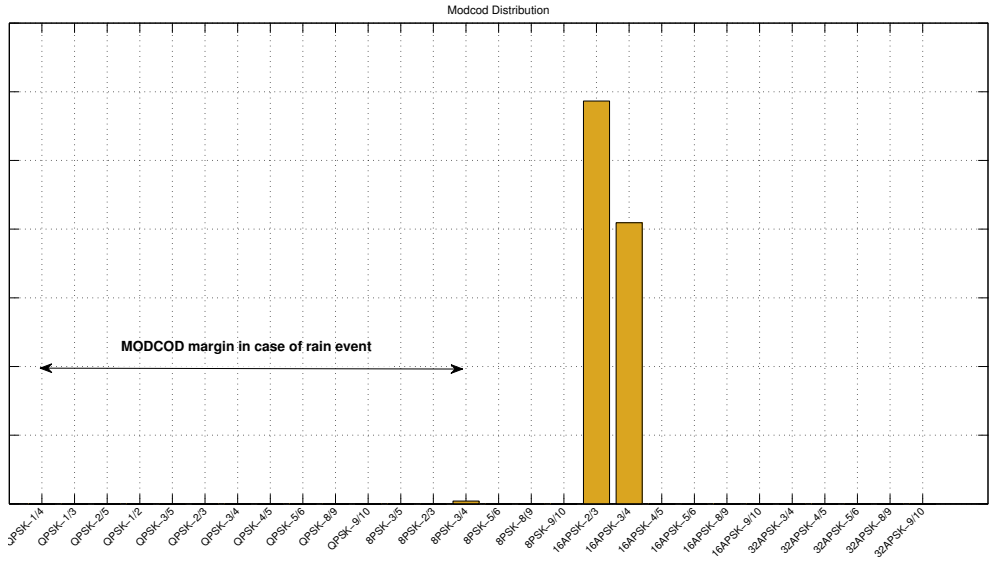


Figure 9: MODCOD distribution for *CONV* system.

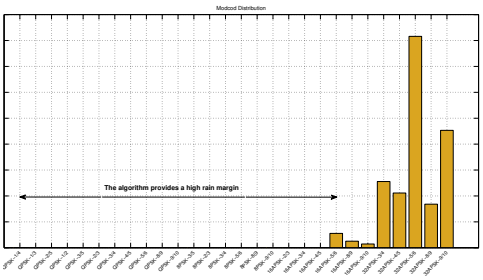


(a) MODCOD distribution for *minCCI* algorithm

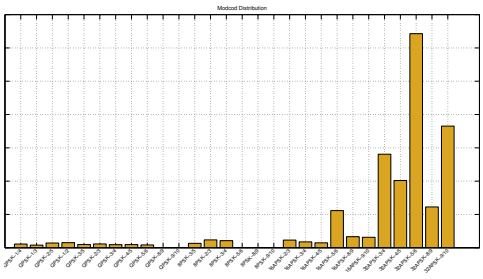

(b) MODCOD distribution for *maxSINR* algorithm

Figure 10: MODCOD distributions for BH algorithms.

On the other hand *maxSINR* algorithm (and the rest of studied BH algorithms) shows a very sparse MODCOD distribution. These allows to obtain higher USC values but could cause UTs incur in outage periods in case of rain events which is drawback for this algorithm.

### D.4.3 *BH Boundaries*

Observe from Figure 7 and Figure 8, that despite of dual polarizing certain beams is still not possible to satisfy them. Therefore, we seek which is the maximum amount of capacity that can be offered to just one beam with the characteristics of our BH system.

In order to find heuristically this value, a simulation illuminating only beams 29 and 52 during all the window length is carried out. Note that this two beams are far enough from each other such that CCI effects can be neglected. The of-

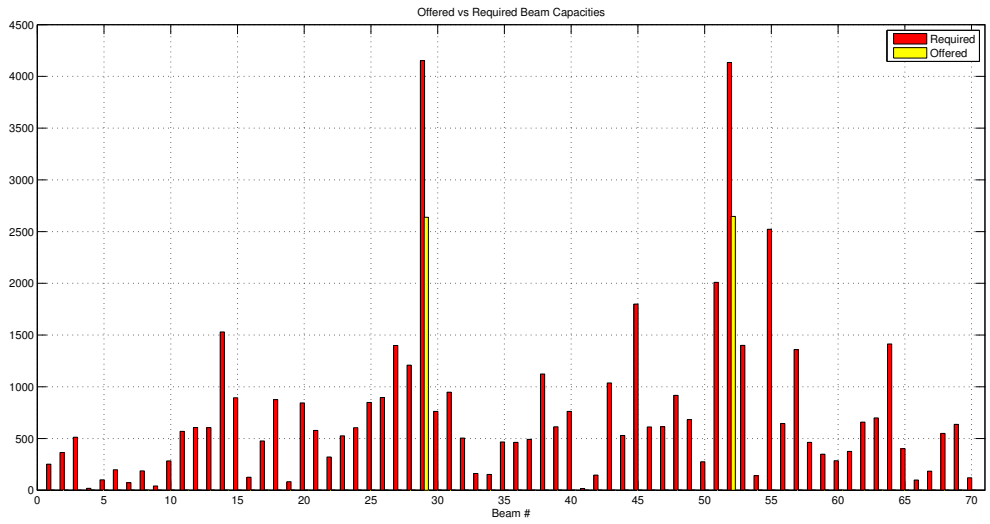


Figure 11: BH upper bound.

fered capacity to these beams under these conditions can be seen in Figure 11. Note from the figure that the maximum capacity that can be offered to a beam is 2.5$Gbps$. However, there are some beams in each of the traffic distributions that are requiring much higher quantities. Two conclusions can be extracted from this result:

- The fact that some beams can not be satisfied even when are illuminated during all the window length implies that the traffic distributions are too demanding for the depicted system. Moreover, this leads to a bias in the performance of the BH algorithms since the algorithms try to serve beams that is not possible to satisfy.
- In order to satisfy this hot-spot beams a satellite system that can offer higher capacities is needed. Current studies are already targeting satellite systems that can offer capacities up to Tb/s, by increasing even more the number of beams.

## D.5 CONCLUSIONS AND DISCUSSION

Results obtained in this work show that BH systems clearly outperform CONV ones in terms of usable capacity and in terms of DC power consumption. Moreover, the satellite payload needs a fewer number of elements resulting in a cheaper satellite launcher and payload. However, some intelligence is necessary in the GW or the satellite side in order to perform the illuminations of the beams and the setting of the input power back-off of the amplifiers in each time-slot properly.

At algorithm level, we have studied the state of the art of current algorithms and we have proposed two new algorithms. From this point of view the fol-

lowing conclusions can be drawn. Our proposed algorithms, *minCCI* and *maxSINR*, improve the performance of the reviewed algorithms in terms of usable capacity. This increase depends on the traffic distributions and is comprehend between a 2% and a 9%. Although the percentage increase is not very high in terms of absolute values is translated in few *Gbps* and comes at no cost. Moreover, we have designed a dual-polarization technique for satisfying hot-spot beams. The technique manages to highly increase the offered capacity to dual polarized beams, however the overall performance of the system in terms of capacity decreases. In terms of power consumption our algorithms perform better than CONV systems while keeping a similar performance with respect to the rest of BH algorithms. Finally, a brief discussion on the suitability of the traffic distributions used has been presented. The main conclusion is that some of the beams in the traffic distributions are demanding too high capacity values for the assumed characteristics of the system. This leads to a false decrease in the performance of the BH algorithms.

## ACKNOWLEDGMENTS

The research leading to these results has received funding from the European Space Agency (ESA) under the PRESTIGE programme.

## REFERENCES

[1] X. Alberti, J.M. Cebrian, A. Del Bianco, Z. Katona, J. Lei, M.A. Vazquez-Castro, A. Zanus, L. Gilbert, and N. Alagha. System capacity optimization in time and frequency for multibeam multi-media satellite systems. In *ASMA Conf. and SPSC Workshop*, pages 226–233, Sept 2010.

[2] J. Anzalchi, A. Couchman, P. Gabellini, G. Gallinaro, L. D'Agristina, N. Alagha, and P. Angeletti. Beam hopping in multi-beam broadband satellite systems: System simulation and performance comparison with non-hopped systems. In *ASMA Conf. and SPSC Workshop*, pages 248–255, Sept 2010.

[3] J.P. Choi and V.W.S. Chan. Optimum multibeam satellite downlink power allocation based on traffic demands. In *Global Telecommunications Conference (GLOBECOM), IEEE*, volume 3, pages 2875–2881, Nov 2002.

[4] J.P. Choi and V.W.S. Chan. Optimum power and beam allocation based on traffic demands and channel conditions over satellite downlinks. *Wireless Communications, IEEE Transactions on*, 4(6):2983–2993, Nov 2005.

[5] F. Joly MP. Kluth S. Taylor C. Elia L. Thomasson, M. Vaissire and R. de Gaudenzi. Ddso: the satellite contribution to european government actions for the e-inclusion of citizens and regions. In *Proceedings of the AIAA International Space Communication Systems Conferences*, 2005.

[6] J. Lei and M.A. Vázquez-Castro. Multibeam satellite frequency/time duality study and capacity optimization. *Communications and Networks, Journal of*, 13(5):472–480, Oct 2011.

[7] M.J. Neely, E. Modiano, and C.E. Rohrs. Power allocation and routing in multibeam satellites with time-varying channels. *Networking, IEEE/ACM Transactions on*, 11(1):138–152, Feb 2003.

# E

# OFFERED CAPACITY OPTIMIZATION MECHANISMS FOR MULTI-BEAM SATELLITE SYSTEMS

**R. Alegre Godoy*, N. Alagha† and M. Á. Vázquez-Castro***

*IEEE ICC*, pages 3180-3184, 2012

ABSTRACT

In this paper we investigate capacity optimization mechanisms for multi-beam satellite systems built on a realistic payload model. The first proposed mechanism deals with long term traffic variations, for which capacity optimization algorithms are proposed based on per-beam traffic requests. Due to the high asymmetry of the traffic, our algorithms provide time and spatial flexibility illuminating a specific set of beams within a window of several time-slots. Our algorithms maximize the amount of capacity actually offered while providing reduced power consumption. The second proposed mechanism deals with short-term traffic variations, for which we propose Network Coding (NC) based techniques at the link layer. The aim is to increase the offered capacity taking advantage of overlapping beam coverage, usually considered as a source of interference. This technique is meant to be applied not only in classical multi- beam systems, but also on top of the per-beam capacity optimization as a method to deal with fast traffic unbalances not evaluated in the first mechanism. Analysis and simulations results show that system capacity can be increased up to 13% in the first case and up to 90% in the second case.

## E.1 INTRODUCTION AND PROBLEM STATEMENT

Increasing the capacity is the main focus in the design of new satellite systems. To this aim, satellite systems have moved from payloads generating one single beam to multi-beam.

* The authors are with the department of Telecommunications and Systems Engineering, Universitat Autònoma de Barcelona.

† The author is with the TEC-ETC section at ESA-ESTEC.

Technologically, increasing the number of beams to very high values in order to offer even higher capacities is not possible without facing important side issues such as the design of complex satellite payloads and the higher impact of satellite instabilities that cause beam displacements [6, 7]. Hence, there is a clear necessity for optimizing the capacity delivered to the User Terminals (UTs) in the system.

The two mechanisms presented in this paper deal with the offered capacity optimization in multi-beam satellite systems from two different points of view. Since traffic requests throughout the coverage are not uniform we propose using an optimization based on a beam-hopping approach to cope with long term traffic variations. Specifically, a window of several time-slots is defined and within each of them a different subset of all the beams is illuminated such that the offered per-beam capacity matches as much as possible the requested. However, traffic is also affected by short term variations due to Internet rush hour or punctual sportive events. For this case, we propose using NC-based techniques in order to increase the offered capacity to UTs under multicast applications by taking advantage of fast traffic unbalances in the requested capacities and latent multiple routes in multi-beam systems. The coding is performed at the link layer, based on finite field coding.

Algorithms for long term traffic variations exploiting time and space flexibility are also proposed in [8] and [4]. The algorithm proposed in [8] is based on the maximization of the Signal to Interference plus Noise Ratio (SINR), i.e. in each iteration all non-satisfied beams are allocated to the time-slot that maximizes its individual SINR until no more beams can be assigned. Optimization process performed in [4] is based on a combination of Genetic Algorithm (GA), Neighborhood Search (NS) and Iterative Local Search (ILS) algorithms. It is worth mentioning that these algorithms do not consider some satellite payload issues that will be described in Section II. Regarding NC techniques over satellite systems there is only little work in the area [5, 10, 2].

This paper complements our previous work in [10] and [2]. In [1] we study algorithms providing spatial and time flexibility comparing the per-beam offered and required capacity and the modulation and codification (MODCOD) distribution of the users. In this paper we simplify the algorithm explanation and provide results from a system point of view rather than the per beam point of view. In [2] we investigate NC techniques for multi-beam satellite systems under Digital Video Broadcasting over IP (DVB-IP) applications. In this work we pose the problem from a traffic requirements perspective in order to deal with short traffic variations. Moreover, we propose a simple criterion to assess the performance gain of NC versus a conventional scheme.

The paper is organized as follows. Section E.2 introduces our proposed payload model, more realistic than in previous works. Section E.3 introduces our proposed optimization for long-term variations. Section E.4 introduces our proposed optimization for short-term variations, in particular a multicast scenario is assumed. Finally, section E.5 draws conclusions from our results.

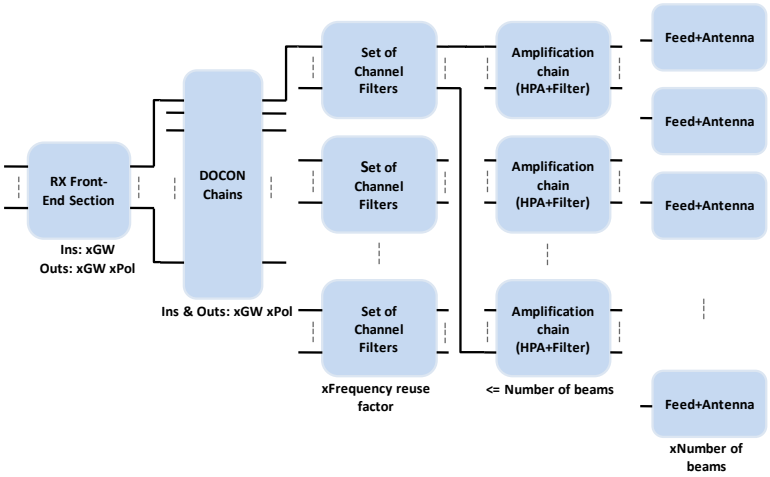


Figure 1: Payload model.

## E.2 SYSTEM AND PAYLOAD MODEL

In this paper we assume a dual-polarized multi-beam system with $N_b$ beams, where the forward link beam to time-slot resource allocation takes place over $W$ time-slots in a beam- hopping fashion. Beams are assigned the entire bandwidth, in one or both polarizations and UTs within a beam are multiplexed using Time Division Multiplexing (TDM).

The satellite payload model assumed is shown in Figure 1 [3]. Signals coming from the gateways (GWs) are filtered in each polarization and amplified using a Low Noise Amplifier (LNA) in the reception front-end section. Then, down- converters (DOCONs) translate each of the information segments to the corresponding downlink frequency. Subsequently, information is separated in the corresponding channels per frequency color and amplified by a combination of a High Power Amplifier (HPA) and a filter. The amplified signal is passed to the beam feeds and antennas such that it can down-shifted to the UTs.

Classically, the number of amplification chains is the same as the number of beams since illumination is continuous. Nevertheless, when allowing spatial and time flexibility the number of amplification chains can become lower, as adopted in this paper. This reduction leads to cheaper satellite launchers and less satellite Direct Current (DC) power consumption. Therefore, beams are grouped and a HPA must be shared among them bringing up a new constraint for the capacity optimization mechanisms.

According to this description, the following parameters characterize the system and payload model:

- $P_{tot}$ denotes the available payload RF power.
- $N_{max}$ is the total number of beams that can be illuminated simultaneously.

- HPAs can be back-offed applying different Output Back-Off (OBO) values from a set of all possible values of back-offing $\Omega$.

## E.3 CAPACITY OPTIMIZATION BASED ON PER-BEAM TRAFFIC REQUESTS

### E.3.1 *Optimization Problem*

Let $R_i$ be the offered capacity per beam defined as:

$$R_i = \frac{BW}{W} \sum_{j=1}^{W} T_{i,j} \log_2(1 + SINR_i^j) \tag{1}$$

where $T_{i,j} = \{0, 1\}$ is a flag indicating if beam $i$ is allocated to time-slot $j$ ($T_{i,j} = 1$) or not ($T_{i,j} = 0$), $BW$ denotes the bandwidth of the system and $SINR_i^j$ denotes the SINR of beam $i$ at time-slot $j$. Assuming that the Digital Video Broadcasting over Satellite, second generation (DVB-S2) is used in the satellite forward link, Eq. (1) can be re-written as:

$$R_i = \frac{R_s}{W} \sum_{j=1}^{W} T_{i,j} f_{DVB-S2}(SINR_i^j) \tag{2}$$

being $R_s$ the system symbol rate and $f_{DVB-S2}$ a function which relates the SINR with a corresponding spectral efficiency value according to DVB-S2 physical layer capabilities. Eq. (2) can be re-formulated as:

$$R_i = \frac{R_s}{W} i \begin{bmatrix} f_{DVB-S2}(SINR_i^1) \\ \vdots \\ f_{DVB-S2}(SINR_i^W) \end{bmatrix} \tag{3}$$

where $i \in \{0, 1\}^{1 \times W}$ is a vector containing all $T_{i,j}$ flags for beam $i$. SINR for the $i$-th beam at time-slot $j$ can be retrieved by:

$$SINR_i^j = \frac{A_i P_{i,j}}{N_0 + \sum_{r \in \phi_{cc}} A_r P_{r,j}} \tag{4}$$

where $P_{i,j}$ is the power allocated to beam $i$ in time-slot $j$, $N_0$ is the spectral noise density, $A_i$ denotes the channel and propagation attenuation at beam $i$ and $\phi_{cc}$ is the set of beams simultaneously illuminated except for beam $i$. Let $\hat{R}_i$ be the required capacity per beam. Now, the objective of the optimization is accommodating beams to time- slots such that each beam $i$ is offered a capacity value $R_i$ as close as possible to the required capacity $\hat{R}_i$, *i.e.* maximize the offered capacity. This can be mathematically formulated as:

$$\begin{aligned} &\max_{i,P_{i,j}} \sum_{i=1}^{N_b} R_i(i, P_{i,j}) \\ &\quad subject \quad to \qquad R_i \leq \hat{R}_i \\ &\qquad\qquad \sum_{i=1}^{N_b} \sum_{j=1}^{W} P_{i,j} \leq P_{tot} \\ &\qquad\qquad \sum_{i=1}^{N_b} T_{i,j} \leq N_{max} \end{aligned} \tag{5}$$

The optimization problem in Eq. (5) is not convex as stated in [8]. A number of heuristic solutions based on iterative/combinatorial algorithms have already been proposed in the literature. Usually, the proposed approach is based on filling a power plan and frequency plan matrices, $\mathbf{F}_p \in \{0,1\}^{N_b \times 2W}$ and $\mathbf{P}_p \in \mathbb{R}^{N_b \times 2W}$ respectively. $\mathbf{F}_p$ and $\mathbf{P}_p$ indicate if a beam is illuminated in certain time-slot and the power assigned to that beam respectively. Each of the matrices is divided in two blocks, the first one including the columns 1 to $W$ indicating allocations in one polarization. The second block includes columns $W$+1 to $2W$ and indicates allocations in the alternate polarization.

### E.3.2 *Heuristic Algorithms*

We propose two new algorithms which follow the same procedural approach as described above but introducing additional modifications. Both algorithms share a pre- allocation stage that allocates each of the beams to one single time-slot. The reason for this pre-allocation is that when HPAs are shared it can cause some of the beams not being illuminated at any time during the window length. Hence, this stage ensures that each beam is at least allocated once in $\mathbf{F}_p$ and $\mathbf{P}_p$. Following, we introduce our two proposed algorithms, namely Iterative Minimal Co-channel Interference (minCCI) and Iterative SINR Maximization (maxSINR) algorithms.

MinCCI algorithm is based on the observation that it is possible to illuminate beams far from each other such that CCI is almost negligible. This causes an increase in the SINR and therefore in the offered capacity. To this aim, the set $\psi_{i,j}$ containing the beams adjacent to i that are illuminated in time- slot j is defined. The algorithm also performs an optimization through the different OBO values to find the optimal one.

MaxSINR algorithm follows the principles of the one described in [8], assigning beams to the time-slots that maximize the individual SINR of the beam. However, in this case also an optimization through different OBO values is performed. Note that both proposed algorithms use the payload model described in Section E.2 by implementing the sharing of the HPAs using the flag $\chi_{i,j}$. The latter indicates whether HPA assigned to beam $i$ is in use in time-slot $j$ ($\chi_{i,j} = 1$) or not ($\chi_{i,j} = 0$). Moreover, an additional degree of freedom for the optimization process is added, *i.e.* the optimization through different OBO values. Under certain CCI patterns reducing the power transmitted can increase the SINR, and hence the offered capacity at the same time that consumption

Table 1: Iterative minimal CCI Algorithm.

1. **Build set** $A_s$ **with non satisfied beams** $(R_i/\hat{R}_i) < 1$
2. **Sort set** $A_s$ **from less-satisfied to more satisfied**
3. **while** $A_s \neq 0$ **and** $\sum_{i=1}^{N_b}\sum_{j=1}^{2W} P_{i,j} < P_{tot}$ **and** $j < W$
   **for each** $j$
   **Illuminate in** $\mathbf{F}_p$ **a beam of** $A_s$ **s.t.** $\chi_{ij} = 0$**,** $\psi_{ij} = 0$ **not** $N_{max}$ **beams illuminated**
   **Compute optimal OBO value from** $\Omega$ **and assign it to** $\mathbf{P}_p$
   **Update** $R_i$
   **Re-build and re-sort set** $A_s$

Table 2: Iterative SINR Maximization Algorithm.

1. **Build set** $A_s$ **with non satisfied beams** $(R_i/\hat{R}_i) < 1$
2. **Sort set** $A_s$ **from less-satisfied to more satisfied**
3. **while** $A_s \neq 0$ **and** $\sum_{i=1}^{N_b}\sum_{j=1}^{2W} P_{i,j} < P_{tot}$
   **for each** $i$ **in** $A_s$
   **Allocate beam in** $\mathbf{F}_p$ **to** $j$ **that maximizes of** $SINR_i^j$ **s.t.** $\chi_{ij} = 0$**, not** $N_{max}$ **beams illuminated**
   **Update** $R_i$
   **Re-build and re-sort set** $A_s$
4. **Compute optimal OBO value from** $\Omega$ **for each** $j$ **and assign it to** $\mathbf{P}_p$
5. **Update** $R_i$

**end**

is reduced. We also allow beam dual-polarization in order to increase the offered capacity to hot spot-beams. Table 1 and Table 2 show the two different proposed optimization stages, in pseudo-code with indentation.

Note that both algorithms are designed for long term traffic variations because the optimization process is not immediate and can not be applied in a time-slot basis.

### E.3.3 *Results*

In order to compare the performance of our proposed algorithms with those in [8] and [4], we carry out simulations over a 70 beam system covering Europe. For comparison purposes performance of a conventional scheme is also included. Table 3 shows the system characteristics. Figure 2 shows the required capacity for some pre-selected beams versus the offered capacity by each of the algorithms. Algorithms in [8] and [4] are abbreviated *Convex* and *Genetic*

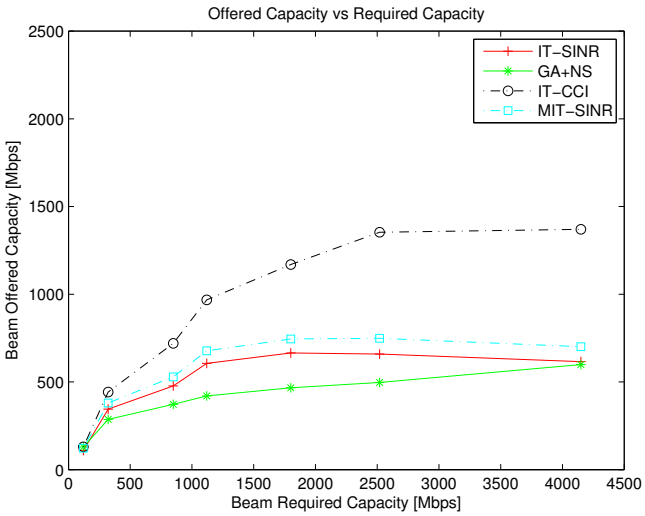


Figure 2: Required vs Offered Capacities.

respectively. Note that our proposed minCCI and maxSINR algorithms assign higher offered capacities to the beams than the rest of the algorithms providing time and space flexibility. Specifically, minCCI algorithm achieves the best results and manages to offer high capacity values even to beams with high capacity requests. A conventional system with the characteristics depicted in Table 3 offers a 500 Mbps capacity to each beam independently of the requested capacity, showing an important waste of resources.

## E.4 CAPACITY OPTIMIZATION BASED ON NETWORK CODING

In this section we introduce a preliminary study on the capacity optimization based on NC. Obtained results are based on the analysis of a fictitious simple scenario of three beams. In order to obtain reference values for the simulations we use the reference numerical values in Table 3 of a typical multi- beam

Table 3: System Characteristics

| **Parameter** | **Value** | |
|---|---|---|
| System Type | Flexible | Conventional |
| $P_{twta}$ | 131W | |
| Coloring | 2 | 4 |
| $W$ | 12 | - |
| $R_s$ | 360Mbauds | |
| Number of HPAs | 35 | 70 |
| OBO | Variable | 1.11dB |
| Traffic demand | 50.6Gbps | |

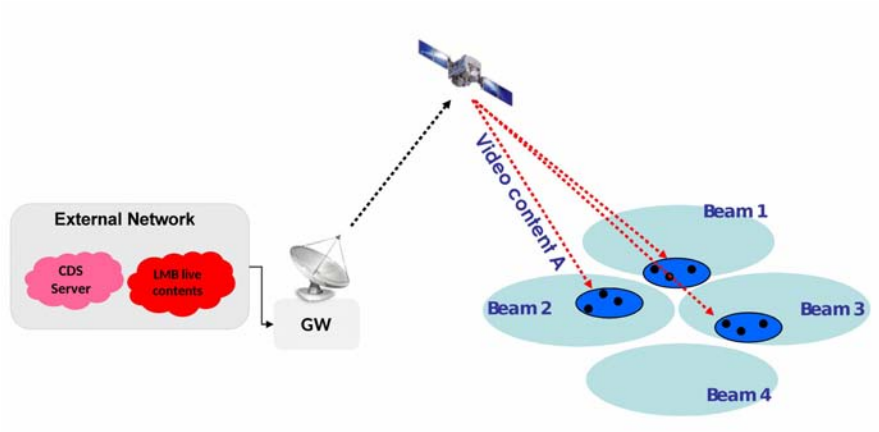


Figure 3: Fictitious scenario for NC technique analysis.

scenario. The applicability of the technique to a realistic system needs further investigation.

### E.4.1 *Optimization Problem*

While the previously shown algorithms are applicable to long term variations, there may still be traffic unbalances due to fast traffic variations that require of additional optimization techniques. For this short-term variations we propose to optimize the coding at link layer level of transmitted flows, such that offered capacity in multicast applications can be increased. Our technique takes also advantage of the fact that UTs close to the border with an adjacent beam receive enough SINR level from it to decode the signal. This effect that traditionally has been considered as interference can be seen as an extra path to reach a user.

### E.4.2 *NC Based Optimization*

In order to illustrate our proposed optimization algorithm based on NC we identify the fictitious scenario shown in Figure 3 not thorough for a realistic system. The example shows an architecture consisting of a GW and a set of multicast groups $MG_i$ spread throughout the coverage. Multicast groups are defined as set of UTs which are under similar channel conditions and request the same type of video content [9]. This example could represent upcoming IPTV services such as Content Delivery Services (CDS) or Live Multimedia Broadcast (LMB).

Figure 4 shows the equivalent network graph, where node $S$ represents the satellite and nodes $B_{i=1,2,3}$ and $MG_{i=1,2,3}$ represent the user beams and multicast groups respectively. Note that each multicast group is reachable from two different paths. Additionally, we assume there is an adjacent beam to the location of the UTs where $\hat{R}_i \leq R_i$ due to a short term variation, *e.g.* beam 1 in Figure 3. In a traditional system the offered multicast capacity can be written as:

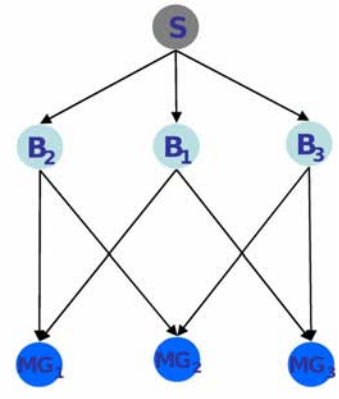


Figure 4: Theoretical NC graph.

$$R_{MG_i}^{CONV} = R_s \eta_{LL} \eta_{i,j} \tag{6}$$

where $\eta_{LL}$ is the encapsulation efficiency at the link layer and and $\eta_{i,j}$ is the physical layer spectral efficiency assigned to multicast group $i$ observed from assigned beam $j$ and its value is a function of the multicast group SINR. When using NC, in each of the paths $\{B_i, MG_i\}$ a coded packet is sent. Therefore, offered multicast capacity can be expressed as:

$$R_{MG_i}^{NC} = 2R_s \eta_{LL} \min(\eta_{i,1}, \eta_{i,2}, ..., \eta_{i,h}) \tag{7}$$

where $h$ is the total number of paths observed by the multicast group, e.g. two in Figure 4. From this theoretical analysis we build the algorithm shown in Table 4. The algorithm finds a beam with sparing resources adjacent to the multicast groups. Then, is selected the scheme that provides more favorable offered capacity to all $C$ multicast groups, (with or without NC). Subsequently, the GW changes the operation mode.

### E.4.3 *NC System Level coding process*

The coding process is performed at the link layer using Random Linear Network Coding (RLNC). Specifically, a link layer packet $P_i$ of length $L$ is divided in $N$ symbols $S_{i1}, S_{i2}, ..., S_{iN}$ of $m$ bits, *i.e.* each $S_{ij}$ belongs to a finite field $\mathbf{F}_q$ with $q = 2^m$. Each link layer coded symbol of a coded packet is generated by mixing h symbols of native packets:

$$c_{xj} = \alpha_{x1} S_{1j} + \alpha_{x2} S_{2j} + ... + \alpha_{xh} S_{hj} \in \mathbf{F}_q \tag{8}$$

where $c_{xj}$ is the $j$-th coded symbol of coded packet $x$ and $\alpha_{x1}, \alpha_{x2}, ..., \alpha_{xj}$ are coefficients chosen at random from $\mathbf{F}_q$. Hence, each coded packet is built joining the $N$ generated coded symbols, $C_x = c_{x1}, c_{x2}, ..., c_{xN}$. The coefficients used or generating the coded symbols, $\alpha_{x1}, \alpha_{x2}, ..., \alpha_{xj}$, are added in the packet header. UTs belonging to multicast groups receive $h$ different coded

Table 4: NC Multicast Capacity Optimization Algorithm

1. **if adjacent beam with** $R_i/\hat{R}_i<1$
   **for each** $MG_i$ **compute** $R_{MG_i}^{CONV}$ **and** $R_{MG_i}^{NC}$
   **if** $\sum_{i=1}^{C} R_{MG_i}^{CONV} > \sum_{i=1}^{C} R_{MG_i}^{NC}$
   **Send packets conventionally**
   **else**
   **Send packets network coded through each path**

**end**

packets (2 packets in Figure 4) and must solve a linear system of equations in $\mathbf{F}_q$ as Eq. (9) shows.

$$\begin{bmatrix} \alpha_{11} & \alpha_{12} & \cdots & \alpha_{1h} \\ \alpha_{21} & \alpha_{22} & \cdots & \alpha_{2h} \\ \vdots & \vdots & \ddots & \vdots \\ \alpha_{h1} & \alpha_{h2} & \cdots & \alpha_{hh} \end{bmatrix}^{-1} \begin{bmatrix} c_{1j} \\ c_{2j} \\ \vdots \\ c_{hj} \end{bmatrix} = \begin{bmatrix} S_{1j} \\ S_{2j} \\ \vdots \\ S_{hj} \end{bmatrix} \tag{9}$$

Note that both the GW and the UTs need an added complexity in order to perform the encoding/decoding.

### E.4.4 *Results*

In order to test the performance of our algorithm, we build the simple scenario shown in Figure 3. Each multicast group is assigned a MODCOD from DVB-S2 16APSK-3/4 with respect its own beam, since this is the most common MODCOD for users out of the center of the beam in multi-beam satellites. The rest of system parameters are set as in Table 3. Link layer encapsulation efficiency is set to 5%, high enough to include the encoding coefficients in the headers of the packets. Figure 5 shows the offered capacity by a traditional and a network coded scheme as a function of the spectral efficiency observed by the additional beam.

The figure shows when to switch from the traditional scheme to a NC-based scheme. Note that the offered capacity improvement obtained by the NC-based scheme respect to the traditional one for those multicast groups observing two paths is up to a 90%. Such improvement is obtained when the spectral efficiency observed from the external beam is the same as the own beam, *i.e.* in the edge of the beam.

These preliminary good results in our simple scenario show the potential of our presented ideas. Further work includes tests in a realistic setting both at system and traffic levels.

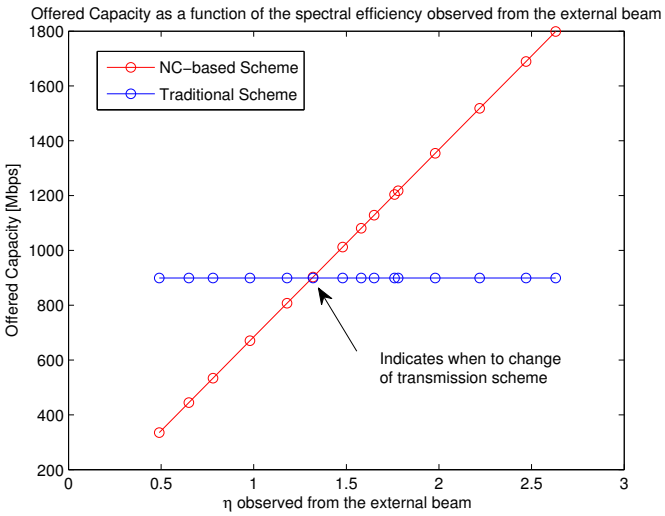


Figure 5: Theoretical offered capacity.

## E.5 CONCLUSIONS

In this paper we have presented two optimization techniques which deal with long-term and short-term traffic variations in multi-beam satellite systems built on a realistic payload model. For the long-term variations we have proposed an optimization based on the per-beam traffic requests. Specifically, the two algorithms we propose increase the offered capacity up to 13% with respect to other algorithms in the literature. Such improvement is obtained due to key modifications introduced such as realistic OBO values and beam dual-polarization.

For the short-term variations a NC-based optimization for multicast traffic is adopted. Our technique takes advantage of overlapping beam coverage, traditionally considered as interference. Depending on the channel conditions observed by the multicast group, the algorithm we propose can change the transmission scheme from a traditional to NC-based one. The combination of data flows allows obtaining a significant improvement in the offered multicast capacity to be proved in realistic set-ups.

## ACKNOWLEDGEMENTS

The research leading to these results has received funding from the European Space Agency (ESA) under the PRESTIGE programme.

## REFERENCES

[1] R. Alegre-Godoy, N. Alagha, and M. A. Vázquez-Castro. Heuristic algorithms for flexible resource allocation in beam hopping multi-beam

satellite system. In *29th AIAA International Communications Satellite Systems Conference*, 2011.

[2] R. Alegre-Godoy, S. Gheorghiu, N. Alagha, and M. A. Vázquez-Castro. Multicasting optimization methods for multi-beam satellite systems using network coding. In *29th AIAA International Communications Satellite Systems Conference*, 2011.

[3] Ricard Alegre-Godoy, Maria Angeles Vázquez-Castro, and Lei Jiang. Unified multibeam satellite system model for payload performance analysis. In *PSATS*, volume 71, pages 365–377, 2011.

[4] J. Anzalchi, A. Couchman, P. Gabellini, G. Gallinaro, L. D'Agristina, N. Alagha, and P. Angeletti. Beam hopping in multi-beam broadband satellite systems: System simulation and performance comparison with non-hopped systems. In *ASMA Conf. and SPSC Workshop*, pages 248–255, Sept 2010.

[5] G. Cocco, C. Ibars, and O. del Rio Herrero. Cooperative satellite to land mobile gap-filler-less interactive system architecture. In *ASMA Conf. and SPSC Workshop*, pages 309–314, Sept 2010.

[6] P. Gabellini and N. Gatti. Advanced optimization techniques for satellite multi - beam and reconfigurable antenna and payload systems. In *Antennas and Propagation (EuCAP), The Second European Conference on*, pages 1–6, Nov 2007.

[7] J.-D. Gayrard. Terabit satellite: Myth or reality? In *Advances in Satellite and Space Communications (SPACOMM), First International Conference on*, pages 1–6, July 2009.

[8] J. Lei and M.A. Vazquez-Castro. Multibeam satellite frequency/time duality study and capacity optimization. *Communications and Networks, Journal of*, 13(5):472–480, Oct 2011.

[9] D. Pradas and M.A. Vazquez-Castro. Num-based fair rate-delay balancing for layered video multicasting over adaptive satellite networks. *Selected Areas in Communications, IEEE Journal on*, 29(5):969–978, May 2011.

[10] F. Rossetto. A comparison of different physical layer network coding techniques for the satellite environment. In *ASMA Conf. and SPSC Workshop*, pages 25–30, Sept 2010.

F

# MULTICASTING OPTIMIZATION METHODS FOR MULTI-BEAM SATELLITE SYSTEMS USING NETWORK CODING

**R. Alegre Godoy*, S. Gheorghiu†, N. Alagha‡ and M. Á. Vázquez-Castro***

*AIAA ICSSC*, 2011

ABSTRACT

In this paper we propose using Network Coding (NC) techniques to increase the ca- pacity in the forward link of multi-beam satellite systems. In particular, we focus on upcoming multicast applications over satellite systems such as Digital Video Broadcasting over IP Networks offering TV services (DVB-IPTV). Our proposed coding scheme takes advantage of inter-beam interference, usually considered as a waste of capacity. Network coded packets are sent from the Gateway (GW) to the user terminals (UTs) through the latent multiple available routes from beam overlapping. We present a theoretical analysis of the upper-bound of the obtained capacity improvement assuming ideal error-free channel based on the equivalent network graphs. Further, we obtain from simulation the overall performance showing the additional improvement in reliability for users in the inter-beam interference areas. Theoretical analysis and simulation results over a reference 70 beam system show that multicast capacity can improve up to 90% in the inter-beam interference areas while overall reliability can improve up to 25% for admissible multicast transmission delay.

* The authors are with the department of Telecommunications and Systems Engineering, Universitat Autònoma de Barcelona.

† The author is with the Universitat Politècnica de Catalunya.

‡ The author is with the TEC-ETC section at ESA-ESTEC.

## F.1 INTRODUCTION

New satellite systems aim to offer highly personalized contents in order to equate to the services provided to traditional terrestrial networks such as 3G and optical fiber networks. Hence, the general system design framework focuses on increasing the offered capacity to the users, which has lead satellite systems moving from sigle beams scenarios to scenarios with a larger number of beams. The smaller size of the beams and the frequency re-use throughout the coverage manages to highly increase the offered capacity.

However, multicasting, which is one of the cornerstones for providing personalized contents, is still based on the simple approach of duplicating packets through each of the beams without performing any optimization [6]. More recent work approach the multicasting by applying Network Utility Maximization (NUM) over a cross-layer differentiated services (Diffserv) architecture, however NUM is applied in a per-beam basis [7].

In this work we propose to optimize the coding at link layer of transmitted flows such that the offered multicast capacity can be increased. To this aim, we design a NC method for multi-beam satellite systems. The NC paradigm is known to increase the offered system capacity in multicast applications by mixing the information coming from several paths rather than assuming the conventional "store and forward" way of sending the information. Although the topic has been already studied for satellite networks [6, 7], none of them approaches the multi-beam scenario. Specifically, we propose to send random linear combinations in a finite field of link layer packets to each user beam. Since we consider beam overlapping as a source of information rather than interference, UTs are able to receive coded packets from multiple routes. For the proposed technique we obtain an upper bound for its performance by assuming ideal channel conditions. Moreover, we investigate the performance of our NC method over a realistic lossy channel. Theoretical analysis and simulation results show that multicast capacity can be highly increased, with a small increase in complexity.

The reminder of the paper is organized as follows. Section F.2 introduces the assumed multi-beam system model by describing each of the elements constituting the architecture. Section F.3 describes the proposed NC method in details and includes an analysis of the performance over the ideal and realistic channel model. In Section F.4 we analyze theoretically the upper bound obtained in Section F.3. Finally Section F.5 shows simulation results for the realistic channel and Section F.6 draws conclusions on the work done.

## F.2 SYSTEM MODEL

### F.2.1 *Architecture*

Throughout this paper we assume a multi-beam satellite system under a multicast application. Figure 1 shows the reference system architecture.

The elements constituting the architecture are the following:

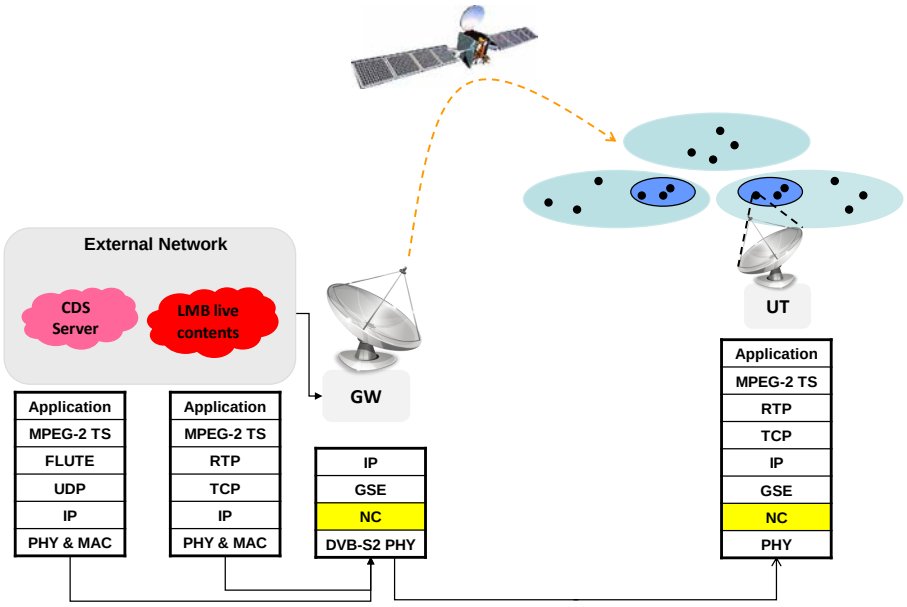


Figure 1: Reference system architecture.

- A GW which sends multicast information to a set of users.
- A satellite which down-shifts the information received from the GW to sets of users.
- Sets of UTs which are grouped into multicast groups. A multicast group is defined as a set of UTs which are under similar channel conditions and aiming to receive the same information [7].

The process to send the information is as follows. Each satellite GW is associated to a server that provides multicast content. The foreseen multicast application comprising encapsulation from the application to the network layer will be described in the next section. The lower layers are structured as in Table 1. IP packets are encapsulated using the Generic Stream Encapsulation (GSE) protocol. At this point an intermediate NC sub-layer is defined such that coding operations are performed right before the Digital Video Broadcasting over Satellite $2^{nd}$ generation (DVB-S2) physical layer frame is built and the information is sent to the satellite.

On the receiver side the reverse process is carried out, i.e. after physical layer de-encapsulation has been performed, network coded packets must be decoded in order to obtain the former GSE packets. Once the GSE headers have been extracted the information can be sent to upper layers. Although Multi-Protocol Encapsulation (MPE) is the most common standard used in the link layer of satellite systems, we rather prefer to use the GSE standard because it allows us to extend the headers of the packets by adding extra fields [5]. This

Table 1: Lower layers protocol stack

| OSI | User Plane |
|---|---|
| **Link Layer** | GSE |
| | NC |
| **Physical Layer** | DVB-S2 PHY |

is a key feature for the practical implementation of NC in satellite systems as it will be shown in Section F.3.

Moreover, for the reference architecture in Figure 1 we assume the following. First, UTs located in a certain beam are able to receive information from an adjacent beam since the observed Signal to Interference plus Noise Ratio (SINR) is high enough. This is a feasible assumption produced by beam overlapping areas which are traditionally considered as interference. Figure 2 shows the effect for two beams of a reference 70 beams scenario. The figure describes a scenario where the satellite is transmitting, in a certain polarization and frequency band, to beam A with center coordinates $U, V = [-2.05, 8]$ and to the red circled beams following the typical conventional scheme of coloring generating a certain co-channel interference level (CCI). Points inside the beam indicate the received SINR at such coordinates. Note that beam B with center coordinates $U, V = [-2.1, 7.5]$ should be operating in another frequency and/or polarization. However, the figure shows that some UTs of beam B are potentially able to decode the signal transmitted to A since the SINR that they receive is high enough. Specifically, note that points inside beam B close to beam A experience higher SINR values than points in B that are further from A. As a DVB-S2 physical layer has been assumed, the lowest SINR that can be decoded by a terminal is -2.2dB corresponding to the modulation and codification pair (MODCOD) QPSK-1/4 [3]. Therefore, in the figure shown all the UTs of beam B situated between its center and the border with A would be able to decode the signal in A.

Second, we assume that UTs have extended reception capabilities in order to be able to decode information from its own beam and from an adjacent one. Hence, UTs are able to listen and decode two polarizations or two frequency bands or both, simultaneously. Finally, we assume UTs are able to perform algebraic operations in finite fields.

### F.2.2 *Target Application*

The target multicast application we consider is the transmission of IP and IPTV contents which are strongly based on multicast. Specifically, we focus on DVB-IP and DVB-IPTV [2] standards which include two services intended for multicasting, Content Download Services (CDS) and Live Multimedia Broadcasting (LMB):

- CDS allows UTs to download a set of video contents and save it in a local storage for further reproduction. This application is used for providing

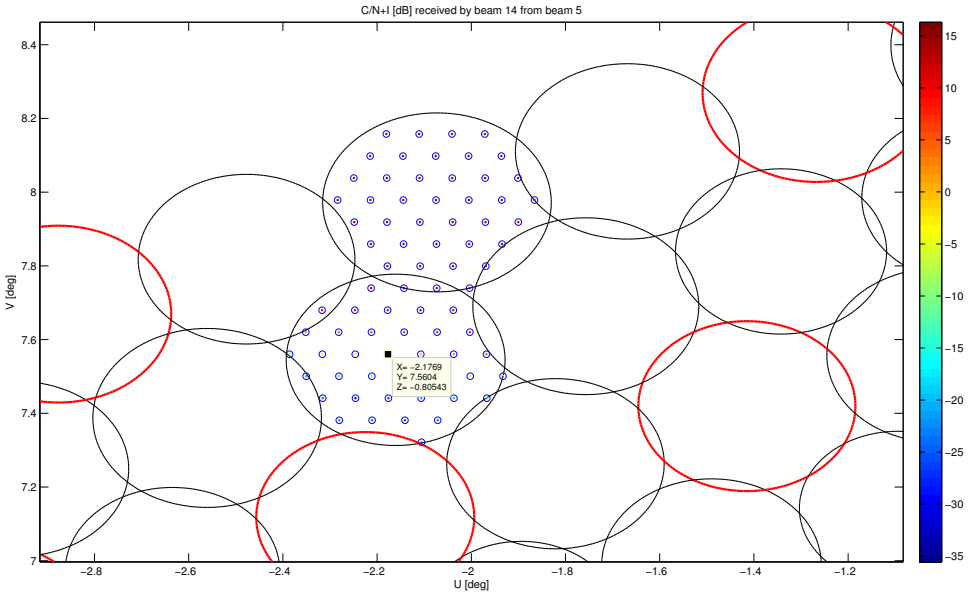


Figure 2: SINR beam grid.

IPTV services in geographic areas where the broadband connection is not suitable for real streaming services. CDS dispose of two operation modes:

  - Push Download: The content distribution is decided by the Service Provider.
  - Pull Download: The content distribution is decided by the user.

- LMB allows UTs to receive live TV contents as in traditional broadcast, however the information is sent in a multicast manner.

Table 2 and Table 3 show the protocol stack, user and control plane, for CDS and LMB services respectively.

Both CDS and LMB encapsulate video into MPEG-2 Transport Streams (MPEG-2 TS). However since LMB transmit real time contents transport layer encapsulation is performed through a combination of Real Time Protocol (RTP) and Transport Control Protocol (TCP) in order to ensure reliability in the data

Table 2: CDS Protocol Stack

| **OSI** | **User Plane** | **Control Plane** |
|---|---|---|
| **Application Layer** | Video Content | Multicast Group |
| | MPEG-2 TS | |
| **Transport Layer** | FLUTE | IGMP |
| | UDP | |
| **Network Layer** | IP | IP |
| **Lower Layers** | - | - |

Table 3: LMB Protocol Stack

| OSI | User Plane | Control Plane |
|---|---|---|
| **Application Layer** | Video Content | Multicast Group |
| | MPEG-2 TS | 33 |
| **Transport Layer** | RTP | IGMP |
| | TCP | |
| **Network Layer** | IP | IP |
| **Lower Layers** | - | - |

delivery. On the other hand CDS performs the encapsulation through a combination of File Delivery Over Unidirectional Transport (FLUTE) protocol and User Datagram Protocol (UDP). The obtained transport layer datagrams in both cases are encapsulated into IP packets resulting in the encapsulation process shown in Figure 1. Note that both services use Internet Group Membership Protocol (IGMP) in order to discover the sets of UTs belonging to each multicast group at any time.

### F.2.3 *Multi-beam Scenarios to graphs mapping*

The fact that UTs within a beam are able to listen information from an adjacent beam means that UTs can be reached through multiple routes. Hence, a multi-beam scenario with $N_b$ and $N_c$ multicast groups composed of several UTs can be conceptually translated into the network graph shown in Figure 3.

Node S represents the satellite which spans to $N_b$ beam nodes $B_i$. After each beam node we add a virtual node that models the broadcast nature of the channel. Finally, $N_C$ multicast groups $MG_j$ receive information from one or two beams. This mapping from a general scenario to a network graph allows us to analyze the problem from a theoretical perspective, away from practical bounds. Note that it is even possible that a UT observe up to three different paths simultaneously if the overlapping areas comprised three beams. However, the physical layer of the UT would become very complex. For this reason we keep the maximum number of paths that can be observed up to a maximum of 2.

## F.3 NETWORK CODING METHOD

In order to illustrate our proposed NC technique we identify a representative example shown in Figure 4. The example shows an architecture consisting of a GW transmitting CDS and/or LMB contents to a set of multicast groups $MG_{i=1,2,3}$ spread throughout the coverage.

The coding process is performed at the link layer, on the GW side, using Random Linear Network Coding (RLNC). Specifically, we consider NC operations are performed over groups of $h$ link layer packets. Then, we assume link layer packets $P_1, ..., P_h$ are all of length $L$ and divided in $N$ symbols $S_{i1}, S_{i2}, ..., S_{iN}$ of

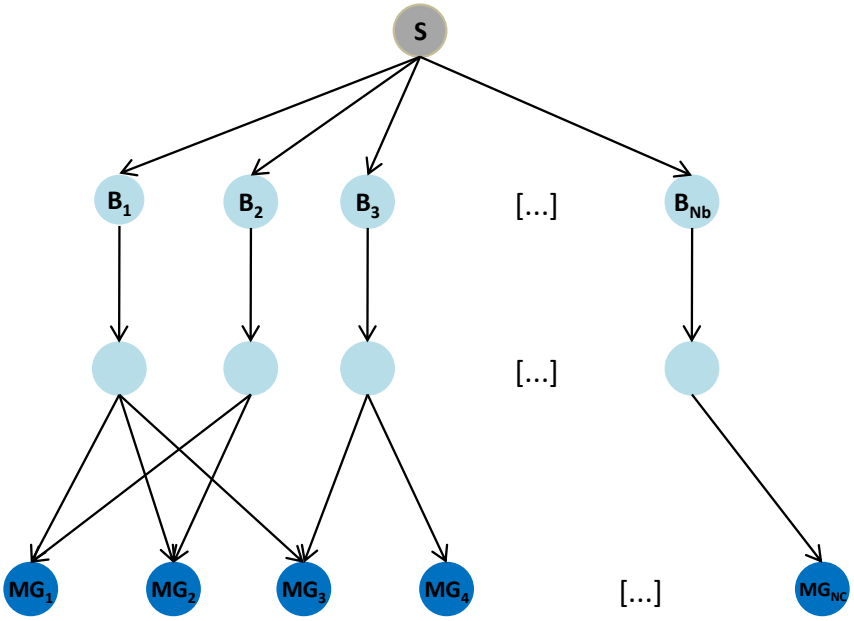


Figure 3: Multi-beam satellite scenario to graph mapping.

$m$ bits, i.e. each $S_{ij}$ belongs to a finite field $\mathbf{F}_q$ with $q = 2^m$. Link layer coded symbols of a coded packet are generated by:

$$c_{xj} = \alpha_{x1} S_{1j} + \alpha_{x2} S_{2j} + ... + \alpha_{xh} S_{hj} \in \mathbf{F}_q \tag{1}$$

where $c_{xj}$ is the $j$-th coded symbol of coded packet $x$ and $\alpha_{x1}, \alpha_{x2}, ..., \alpha_{xj}$ are coefficients chosen at random from $\mathbf{F}_q$. Hence, each coded packet is built by joining the $N$ generated coded symbols, $C_x = \{c_{x1}, c_{x2}, ..., c_{xN}\}$. Since we adopt the GSE protocol for the link layer packets, the coefficients $\alpha_{x1}, \alpha_{x2}, ..., \alpha_{xj}$ used for generating the coded symbols can be added in the header of the packets as an extra field. Although this implies a small overhead, it allow the receivers knowing the encoding coefficients in order to retrieve again the native packets [1]. The number of coded packets $h$ to be sent is chosen by the GW and depends on the path diversity and the channel conditions of the multicast groups.

In the receiver side, UTs belonging to multicast groups must receive at least $h$ different coded packets. The terminals read the headers of the packets to obtain the encoding coefficients and solve a linear system of equations in $\mathbf{F}_q$ to retrieve the native packets as shown in Eq. (2).

$$\begin{bmatrix} \alpha_{11} & \alpha_{12} & \cdots & \alpha_{1h} \\ \alpha_{21} & \alpha_{22} & \cdots & \alpha_{2h} \\ \vdots & \vdots & \ddots & \vdots \\ \alpha_{h1} & \alpha_{h2} & \cdots & \alpha_{hh} \end{bmatrix}^{-1} \begin{bmatrix} c_{1j} \\ c_{2j} \\ \vdots \\ c_{hj} \end{bmatrix} = \begin{bmatrix} S_{1j} \\ S_{2j} \\ \vdots \\ S_{hj} \end{bmatrix} \tag{2}$$

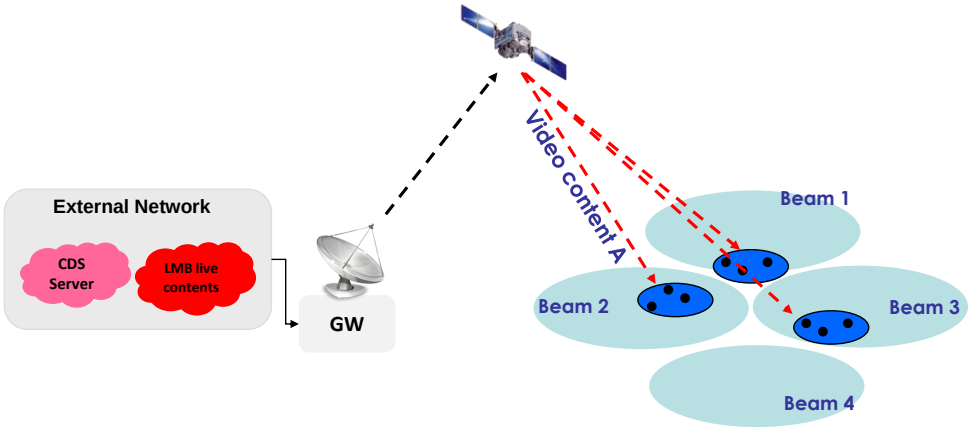


Figure 4: Representative example for the NC technique analysis.

Note that in order to perform such encoding and decoding operations both the GW and the UTs need an added complexity.

### F.3.1 *Theoretical upper bound*

In order to obtain a theoretical upper bound we analyze the network graph in Figure 5. Note that this graph is equivalent to the scenario in Figure 4 assuming an ideal channel and that each of the the multicast groups is able to observe information from two different beams, i.e. from two different paths. Therefore, this is a best case scenario that allows us to derive an upper-bound performance.

In a traditional multi-beam system, where packets are sent uncoded and beam overlapping is considered as interference, the offered multicast capacity at the link layer to multicast group $MG_i$ can be expressed as:

$$R_{MG_i} = R_s \eta_{LL} \eta_{i,j} \qquad \forall i \tag{3}$$

where $R_s$ is the system symbol rate, $\eta_{LL}$ is the encapsulation efficiency at the link layer and $\eta_{i,j}$ is the spectral efficiency assigned to multicast group $i$ observed from assigned beam $j$ and its value is a function of the multicast group SINR. When using NC in this scenario, in each of the paths $\{B_i, MG_i\}$ is sent one coded packet. Therefore, the offered multicast capacity can be expressed as:

$$R_{MG_i} = h R_s \eta_{LL} \min(\eta_{i,1}, \eta_{i,2}, ..., \eta_{i,h}) \qquad \forall i \tag{4}$$

where $h$, the number of sent to each multicast group, equates in this case to the number of the paths observed. For the graph shown in Figure 5, $h = 2$. Note that Eq. (4) states that in an ideal channel, our proposed NC technique can offer, for each of multicast group, $h$ times the capacity of the path with worst channel conditions.

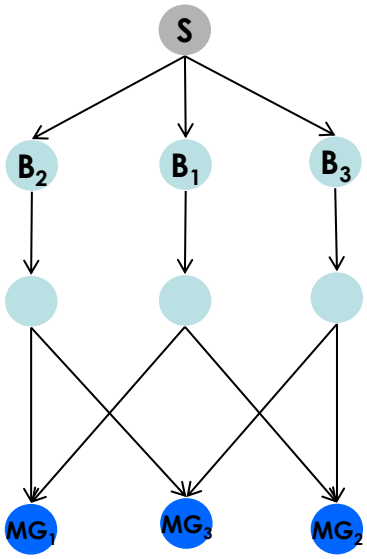


Figure 5: Theoretical graph for error free channel.

### F.3.2 *Reliability improvement*

In the previous section we assumed each multicast group was able to observe information from two beams (paths) simultaneously. However, in a real scenario just some of the multicast groups will observe such path diversity. Moreover, those multicast groups located in the overlapping areas of two beams might experience packet losses. Within a multicast application those errors can be produced by the following reasons:

- The UTs belonging to the multicast group in the overlapping areas attempt to decode a MODCOD with the same order than multicast groups located in more centered zones within the beam. Since the SINR observed in the edge of the beam is lower than in the center some of the packets can not be decoded causing packet losses.
- Multicast groups in the overlapping areas, i.e. in the edge of the beams, are more affected by climatological events than multicast groups in the center of the beams causing that some packets are lost during the transmission.

In order to model such realistic scenario we map the scenario in Figure 4 into the network in Figure 6. The GW sends $h$ network coded packets to $MG_1$ and $MG_2$ which are located in the center of the beam such that packets are decoded with o error probability. $MG_3$ is able to decode information from two beams but since UTs are located in the overlapping area, they experience some packet losses.

Specifically, $MG_3$ receives packets according to a two-state Gilbert model for a bursty wireless channel. When a channel is in state $S_i$, then it receives a packet erroneously with probability $e_i$, with $0 \leq e_i \leq 1$ for $i \in \{1, 2\}$. Moreover,

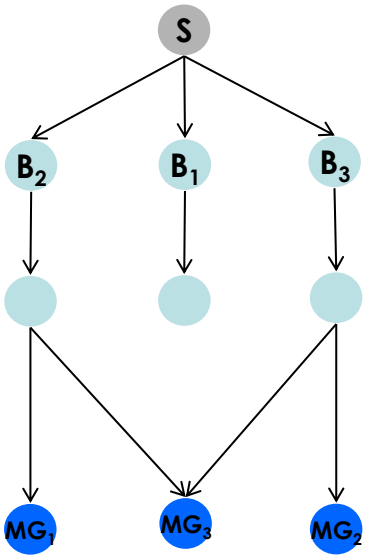


Figure 6: Theoretical graph for erasure channel.

$e_0 < e_1$, which means that the state $S_0$ is associated to a "good" channel state, where the packets are received with a high probability, and $S_1$ represents a "bad" channel state, where the packets are lost with a high probability. The transition matrix $\mathbf{Q}$ for the channel, for the Gilbert model under consideration is given by:

$$\mathbf{Q} = \begin{pmatrix} 1-q_0 & q_0 \\ q_1 & 1-q_1 \end{pmatrix} \tag{5}$$

Let $\mathbf{\Pi}$ denote the stationary distribution for our model, with:

$$\begin{aligned} \mathbf{\Pi} &= (\Pi_0, \Pi_1) \\ &= \left( \frac{q_1}{q_0+q_1}, \frac{q_0}{q_0+q_1} \right) \end{aligned} \tag{6}$$

Then, the total error probability $p$ is given by Eq. (7).

$$\begin{aligned} p &= e_0\Pi_0 + e_1\Pi_1 \\ &= \frac{e_0q_1 + e_1q_0}{q_0+q_1} \end{aligned} \tag{7}$$

Note that now the GW will need to send more than two coded packets, as opposite to the previous case analyzed. The reason for this is that some coded packets are going to be lost during the transmission. Hence the GW will need to generate more packet diversity to let the UTs in $MG_3$ obtain a sufficient number of coded packets to retrieve the originals. However, due to NC robustness

to errors, even if a subset of the packets are lost in one path, $MG_3$ is still able to recover the original video by relying the packets received from the adjacent beam, providing, in this way, an increased reliability. Such a realistic model does not allow extracting straightforward theoretical expressions, however in Section F.5 we provide preliminary simulation results for this scenario.

## F.4 UPPER BOUND ANALYSIS

In order to analyze the theoretical expression obtained in Eq. (4) we compare the performance of the NC technique we propose with the performance of the traditional scheme given by Eq. (3). Note that this is a preliminary theoretical analysis that needs further investigation on the Adaptive Coding and Modulation (ACM) effects. Moreover, also a generalization to any number of beams and multicast groups is required. In order to provide some indicative results, we set up the following parameters for the network in Figure 5:

- The system symbol rate $R_s$ is set to $360 Mbauds$.
- Multicast groups are assigned MODCOD 16APSK-3/4 with respect its own beam since this is the most common assigned MODCOD in real systems for UTs located out of the center of the beam in clear-sky conditions.
- The encapsulation efficiency $\eta_{LL}$ for NC technique is set to 95%. This efficiency takes into account the necessary overheads for adding the encoding coefficients used for generating the coded packets in the headers.

Figure 7 shows the offered multicast capacity in a traditional scheme and using our proposed NC method as a function of the spectral efficiency observed from the additional (external) beam. This spectral efficiency increases from 0.5 (QPSK-1/4) to 2.63 (16APSK-3/4) since a UT could, at most, observe the same spectral efficiency from an external as from its own beam.

Note that there is a range of values where the spectral efficiency observed from the additional/external beam is so low that traditional scheme achieves more gain because received packets are not network coded. When the location of the multicast groups are close to the edge of the beam, i.e. observed spectral efficiencies from both beams are similar, NC technique achieves up to 90% improvement in the offered multicast capacity with respect to the traditional approach. The intersection point between the traditional and NC curves could be understood as an indicator for the system to switch from the traditional way of sending to information to the network coded scheme.

## F.5 SIMULATION RESULTS

In this section we simulate the network in Figure 6 over the bursty wireless channel introduced in Section F.3.2. As in the previous case, simulation results are very preliminary and require further analysis on the ACM effect and a

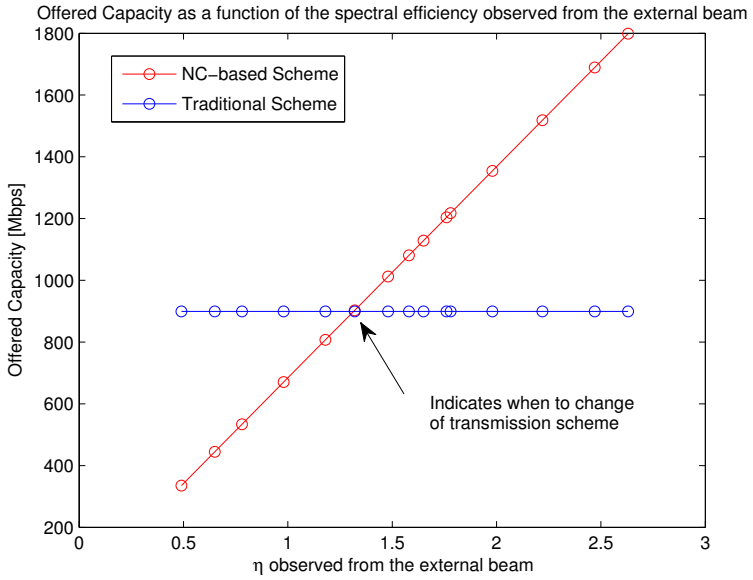


Figure 7: Theoretical upper bound.

generalization on the number of beams and multicast groups. Moreover, implications of NC when using TCP need to be assessed. Therefore, we carry out simulations using the network simulator *ns2* and assuming UDP. To this aim, we set up the following parameters:

- The system symbol rate $R_s$ is set to $360 Mbauds$.
- The GW generates constant bit rate traffic stream of High Definition (HD) video at 2Mbps during 180 seconds. Moreover, the GW sends $h = \{5, 10\}$ coded packets through each user beam.
- $MG_{i=1,2}$ are assigned MODCOD 16APSK-2/3 as in the theoretical analysis performed right above. However, since $MG_3$ is located in the edge of the beam, its assigned MODCOD is QPSK-8/9, e.g. physical layer frames are received $\alpha = 5.37$ times slower.
- For $MG_3$ we vary $q_0$, the probability to change from the good state $S_0$ to the bad state $S_1$, from 0 to 0.5, and we fix the probability to change from the bad state $S_1$ to the good state $S_0$, $q_1 = 0.5$. Then, the total loss probability $p$ is illustrated in Table 4. Note that is a worst case scenario since the $p$ probabilities in Table 4 are very high. Also note that UTs from $MG_1$ and $MG_2$ do not experience any loss, and they receive all the packets sent to their corresponding beams.
- We measure the video throughput at each multicast group and the packet delay, i.e. the elapsed time from the moment when the native video packet is produced at the application layer to the moment when that packet is delivered to the application layer at the UTs.

Table 4: Total loss probability, $p$, for $q_0$ varying from 0 to 0.5 and $q_1 = 0.5$.

| $q_0$ | 0 | 0.1 | 0.2 | 0.3 | 0.4 | 0.5 |
|---|---|---|---|---|---|---|
| $p$ | 0 | 0.16 | 0.28 | 0.37 | 0.44 | 0.5 |

In order to see the benefits provided by NC in this scenario, we compare it against the traditional approach where the GW sends packets as they are. Figure 8 shows the obtained results when $h = 5$ coded packets are sent through each beam. In Figure 8a we plot the average throughput (in Mbps), with increasing loss probability, $p$. For low probability of loss, receivers from $MG_3$ are able to decode the complete information, similar to the other receivers from the center of the beam, due to the robustness provided by NC. In other words, even if a UT at the border of a beam receives only a subset of the packets transmitted to that beam, it is still able to recover the original video by relying the packets received from the adjacent beams. Since all the information sent to each of the beams is processed by means of NC, any receiver from $MG_3$ that receives a sufficient number of independent linear combinations, can decode the original file. However, as $p$ grows, these receivers do not obtain enough independent coded packets, hence the decoding rate starts to decrease.

On the other hand, when the gateway does not employ NC the throughput decreases linearly with $p$. Note that when the loss is higher than 0.40, sending the native packets instead of mixing them by means of NC achieves a higher throughput. In this case, the NC approach is penalized by the fact that if a user terminal does not obtain enough linear combinations for a generation, then it is not able to decode. As in the theoretical analysis performed, this intersection point indicates us when to switch from the traditional way of sending the information to the proposed NC scheme in order to achieve larger throughputs. Note that obtained reliability improvement by means of the proposed NC scheme in a realistic channel with $h = 5$ is up to 10%.

Figure 8b shows the average packet delay with increasing $p$. Obviously, the non-coded scheme achieves lower delays since every single packet is already useful for the UT while in the coded scheme $h = 5$ packets must be received to deliver original video streams to the application layer. However, note that the added delay to both $MG_{i=1,2,3}$ when using NC is very low since the system symbol rate is very high. For a final user, this added delay of tens of milliseconds is imperceptible.

Since this added delay is so low, we can think of increasing the number of coded packets sent through each beam, such that reliability in the system is increased. Figure 9a and Figure 9b show the average throughput and the average packet delay respectively for $h = 10$. It can be seen that the throughput improvement obtained due to NC robustness is now up to 25% whilst the packet delay is just few miliseconds higher than $h = 5$ case.

Hence, we can state that for the realistic scenario, exists a trade-off between the reliability obtained due to NC and the delay introduced at the application level. Such trade-off is driven by the number of coded packets sent through each beam $h$.

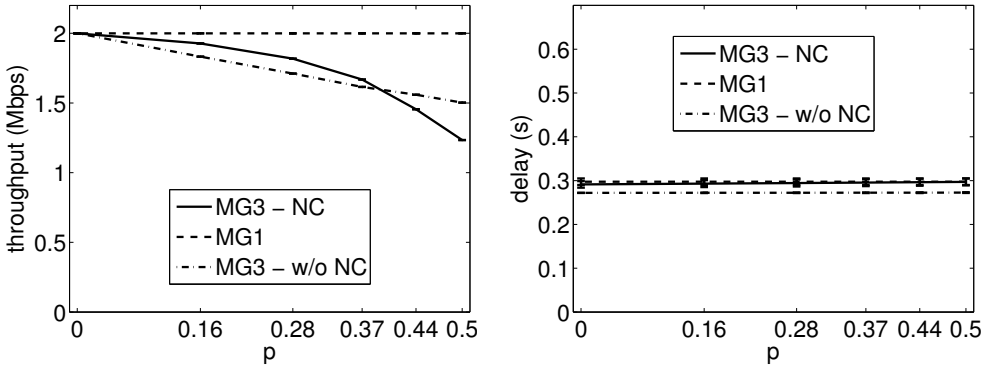


(a) Throughput. (b) Packet delay.

Figure 8: 2Mbps HD quality. $h = 5$ coded packets are sent through each beam.

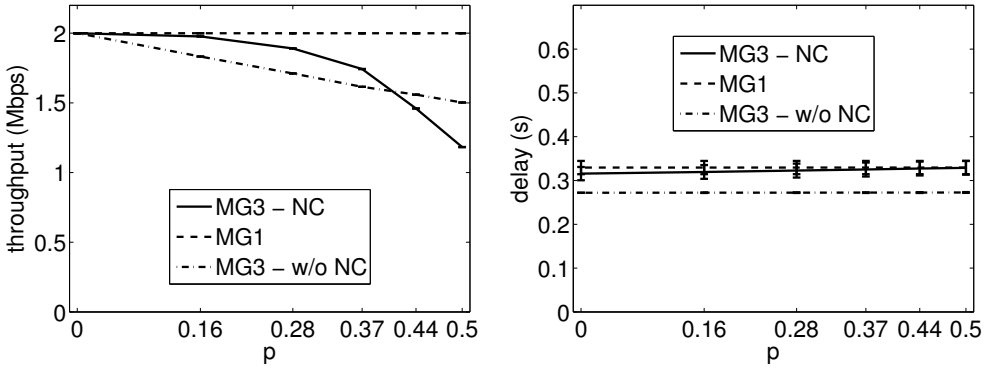


(a) Throughput. (b) Packet delay.

Figure 9: 2Mbps HD quality. $h = 10$ coded packets are sent through each beam.

## F.6 CONCLUSIONS

In this work we have introduced a NC technique to increase the offered capacity to UTs under multi- cast applications in the forward link of multi-beam satellite systems. Specifically, the proposed technique randomly codes link layer packets in a finite field and obtained linear combinations are sent through each beam. UTs belonging to multicast groups can retrieve the original packets when gathering enough linear combinations. Since we consider beam overlapping as an extra source of information rather than interference, coded packets can be received from up to two paths simultaneously.

In order to analyze the performance of the proposed NC technique we have chosen a representative scenario for which a theoretical upper bound and simulations over a realistic channel have been obtained. For the theoretical upper bound, the expressions obtained show that is possible to achieve up to 90% improvement in the inter-beam interference areas by just sending one coded packet through each of the paths observed by the terminals. On the other hand, simulations over the realistic scenario have been performed generating 2Mbps

HD video which is sent in a network coded manner. Results show that up to 25% reliability improvement can be achieved. Moreover, we show that exists a trade-off between the reliability and the packet delay. Such trade-off is driven by the number of coded packets sent through each beam $h$.

Theoretical analysis and simulation results obtained in this work are preliminary and need further inves- tigation on the ACM effects and on the scalability to a general number of beams.

## ACKOWLEDGMENTS

The research leading to these results has received funding from the European Space Agency (ESA) under the PRESTIGE programme.

## REFERENCES

[1] Philip A. Chou, Yunnan Wu, and Kamal Jain. Practical network coding, 2003.

[2] G. Cocco, C. Ibars, and O. del Rio Herrero. Cooperative satellite to land mobile gap-filler-less interactive system architecture. In *ASMA Conf. and SPSC Workshop*, pages 309–314, Sept 2010.

[3] ETSI EN 302 307 v1.2.1. *Digital Video Broadcasting (DVB); Second generation framing structure, channel coding and modulation systems for Broadcasting, Interactive Services, News Gathering and other broadband satellite application (DVB-S2)*. 2009.

[4] ETSI TS 102 034 v1.4.1. *Digital Video Broadcasting (DVB); Transport of MPEG-2 TS based DVB Services over IP Based Networks*. 2009.

[5] ETSI TS 102 606 v1.1.1. *Digital Video Broadcasting (DVB); Generic Stream Encapsulation (GSE) Protocol*. 2010.

[6] F. Filali, G. Aniba, and W. Dabbous. Efficient support of ip multicast in the next generation of geo satellites. *Selected Areas in Communications, IEEE Journal on*, 22(2):413–425, Feb 2004.

[7] D. Pradas and M.A. Vazquez-Castro. Num-based fair rate-delay balancing for layered video multicasting over adaptive satellite networks. *Selected Areas in Communications, IEEE Journal on*, 29(5):969–978, May 2011.

[8] F. Rossetto. A comparison of different physical layer network coding techniques for the satellite environment. In *ASMA Conf. and SPSC Workshop*, pages 25–30, Sept 2010.

Part IV

# BOOK CHAPTER CONTRIBUTIONS (COMPLEMENTARY ANNEX)

# G

# COGNITIVE DUAL SATELLITE SYSTEMS

**S. Gupta, M. Á. Vázquez-Castro and R. Alegre- Godoy***

In Book: *Cooperative and Cognitive Satellite Systems*, Elsevier, 2015

Extract of Section 12.5

## G.1 NETWORK CODING DSS

As explained in subsection 4.1.3, NC is a potential technique for CR in DSS and more specifically in LMS-DSS because it can be applied at MAC layer to coordinate how users access the system. For illustration purposes, this section extends the work in [1] in order to give a concrete example on how NC is applied in CR LMS-DSS.

### G.1.1 *System Model and Channel Model*

We assume a DSS with $|S|$ mobile sources and one receiver as Figure 1 shows. The system has two satellites and the per-satellite channel per source is modeled using the Lutz channel model introduced in 3.3.2, with independent identical statistics per source. This means that the connection of each source with the satellites is described by a pair "good-good", "good-bad", "bad-good" or "bad-bad". In order to capture whether or not channel correlation affects performance, three different cases are considered:

- |S| source - satellite 1 and |S| source - satellite 2 links are uncorrelated.
- |S| source - satellite 1 and |S| source - satellite 2 links are correlated.
- |S| source - satellite 1 and |S| source - satellite 2 links are totally correlated.

* The authors are with the department of Telecommunications and Systems Engineering, Universitat Autònoma de Barcelona.

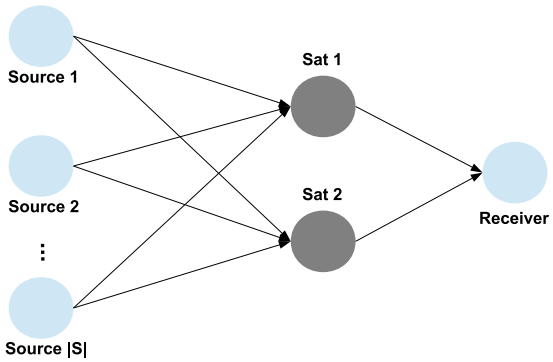


Figure 1: Dual satellite multiple source single receiver system model.

We assume sources are able to exchange their packets via a certain mechanism. Note that this a feasible approach that has been adopted for Wireless Sensor Networks (WSN) in [2], for smart gateways in [2] and for Delay Tolerant Networks (DTN) in [3]. Then, sources select a subset of the packets and broadcast them to the satellites using a certain technique such that the outage probability, i.e. the probability that the receiver is unable to collect all the packets, is low. To this aim, two different techniques are studied, Cognitive Radio Spatial Diversity (CR SD) and Cognitive Radio Spatial Diversity with Network Coding (CR SD+NC).

A number of scenarios match the described system. For instance, a number of sensors attached to animals in remote areas like forests. These sensors would transmit the sensed information to a reduced number of sinks with advanced capabilities. These sinks would cooperate before sending the information to a remote host through any available satellite [2]. Due to the randomness of the surrounding environment (trees blocking the line of sight, rain, etc.) channel becomes available/unavailable at certain periods of time. Another example would involve several military mobile base stations which gather information send by the troops deployed in a military zone, e.g. a city under attack. Again, note that this is a realistic assumption, mobile stations would exchange their packets before sending them to the satellites. The channel would become available/unavailable to the sources by tall buildings blocking the line of sight or by temporary disruptions caused by the enemy.

### G.1.2 *Proposed techniques*

#### G.1.2.1 *Cognitive Radio Spatial Diversity (CR SD)*

Under this scheme, the set of $|S|$ sources, $S = \{s_1, ..., s_{|S|}\}$ coordinate to transmit $N$ packets ($N \leq |S|$), $P = \{p_1, ..., p_N\}$ as follows. Let $s_1$ to $s_N$ transmit each a packet $p_1$ to $p_N$. The CR SD scheme is such that sources $s_{N+1}, s_{N+2}, ..., s_{|S|}$ transmit packets $p_1, p_2, ..., p_{|S| \bmod N}$. Hence, for $N < |S|$ at least one of the packets is sent by more than one source and packets are sent towards two satellites achieving in this way a simple spatial diversity scheme. Since the system has limited resources, the sources access the system via spectrum sensing,

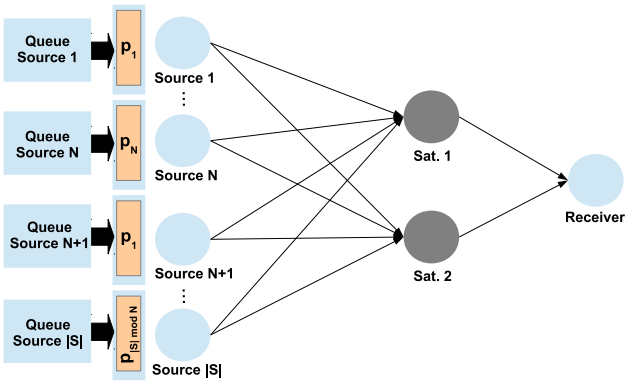


Figure 2: CR SD scheme. Sources have already exchanged their packets and coordinate to select the packets each source sends. $s_i$ sends packet $p_{i \, mod \, N}$. When $N < |S|$ at least one of the packets is sent by more than one source and packets are sent towards two satellites, hence a simple spatial diversity scheme is achieved.

a CR spectrum management technique introduced in 4.1.1. More specifically, sources could employ spectrum sensing as in the return link case briefly introduced in 4.1.3, (Network Coding part) and detailed in [8, 9]. It is worth mentioning that for satellite scenarios the proposed spectrum sensing techniques may present some limitations, mainly due to the large physical separations between the nodes which may difficult the sensing. Hence, the use of the technique could be limited to scenarios where nodes are relatively close. Figure 2 shows a graphical illustration of the CR SD scheme.

#### G.1.2.2 *Cognitive Radio Spatial Diversity with Network Coding (CR SD+NC)*

Under this scheme each of the $|S|$ sources employ CR SD+NC to send a single coded packet as a combination of a number of packets. Specifically each source employs Random Linear Network Coding (RLNC) to generate a single coded packet from the same native $N$ packets, where we assume $N \geq 1$. The encoding coefficients are signaled in the packet headers. In the receiver side at least $N$ coded packets must be received to retrieve the original packets. As before users access the system via spectrum sensing. Figure 3 shows the proposed CR SD+NC scheme where coded packets are indicated as C(·).

### G.1.3 *Analysis and results*

Now, a conceptual performance is discussed in the following:

- Under the CR SD scheme a high probability exists that the receiver obtains duplicated packets, e.g. sources sending a certain packet $p_j$ are the ones under good state with one or both satellites (“good-good”, “good-bad”, “bad-good).
- Under the CR SD+NC scheme it is still possible to receive duplicated packets, but only when both satellites receive a packet from the same

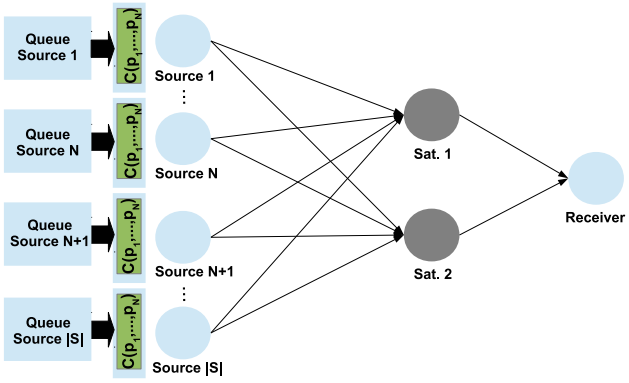


Figure 3: Proposed CR SD+NC scheme. Each source sends a random linear combination of the same $p_1$ to $p_N$ packets.

source. Packets from different sources are fundamentally different although they contain information from the same $N$ packets. This provides fair protection of the packets, because if one source observes a satellite or both in bad state, it equally affects all the packets and not a single packet as in the CR SD case. Moreover, NC also improves the CR part of the system. Transitions between busy and idle periods become more predictable due to the packet accumulation and batch-based transmission. Hence, sources reduce the need for sensing and also their chances to find a free carrier will improve [8].

A simple way forward to extend [1] to cognitive-aided DSS is as follows. Instead of using Markov channel model (that becomes too complex for two satellites or more), availability models like in [7] may simplify the practical design. In this specific scenario, it is more convenient to model the channels in terms of availability (i.e. whether the system is available to the source or not) rather than in terms of pairs of states. If a packet from a source is received by two satellites it does not provide an added value to the system. Nevertheless, the fact that it has been received by at least one satellite is important. Hence, if we transform the 4 state Lutz model of each source to the service availability also introduced in 3.3.2, all the expressions and theoretical derivations in [1] can be directly applied to the DSS scenario just by substituting $p_G$ and $p_B$ (average probability that the channel is in good and bad state in a single satellite system respectively) with the adequate values of $p_A$ and $p_B$, i.e. the average probability that system is available and the probability the system is unavailable respectively. The correlation coefficient has a key influence on the values of $p_A$ and $p_B$ [6]. Correlated channels tend to occupy equal states, i.e. compared to the four-state model for uncorrelated channels (introduced in 3.3.2), the probabilities of states "bad-bad" and "good-good" are higher, and the probabilities of states "good-bad" and "bad-good" are lower (higher $p_B$). Uncorrelated channels show the opposite behavior (higher $p_A$).

Table 1 shows the characteristics of the systems simulated. First, a WSN scenario where sensors cooperate and transmit sensed data to a remote host through satellite. Packet sizes and transmission rates are low according to this

| Parameter | System 1: WSN [2] | System 2: DTN [4] |
|---|---|---|
| Number of satellites | 1(SSS)/2(DSS) | 1(SSS)/2(DSS) |
| Packet Size (bytes) | 200 | 1500 |
| Packet Rate (kbps) | 200 | 10 |
| Number of sources | 1-10 | 1-10 |
| Mean dur. ON state (s) | 4 | 1200 |
| Mean dur. OFF state (s) | 4 | 600 |
| Correlation coefficient | 0/1 | 0/1 |
| $N$ | 2 | 2 |

Table 1: Systems' characteristics.

type of networks. We consider a fast variable channel, i.e. fast transitions of the ON/OFF states modeling a developing hurricane or sandstorm. Second, a DTN where several earth stations cooperate and send information to a spacecraft through a relay satellite. Packet size is set to 1500 bytes, a typical IP protocol value, and transmission rate is very low according to the uplinks of these kind of systems which are normally used for telecommand. The mean durations of ON/OFF states are 20/10 minutes modeling intermittent periods of heavy rain. In both scenarios, simulations consider totally uncorrelated, uncorrelated and totally correlated channels between the sources and the two satellites.

Performance results are separated in two parts. First, in G.1.3.1 the CR SD scheme is evaluated under a SSS and under DSS in order to have an insight of the performance improvement introduced by the fact of having to satellites. Second, in G.1.3.2 the CR SD+NC scheme is evaluated within a DSS. Its performance is compared to CR SD scheme.

#### G.1.3.1 *CR-DSS Performance*

Figure 4 shows the performance for System 1 scenario of the CR SD scheme under a SSS and DSS. Figure 5 shows the equivalent performance for System 2.

When the channels between the source and the satellites are totally uncorrelated (left plot of Figure 4 and Figure 5), the DSS provides the maximum gain. The system outage probability is 0 (not seen in the plot due to the logarithmic scale in the Y-axis) since there is always one satellite available per source. When the channels between the source and the satellites are totally correlated (right plot of Figure 4 and Figure 5), the DSS does not provide any advantage in terms of availability since both satellites behave exactly equally per each source (in the plot SSS and DSS performances are superimposed). For any degree of correlation in-between (central plot of Figure 4 and Figure 5), DSS offers advantage with respect to SSS. The more uncorrelated the source to satellite channels the better the performance improvement in terms of system availability.

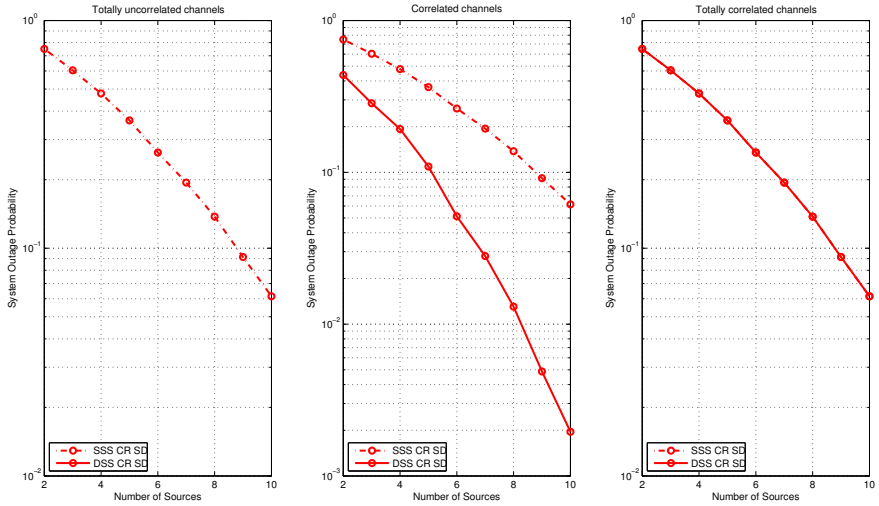


Figure 4: System 1. SSS vs DSS performance for various channel correlations.

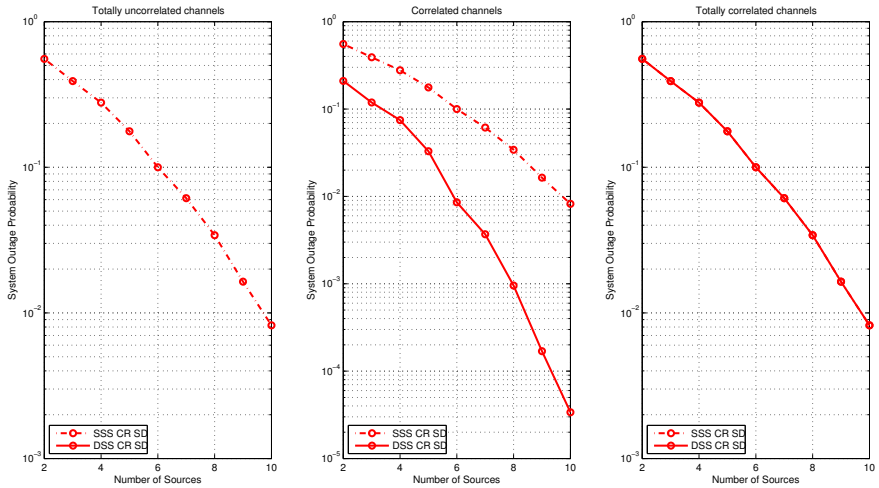


Figure 5: System 2. SSS vs DSS performance for various channel correlations.

### G.1.3.2 *CR-DSS Improvement with NC-Aided CR-DSS*

Figure 6 and Figure 7 show the performance of CR SD+NC compared to CR SD in DSS for System 1 and System 2 respectively. From the analysis in G.1.3.1 we know that if channels are totally uncorrelated, CR SD and CRSD+NC would perform equally and with system outage probability 0, i.e. per each source there is always at least one satellite available and all the packets reach the receiver. When the source to satellites channels are totally correlated, CR SD+NC shows a performance equivalent to CR SD+NC in a SSS because both satellites are either available or not. Hence, the analysis in [1] applies directly, i.e. NC avoids that duplicated packets are received and provides fair protection of the packets. For any degree of correlation in between, CR SD+NC offers always better performance compared to CR SD since the fact of having two satellites is exploited.

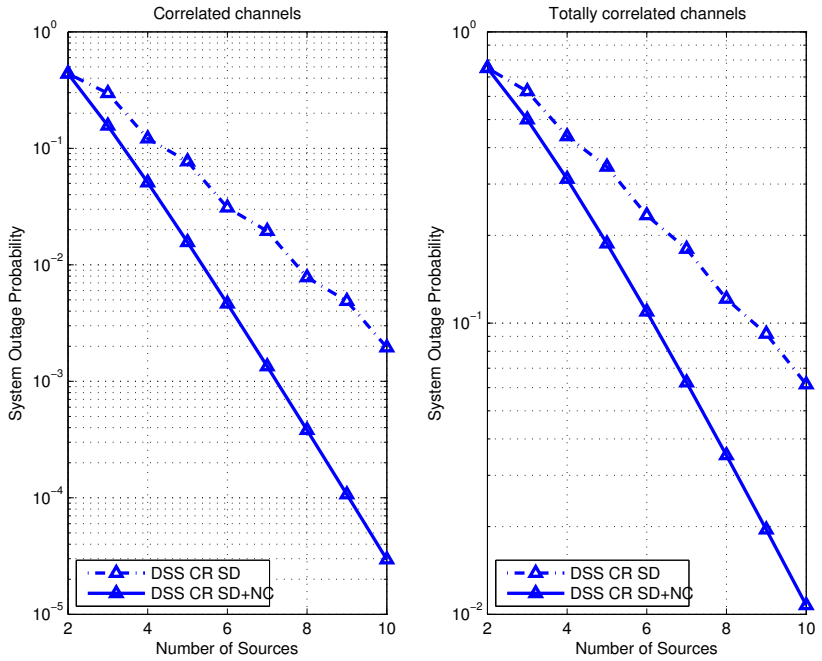


Figure 6: System 1. CR SD+NC vs CR SD in DSS.

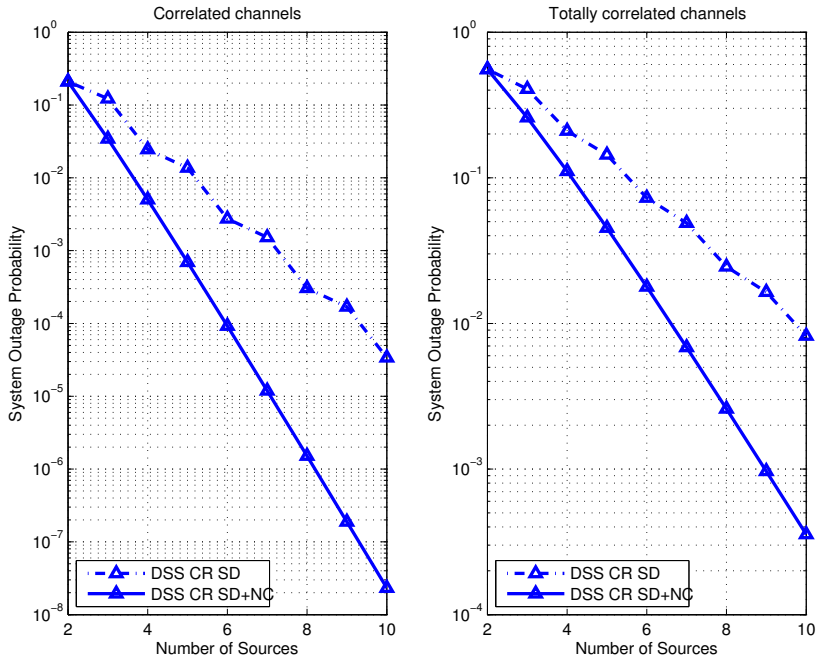


Figure 7: System 2. CR SD+NC vs CR SD in DSS.

## REFERENCES

[1] R. Alegre-Godoy and M. A. Vázquez-Castro. Spatial diversity with network coding for on/off satellite channels. *Communications Letters, IEEE*, 17(8):1612–1615, 2013.

[2] I Bisio and Mario Marchese. Efficient satellite-based sensor networks for information retrieval. *Systems Journal, IEEE*, 2(4):464–475, Dec 2008.

[3] C. Caini and V. Fiore. Moon to earth dtn communications through lunar relay satellites. In *Advanced Satellite Multimedia Systems Conference (ASMS) and 12th Signal Processing for Space Communications Workshop (SPSC), 2012 6th*, pages 89–95, Sept 2012.

[4] T. de Cola and Mario Marchese. Reliable data delivery over deep space networks: Benefits of long erasure codes over arq strategies. *Wireless Communications, IEEE*, 17(2):57–65, April 2010.

[5] A Kyrgiazos, B. Evans, P. Thompson, and N. Jeannin. Gateway diversity scheme for a future broadband satellite system. In *Advanced Satellite Multimedia Systems Conference (ASMS) and 12th Signal Processing for Space Communications Workshop (SPSC), 2012 6th*, pages 363–370, Sept 2012.

[6] Erich Lutz. A markov model for correlated land mobile satellite channels. *International Journal of Satellite Communications*, 14:333–339, 1996.

[7] M. A. Vázquez-Castro, F. Perez-Fontan, and S. R. Saunders. Shadowing correlation assessment and modeling for satellite diversity in urban environments. *International Journal of Satellite Communications*, 20(2):151–166, 2002.

[8] Shanshan Wang, Yalin E. Sagduyu, Junshan Zhang, and Jason H. Li. Spectrum shaping via network coding in cognitive radio networks. *IEEE INFOCOM*, pages 396–400, 2011.

[9] Changliang Zheng, Eryk Dutkiewicz, Ren Ping Liu, Rein Vesilo, and Zheng Zhou. Efficient data transmission with random linear coding in multi-channel cognitive radio networks. *IEEE Wireless Communications and Networking Conference*, pages 77–82, 2013.